NONLINEAR DYNAMICS OF COMPOSITE PLATES AND OTHER PHYSICAL SYSTEMS

by

Jamal Faris Nayfeh

Dissertation submitted to the Faculty of the

Virginia Polytechnic Institute and State University

in partial fulfillment of the requirements for the degree of

Doctor of Philosophy

in

Engineering Mechanics

APPROVED:

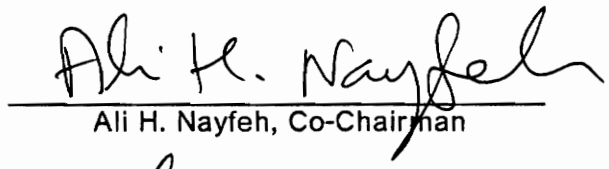

Ali H. Nayfeh, Co-Chairman

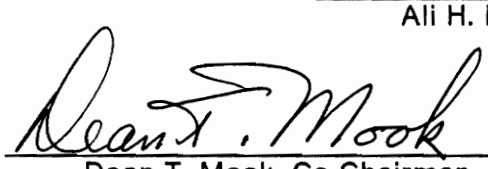

Dean T. Mook, Co-Chairman

Rakesh K. Kapania

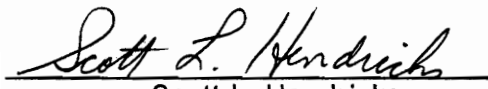

Scott L. Hendricks

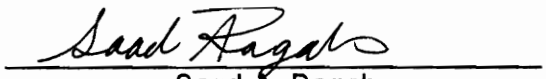

Saad A. Ragab

December, 1990

Blacksburg, Virginia

NONLINEAR DYNAMICS OF COMPOSITE PLATES AND OTHER PHYSICAL SYSTEMS

by

Jamal Faris Nayfeh

Ali H. Nayfeh, Co-Chairman

Engineering Mechanics

(ABSTRACT)

The computer algebra system MACSYMA is used to derive the nonlinear expression for the Lagrangian and the nonlinear equations of motion of composite plates undergoing large deformations by using a higher-order shear-deformation theory. When computer algebra is not used, the derivation of these equations is very involved and time consuming.

A time-averaged-Lagrangian technique is developed for the nonlinear analysis of the response of a wide variety of physical systems. It is a perturbation method that produces accurate second-order approximate solutions in the neighborhoods of different resonances. As an application of the technique, the nonlinear response of a fluid-relief valve is discussed in detail. The different resonances are studied, and in each case the responses are compared to those obtained by using the Galerkin procedure. The shortcomings of the latter procedure are pointed out.

The time-averaged-Lagrangian technique is implemented in a MACSYMA code that produces second-order perturbation solutions. The effects of the quadratic nonlinearities are incorporated into the solution and different cases of resonances are fully investigated. First-order differential equations are derived for the evolution of the amplitudes and phases for the following resonances: primary resonance, subharmonic resonance of order one-half, and superharmonic resonance of order two. The evolution equations are used to determine the fixed point or constant

solutions and the results are then used to obtain representative frequency-response and force-response curves for each case. The stability of the fixed points is investigated. The results show that stable and unstable solutions may coexist when multi-valued solutions are possible, the initial conditions determine which describes the response. The multi-valuedness of the solutions lead to the jump phenomenon. The results show that subharmonic resonances of order one-half cannot be activated unless the excitation amplitude exceeds a threshold value.

Lastly, a numerical-perturbation approach is used to study modal interactions in the response of the surface of a liquid in a cylindrical container to a principal parametric resonant excitation in the presence of a two-to-one internal (autoparametric) resonance. The force-response curves exhibit saturation, jumps, and Hopf bifurcations. They also show that the response does not start until a certain threshold level of excitation is exceeded. The frequency-response curves exhibit jumps, pitchfork bifurcations, and Hopf bifurcations. For certain parameters and excitation frequencies between the Hopf bifurcation values, limit-cycle solutions of the modulation equations are found. As the excitation frequency changes, the limit-cycles deform and lose their stability through either pitchfork or cyclic-fold (saddle-node) bifurcations. Some of these saddle-node bifurcations cause a transition to chaos. The pitchfork bifurcations break the symmetry of the limit cycles. Period-three motions are observed over a narrow range of excitation frequencies.

Acknowledgements

I wish to express my appreciation and gratitude to Professors Ali H. Nayfeh and Dean T. Mook for serving as my major advisors. Their teaching, guidance, and support were essential to the completion of this work. Sincere thanks are also due to the members of the committee: Professors Saad Ragab, Scott Hendricks, and Rakesh Kapania. Their comments and valuable advice were essential in completing this work. In addition, I appreciate the friendship and assistance of fellow graduate students: Raouf Raouf, Marwan Bikdash, Jamal Masad, Balakumar Balachandran, Nestor Sanchez, and Jafar Hadian. The research reported in this dissertation was supported by the Army Research Office under Grant No. DAAL03-89-K-0180 and the Office of Naval Research under Grant No. N00014-90-J-1149. Their support is gratefully acknowledged.

The constant love, support, and encouragement of my family is deeply appreciated. My deepest love and thanks go to my wife, Stephanie, whose unselfish patience and understanding have lifted me in critical times. I am grateful for her unending support in all of my endeavors, academic and otherwise.

Finally, it is a pleasure to acknowledge the brilliant typing skills and friendly helpfulness of Sally Shrader during the preparation of this dissertation.

Table of Contents

1. LITERATURE SURVEY

1.1. Composite Plates

Demands of materials by todays technologies have become so diverse that they often cannot be met by simple single-component materials acting alone. In recent years, the use of laminated anisotropic composites as structural elements has increased significantly. This stems from the fact that laminated composites offer outstanding strength, stiffness, and weight saving to best match the design requirements of different engineering structural configurations. They are extensively used in various industries, such as aircraft, missile, hydrospace, shipbuilding, transportation, and building construction. Composite technology will play an even more important role in the future.

A significant amount of research has been conducted on the modeling and vibration analyses of laminated composite plates. In this section, we present a limited literature review of some of the developments in these areas of research. The literature cited below is divided into three categories: shear-deformation theories for

multilayered composite plates, linear vibrations of laminated plates, and nonlinear vibrations of laminated plates.

1.1.1. Shear-deformation theories for multilayered composite plates

It is well documented that the classical laminated plate theory, based on the Kirchhoff hypotheses of straight inextensional normals to the mid-plane of the plate, yields sufficiently accurate results for only thin composite plates. The wide use of advanced filamentary composite materials in aircraft, automotive, shipbuilding, and other industries demands more accurate predictions of the dynamic response of laminated plates. These advanced composites are susceptible to thickness effects because their effective transverse shear moduli are considerably smaller than their effective in-plane elastic moduli. Therefore, the transverse shear deformations are no more negligible and should be considered in the analysis of such composites.

The shear-deformation theories can be grouped into two classes: stress-based theories and displacement-based theories. Reissner (1944, 1945, 1947) presented the first stress-based transverse shear-deformation plate theory. His theory was based on a linear distribution of the in-plane normal and shear stresses through the thickness of the plate. The pioneering work on the displacement-based theories is due to Basset (1890). Hildebrand et al. (1949) developed a variationally consistent first-order theory for shells based on Basset's representation of the displacement field. Mindlin (1951) extended Hencky's theory (1947) of isotropic plates to account for the dynamics of the plate. The shear-deformation theory based on Mindlin's formulation is referred to as the first-order transverse shear-deformation theory (e.g., Reddy, 1984c).

The literature shows that many researchers extended and applied the above mentioned classes of theories. Khdeir (1986) included a list of these works. Gol'denveizer (1958) generalized Reissner's theory (1944, 1945, 1947) by replacing the linear distribution of stresses through the thickness of the plate by an arbitrary distribution. Following Hildebrand (1949), Librescu (1966, 1969) made the first attempt to formulate a higher-order theory of anisotropic plates and shells.

Kromm (1955) presented a shear-deformation theory in which the transverse shear stresses are assumed to vanish on the bounding planes of the plate. Schmidt (1977) extended Kromm's theory (1955) to account for moderately large deflections of the von Karman type.

Whitney (1969a) and Whitney and Pagano (1970) extended the displacement-based theory to laminated plates. The second- and higher-order displacement shear-deformation theories had been considered by Nelson and Lorch (1974), Lo et al. (1977), Levinson (1980), Murthy (1981), and Reddy (1984c, 1985). The works of Levinson (1980) and Murthy (1981) lead to variationally inconsistent analyses. Reddy (1984a, 1984b) corrected these theories by deriving energy consistent governing differential equations and boundary conditions by means of the principle of virtual work. Moreover, Reddy accounted for the von Karman strains in his third-order theory.

1.1.2. Linear vibrations of laminated plates

The linear vibrations of laminated composite plates has received widespread attention in recent years. The literature pertaining to this subject is rich and diverse. Researchers used both analytical and numerical methods to solve for the free- and

forced-vibration problems of composite plates. Leissa (1981) surveyed the literature on the vibration behavior of anisotropic plates. Bert (1985) reviewed the dynamic response of laminated composites. Reddy (1983a, 1985) reviewed the literature concerning the application of the finite-element method in studying the vibrations of plates.

Bhimaraddi and Stephen (1984) studied the vibrations of thick laminated composite plates by using a higher-order theory. Stein and Jegley (1985) investigated the effects of transverse shear deformation on the cylindrical bending and vibration of laminated plates. Bowlus et al. (1987) studied the effects of transverse shear deformations and rotary inertia on the vibration of symmetrically laminated rectangular plates by using the Galerkin method. Sivakumaran (1987) considered the vibrations of thick symmetrically laminated rectangular plates having free-edge conditions.

Recent research on the free-vibration analysis of rectangular plates by using higher-order shear-deformation theories include the studies by Reddy (1983d, 1984a), Di Sciuva (1986), Bhimaraddi and Stephens (1984), Doong and Chen (1987). Bert and Mayberry (1969) conducted free-vibration analysis of unsymmetrically laminated plates with clamped edges. Whitney (1969b, 1970) studied the effects of boundary conditions on the bending, vibration, and buckling of unsymmetric laminates. Ashton (1969) and Jones (1973) also studied the response of unsymmetric laminates. Baharlou and Leissa (1987) proposed a general method for the analysis of generally laminated thin plates with different boundary conditions by using a technique based on the Ritz method. Khdeir (1988) analyzed the free vibrations of antisymmetric angle-ply laminates with various boundary conditions. He used a generalized Levy-type solution (Reddy et al., 1987) in conjunction with the state-space concept (Librescu et al., 1987). Kamal and Durvasula (1986) studied the free vibrations of

unsymmetric laminates by using a shear-deformation plate theory and considering all possible boundary conditions.

1.1.3. Nonlinear vibrations

It is well known that isotropic plates undergoing large deflections of the order of the plate thickness show an increase in the effective stiffness of the plate and the free-vibration frequencies. The resulting nonlinear equations of motion are the dynamic version of the von Karman equations. The nonlinearity is of the hardening type. A very extensive bibliography, containing references to numerous publications on the nonlinear responses of plates, was compiled and presented in the text by Nayfeh and Mook (1979).

The coupling between bending and stretching in composite plates had been reported experimentally and in applications. Reissner and Stavsky (1961) provided the theoretical background for the study of vibrations of composite plates. The excellent pioneering books by Ashton and Whitney (1970) and Jones (1975) were the books that dealt extensively with the vibrations and bucklings of composite plates. Bert (1976a, 1976b, 1979, 1980) and Bert and Francis (1974) provided outstanding literature reviews on the subject.

The nonlinear analysis of laminated composite plates has been a subject of significant current interest. Whitney (1968) and Whitney and Leissa (1969) were the first to formulate the equations of motion for the large-deflection behavior of laminated anisotropic plates that account for the von Karman geometrical nonlinearity. A comprehensive literature review can be found in the text by Chia (1980), which covers the work in the field until 1979. Bennet (1971) obtained the first

known solutions to the nonlinear coupled equations for angle-ply rectangular composite plates having simply-supported edge conditions. He reported that the bending-stretching coupling appears only in the linear terms, which indirectly affects the nonlinear term in the frequency equation. Wu and Vinson (1971) used Berger's approximation and studied the nonlinear vibrations of laminated plates with clamped and simply-supported edges. Employing the Galerkin procedure, Bert (1973) studied the vibrations of clamped laminated composite plates. Chandra and Raju (1975a, 1975b) investigated the nonlinear vibrations of angle-ply and cross-ply plates by using the Galerkin method and a perturbation technique. They assumed the plate edges to be clamped and simply-supported for out-of-plane boundary conditions and to be movable and immovable for in-plane boundary conditions. They presented a two-term (multimode) solution for the case of angle-ply plates. Chandra (1976) extended this analysis to study nonlinear oscillations of simply-supported clamped cross-ply plates. Multimode nonlinear vibrations of angle-ply and cross-ply plates were investigated by Chia and Parabhakara (1978) for all clamped and all simply-supported stress-free edges. Chia (1982) presented a single-mode solution for the large-amplitude vibrations of rigidly clamped antisymmetric cross-ply plates. He expressed the dynamic von Karman type nonlinear equations in terms of three displacement components. Using the finite-element method, Reddy and Chao (1981, 1982) and Reddy (1982) considered nonlinear oscillations of laminated plates with edges all clamped and all simply supported. Sivakumaran and Chia (1984, 1985) used Hamilton's principle and Reissner's variational principle to determine single-mode vibrations of laminated plates with all edges being clamped, all simply-supported, and two parallel edges clamped and the other edges simply-supported. Reddy and Chao (1981, 1982a), Reddy (1982), and Sivakumaran and Chia (1984, 1985) included in their analyses the effects of transverse shear and rotary inertia. Reddy (1982) and

Sivakumaran and Chia (1985) included rectangular cutouts and transverse normal stresses, respectively. Chia (1985) investigated the amplitude and frequency responses of angle-ply plates on a Winkler-Pasternak elastic foundation having the edges nonuniformly restrained against rotation. He used a single-mode solution to the von Karman nonlinear equations. Hui (1985a, 1985b) investigated the effects of geometric imperfections and in-plane edge compressive loads on the large-amplitude vibrations of simply-supported antisymmetric laminates using a perturbation method and the Galerkin procedure in association with the dynamic von Karman-type plate equations.

Kapania and Raciti (1988a) reviewed recent developments in the analyses of laminated beams and plates with an emphasis on shear effects and buckling. They presented a discussion of various shear-deformation theories for plates and beams and a review of the recently developed finite-element method for the analysis of thin and thick laminated beams and plates. Moreover, they included recent studies on the buckling and postbuckling behavior of perfect and geometrically imperfect plates and the delamination buckling and growth in beams and plates. Kapania and Raciti (1988b) presented a summary of recent advances in the analysis of laminated beams and plates with an emphasis on vibrations and wave propagations. They reviewed the free-vibration analysis of symmetrically laminated plates for various geometric shapes and edge conditions. A detailed review of the various developments in the analysis of unsymmetrically laminated beams and plates was included in their study. Moreover, they presented a survey of the nonlinear vibrations of perfect and geometrically laminated plates. They pointed out that, due to the bending-stretching coupling, the nonlinear behavior of unsymmetrically laminated perfect and imperfect plates may be of the hardening- or softening-type, depending upon the boundary

conditions. In addition, they reviewed wave propagation in and the linear and nonlinear transient response of laminated materials.

Eslami and Kandil (1989a) used the method of multiple scales to study the large-amplitude response of special orthotropic plates to harmonic excitations. They used a single-mode Galerkin's method to transform the nonlinear coupled partial-differential equations into a Duffing-type equation. They studied primary, subharmonic, and superharmonic resonances. Eslami and Kandil (1989b) also studied the multi-mode nonlinear vibration of orthotropic panels by using the method of multiple scales in conjunction with the Galerkin's procedure. They discussed different resonances and compared the solutions in the case of primary resonance with those obtained by using the method of harmonic balance and found good agreement.

1.2. Dynamics of Physical Systems

The text by Nayfeh and Mook (1979) presents a comprehensive literature review of the nonlinear oscillations of diverse physical systems. Nayfeh and Mook studied and explained complicated nonlinear phenomena in the dynamics of discrete single-degree-of-freedom, multi-degrees-of-freedom, and continuous systems. They also showed that modal interactions reduce the dynamics of a continuous system to that of a finite-degree-of-freedom system. A survey paper by Holmes and Moon (1983) contains several examples of diverse physical systems that exhibit complicated dynamics. The examples include experimental studies of postbuckled beams oscillating around their buckled positions; nonlinear circuits (Ueda, 1979);

magnetomechanical devices, such as rotating disks in a magnetic field (Robbins, 1977) and torsional oscillations of a compass needle in an oscillating or rotating magnetic field (Croquette and Pointou, 1981); feedback control systems; and chemical reactions, such as the reaction-diffusion system (Rossler, 1976). Moon (1987) presented a review of mathematical models and experiments of physical systems that display chaotic vibrations. He also presented a variety of theoretical and experimental tools to identify chaos. Nayfeh (1988) discussed several examples of physical systems that exhibit complicated nonlinear behaviors, such as the saturation and jump phenomena, period-multiplying bifurcations, and chaos. He used a numerical-perturbation approach for the analysis of these systems; they include cylindrical shells, experiments with two-beam structures, surface waves in closed cylindrical containers, subharmonic instability of two-dimensional boundary layers on flat plates, and three-dimensional propagation of sound in partially choked ducts.

The literature shows that most of the available studies on the subject of nonlinear dynamics consider only the cases of single- and two-degree-of-freedom systems. Physical and mathematical justifications usually determine the number of degrees of freedom that best represent and explain the dynamics of a given system. The number of degrees of freedom needed to describe the behavior of discrete systems, such as particles, may be obvious, whereas that of continuous systems, such as beams, plates, and shells is not. This is due to the fact that a continuous system has an infinite number of modes, representing an infinite number of degrees of freedom. Nayfeh and Mook (1979) argue that, in the presence of damping, modes that are not directly excited through an external resonance or indirectly excited through an internal resonance will decay with time.

Single-degree-of-freedom systems with nonlinear characteristics are, in general, easier to study and understand than systems with more degrees of freedom.

Therefore, there exists a good and rich amount of the literature about the subject. Nayfeh and Khdeir (1986a, 1986b) investigated the nonlinear rolling of ships in regular seas. They modeled the ship as a single-degree-of-freedom system and found that its response undergoes a cascade of period-doubling bifurcations culminating into chaos. Dowell and Pezeshki (1986) studied the nonlinear single-mode response of a buckled beam and showed that the response undergoes a sequence of period-doubling bifurcations that culminates into chaos. They reported that their results agree with the experimental results of Moon (1980). Zavodney and Nayfeh (1988) and Zavodney, Nayfeh, and Sanchez (1989,1990) studied extensively the response of a single-degree-of-freedom system with quadratic and cubic nonlinearities to fundamental and principal parametric resonances. They presented a second-order perturbation solution to the problem and verified its validity with analog- and digital-computer simulations. They found period-multiplying and -demultiplying bifurcations as well as chaotic motions.

1.3. Nonlinear Response of a Fluid Valve

Here, we present a literature review into the nonlinear response of a fluid valve mechanism, which is the main topic of Chapter 4 of this dissertation. This problem provides an excellent example for demonstrating the solution procedure. An accurate alternative method already exists in the literature (Nayfeh and Bouguerra, 1990) and thus provides a means of checking the validity of the method. The valve is used to protect a fluid system from overpressure and consists, in its simplest design, of a ball held by a helical spring against a valve seat having nonlinear spring

characteristics. The helical spring is modeled as a continuous system and its motion is described by the wave equation with proper damping terms added. One end of the spring is considered to be fixed, whereas the other end is restrained by a force induced by the valve seat and subjected to a constant static pressure and a sinusoidally varying dynamic pressure, resulting from vibrations in the pneumatic transmission lines (see Figures 4.1 and 4.2).

Johnson and Wandling (1969) showed that the actual popping pressure of a relief valve under dynamic loading is frequency dependent. They showed that because of the spring dynamics the actual popping pressure may be a fraction of the static popping pressure. Both experimental and theoretical results, which appear to follow somewhat the same trend, confirm that the actual popping pressure does vary greatly from that for which the valve was statically set. Dokainish and Elmadany (1978) used the method of harmonic balance to analyze the influence of the nonlinear spring characteristics in the absence of damping. They studied the cases of primary resonance, superharmonic resonance of order three, and subharmonic resonance of order one-third. Their assumed solutions do not contain the second harmonic and hence their results are valid only for static pressures that are small compared with the dynamic component (Nayfeh and Bouguerra, 1990).

Nakashima et al. (1986) studied the effects of the configuration of the pressure lines and the elements of the regulator, such as the mass of the valve-spring system and spring constant, on the response of the regulator. In their theoretical analysis, the motion of the spring was modeled as a damped one-degree-of-freedom system under external forces. The results were then compared with those obtained experimentally in order to clarify their validity and determine the conditions under which occasional vibrations may arise during operation. They concluded that occasional vibrations of the regulator may arise when the resistance of the pipe line

becomes large. They also observed that when the adjusting pressure decreases below a threshold value, these vibrations may be easily generated due to severe pressure changes in the chambers of the regulator in the transient response process.

Porter and Billett (1965) used the method of harmonic balance to analyze primary resonances, subharmonic resonances of order one-third, and superharmonic resonances of order three in the longitudinal response of a bar constrained by a nonlinear spring to a harmonic excitation. Using the method of harmonic balance, Watanabe (1978) analyzed primary resonances in the longitudinal response of a bar subject to nonlinear boundary conditions to a harmonic excitation. Paslay and Gurtin (1980) analyzed primary and third-harmonic resonances in the response of a linear system resting on a nonlinear spring to a harmonic excitation. Dowell (1980) employed a component mode analysis for the transverse free oscillations of a hinged-hinged beam constrained by a nonlinear spring mass system. Nayfeh and Asfar (1986) used the method of multiple scales (Nayfeh, 1973, 1981) to analyze the response and the stability of a bar constrained by a nonlinear spring to a harmonic excitation for the cases of primary, subharmonic, superharmonic, combination and ultrasubharmonic resonances.

1.4. Surface Waves in Closed Basins Under Principal and Autoparametric Resonances

The problem of standing waves on the free surface of liquids that are contained in vessels of finite dimensions provides interesting dynamical characteristics. In

Chapter 6 a nonlinear analysis is presented of a class of these waves in cylindrical vessels. The system is subject to a harmonic longitudinal excitation that produces a principal parametric resonance of a mode that is involved in a two-to-one internal (autoparametric) resonance with a lower mode. Reviews of modal interactions in the response of dynamical systems were given by Miles (1984), Nayfeh (1989), Miles and Henderson (1990), and Nayfeh and Balachandran (1989). The following brief discussion of representative examples provides a background for the work done in Chapter 6 of this dissertation.

Linear theory predicts that the surface either grows exponentially with time or is bounded, depending on the amplitude and frequency of the excitation. Because the exponential growth is physically unrealistic, the model should include nonlinear terms, which act as limiters of the response. Moreover, the linear model may predict stability (i.e., decaying response), whereas the actual response may not decay under certain conditions. In this case, the parametric excitation produces a subcritical instability that is only predictable by including nonlinear terms. Recent theoretical and experimental work clearly show that the nonlinearities produce interesting surface-wave motions and that linearizing the problem results in overlooking some of the complex and interesting features of the motion.

Miles (1984) studied the case of a one-to-one autoparametric resonance. He introduced damping and determined the parametric region in which chaotic motions exist. Umeki and Kambe (1989) extended the analysis of Miles for the case of a circular cylinder by taking into account capillary effects. They presented stability and bifurcation diagrams for the case of subharmonic resonance of order one-half. They presented numerical results showing period-doubling bifurcations and chaotic solutions with one positive Lyapunov exponent. Feng and Sethna (1989) also investigated surface waves for the case of one-to-one autoparametric resonances but

in a near square container. Their bifurcation analysis shows that the response of the system may be a periodic or a quasiperiodic standing or traveling wave. Their analysis also identifies parameter values for chaotic behavior. They verified their theoretical findings with the aid of experiments. Simonelli and Gollub (1989) investigated the same problem experimentally; that is, the dynamics of the interaction of two modes that are degenerate in a square container but not in a rectangular container. They determined both stable and unstable fixed points and established the bifurcation sequences. In a nearly square container, they found that mode competition produces both periodic and chaotic states, in agreement with the theoretical and experimental findings of Feng and Sethna.

Other experimental studies have been carried out to detect aperiodic motions on the free surfaces of liquids in containers that are subject to longitudinal harmonic excitations. Keolian et al. (1981) and Keolian and Rudnick (1984) conducted experiments using liquid helium and water in thin angular troughs. They observed period-doubling bifurcations and quasiperiodic motions involving three interacting modes. Gollub and Meyer (1983) used flow visualization and laser detection techniques to measure the time-dependent modal amplitudes. They reported a sequence of four boundaries of symmetry-breaking instabilities: a single axisymmetric mode, a slow precession of the wave pattern with a quasiperiodic overall motion, azimuthal modulations which produced chaotic oscillations, and a discontinuous spatial disordered flow. Ciliberto and Gollub (1984, 1985) examined the case in which the excitation frequency and amplitude are near the intersection of the instability boundary between two degenerate modes and found that they can compete to produce either a periodic or a chaotic motion.

The one-to-one autoparametric resonant case leads to modulation equations with cubic nonlinearities. Another autoparametric case occurs when two of the natural

frequencies are approximately in the ratio of two-to-one. The coupling in this case is quadratic and leads to modulation equations with quadratic nonlinearities. Miles (1984) analyzed the case of a perfectly tuned two-to-one autoparametric resonance (i.e., $\omega_2 = 2\omega_1$) when the lower mode is excited by a principal parametric resonance (i.e., $\Omega \approx 2\omega_1$), where the ω_n are the linear natural frequencies and Ω is the excitation frequency. He found no Hopf bifurcation points and concluded that in the presence of small but finite damping, neither periodic limit cycles nor chaotic motions exist. Nayfeh (1987a) and Gu and Sethna (1987) relaxed the perfectly tuned condition and considered the case $\omega_2 = 2\omega_1 + \sigma_1$ and $\Omega = 2\omega_1 + \sigma_2$, where σ_1 and σ_2 are detuning parameters. For sufficiently small damping, they found Hopf bifurcations. Between the Hopf bifurcation points, they found limit cycles of the modulation equations that undergo a sequence of period-doubling bifurcations, culminating in chaos. Gu and Sethna (1987) used the Silnikov theorem to investigate the routes to chaos. Becker and Miles (1986) and Nayfeh (1987a) analyzed the response of systems with two-to-one internal resonances to a principal parametric excitation of the higher mode.

In Chapter 6, we use the method of multiple scales (1973, 1981) to extend the analysis of Nayfeh (1987a) and Gu and Sethna (1987) to the case of principal parametric resonance of the higher mode; that is, we analyze surface waves in a cylindrical container in the presence of a two-to-one autoparametric resonance when the higher mode rather than the lower mode is excited by a principal parametric resonance. Although the modulation equations are the same as those derived by Becker and Miles (1986) and Nayfeh (1987b), the bifurcation analysis presented in Chapter 6 is far more comprehensive than theirs.

1.5. Organization of Dissertation

The rest of this dissertation is divided into six subsequent chapters organized in the following manner. In Chapter 2, the general nonlinear equations of motion of thick rectangular laminated plates are derived by using a higher-order shear-deformation plate theory. Chapter 3 includes the nonlinear governing equations in terms of the displacement variables and provides the linear solution for the case of simply-supported antisymmetric plates and plate strips in cylindrical bending. The time-averaged-Lagrangian technique is described and applied to a case problem that treats the nonlinear response of a fluid relief valve in Chapter 4. Chapter 5 contains the application of the time-averaged-Lagrangian technique to the nonlinear vibrations of composite plates subject to external transverse harmonic loads in the presence of primary, subharmonic, and superharmonic resonances. In Chapter 6, modal interactions and complicated dynamics of the response of surface waves in closed cylindrical containers under principal and internal (autoparametric) resonances are discussed in detail. Finally, in Chapter 7, conclusions and summaries of the research in this dissertation are presented and topics for further future related research are suggested.

2. NONLINEAR EQUATIONS OF MOTION OF LAMINATED PLATES

2.1. Introduction

In spite of the fact that linearized equations of motion provide no more than a first approximation in a real problem, they are adequate for many engineering applications. However, when The amplitudes of the vibrations are not small, a nonlinear analysis must be used to obtain more accurate results and to explain certain phenomena, such as the dependence of the frequency on the amplitude. The great demand for more realistic (i.e., nonlinear) models of structural responses has resulted in the development of various analytical techniques. Symbolic manipulation and digital computers are of increasing value.

In general, nonlinearities in structural mechanics problems appear in the governing differential equations in different ways. Material or physical nonlinearity exists when the material behavior is nonlinear. Alternatively, the material behavior

can be linear, but the deflection can be large and require nonlinear strain-displacement relations. Combinations of both physical and geometric nonlinearities are also possible. In this dissertation, consideration is limited to geometrical nonlinearities.

One of the assumptions in Kirchhoff's plate theory is that the normals to the mid-plane before deformation remain normal after deformation. This assumption makes Kirchhoff's plate theory insensitive to shear deformation. It is, however, well known that the effect of shear deformations can be significant in laminated plates and thick plates. Reissner (1945) improved Kirchhoff's theory when he considered the shear deformation effects by introducing a complementary energy principle. Mindlin (1951) presented a first-order theory that takes into account the effects of shear deformation of plates by introducing a shear-correction factor. Nelson and Lorch (1974) and Lo et al. (1977) presented higher-order theories that have nine and eleven variables, respectively. Reddy (1984a) simplified the theory of Lo et al. by neglecting the transverse normal strain and satisfying zero transverse shear strains at the top and bottom surfaces of the plates. These assumptions further reduced the number of variables to five.

In the present study, we use Reddy's (1984b) higher-order shear-deformation theory. The theory is based on the assumptions of a cubic variation of in-plane displacements through the plate thickness and a vanishing of the transverse shear strains at the free faces of the plate. The plates under investigation are made of linearly elastic anisotropic constituents.

In this chapter, MACSYMA is used derive the nonlinear equations of motion for the dynamic response of thick rectangular laminates under harmonic transverse loads. The equations of motion are derived by using Hamilton's principle and are

applicable to any lamination scheme. Next a brief review of Reddy's plate theory is given.

2.2. The Displacement Field

We consider a rectangular plate with dimensions $a \times b$ and thickness h. The coordinate system is chosen in such a way that the x-y plane coincides with the mid-plane of the plate, and the z-axis is perpendicular to that plane as shown in Figure 2.1.

Elasticity solutions suggest a parabolic variation of the transverse shear stresses through the thickness of the plate. Reddy (1984c) introduced a displacement field that varies cubically with the thickness coordinate z and satisfies the criterion for the variation of the transverse shear stresses mentioned above. The displacements for the present theory, commonly known in the literature as the Kromm-Reddy refined higher-order shear-deformation plate theory, are assumed to be of the form

$$\begin{aligned} u_1(x,y,z,t) &= u(x,y,t) + z\psi_x(x,y,t) + z^2\xi_x(x,y,t) + z^3\eta_x(x,y,t) \\ u_2(x,y,z,t) &= v(x,y,t) + z\psi_y(x,y,t) + z^2\xi_y(x,y,t) + z^3\eta_y(x,y,t) \\ u_3(x,y,z,t) &= w(x,y,t) \end{aligned} \tag{2.1}$$

Here (u_1, u_2, u_3) denote the components of the displacement in the (x,y,z) directions, respectively; (u,v,w) are the displacements of a point on the mid-plane $(x,y,0)$ in the (x,y,z) directions, respectively, at time t ; ψ_x and ψ_y are the rotations of the normals to the mid-plane about the y and x axes, respectively (see Figure 2.2). In (2.1), u_1 and u_2 are expanded as cubic functions of z and u_3 is constant along z.

The condition that the transverse shear stresses (i.e., σ_{xz} and σ_{yz}) must vanish on the top and bottom faces of the plate is used to determine the unknown functions ξ_x, ξ_y, η_x, and η_y:

$$\sigma_5 = \sigma_{xz}(x,y,\pm\frac{h}{2},t) = 0, \quad \sigma_4 = \sigma_{yz}(x,y,\pm\frac{h}{2},t) = 0 \tag{2.2}$$

These stress-free boundary conditions require the corresponding strains (i.e., ε_{xz} and ε_{yz}) to be zero on the free surfaces of the plate. It follows from (2.1) that

$$\begin{aligned}\varepsilon_5 &= \varepsilon_{xz} = u_{1,z} + u_{3,x} = \psi_x + 2z\xi_x + 3z^2\eta_x + w_{,x}\\ \varepsilon_4 &= \varepsilon_{yz} = u_{2,z} + u_{3,y} = \psi_y + 2z\xi_y + 3z^2\eta_y + w_{,y}\end{aligned} \tag{2.3}$$

where the comma denotes partial differentiation. Setting $\varepsilon_5(x,y,\pm h/2,t)$ and $\varepsilon_4(x,y,\pm h/2,t)$ equal to zero, we obtain

$$\begin{aligned}&\xi_x \equiv \xi_y \equiv 0\\ &\eta_x = -\frac{4}{3h^2}(\psi_x + w_{,x})\\ &\eta_y = -\frac{4}{3h^2}(\psi_y + w_{,y})\end{aligned} \tag{2.4}$$

Now the displacement field given in (2.1) can be rewritten as

$$\begin{aligned}u_1 &= u + z\left[\psi_x - \frac{4}{3}\left(\frac{z}{h}\right)^2(\psi_x + w_{,x})\right]\\ u_2 &= v + z\left[\psi_y - \frac{4}{3}\left(\frac{z}{h}\right)^2(\psi_y + w_{,y})\right]\\ u_3 &= w\end{aligned} \tag{2.5}$$

2.3. Strain-Displacement Relations

The linear theory of small deflections of plates assumes infinitesimal displacements and provides accurate results only for very small displacements. However, when the deflections are the same order of magnitude as the thickness, the results are enormously inaccurate.

A well known theory for large deflections of plates that models the geometric nonlinearities is due to von Karman. In this theory, the basic assumption concerning the strains is that the displacements u, v, ψ_x, and ψ_y are infinitesimal. Moreover, in the strain-displacement relations only those nonlinear terms which depend on $w_{,x}$ and $w_{,y}$ are to be retained. All other nonlinear terms are to be neglected. Hence, the higher powers of the derivatives of u, v, ψ_x, and ψ_y are negligible in comparison with their first powers and the only nonlinear terms to be retained in the strains are the squares and products of $w_{,x}$ and $w_{,y}$. Following Reddy (1984b), we write the von Karman strains associated with the displacement field in equations (2.5) as

$$\begin{aligned}
\varepsilon_1 &= \varepsilon_1^0 + z(\kappa_1^0 + z^2\kappa_1^2) \\
\varepsilon_2 &= \varepsilon_2^0 + z(\kappa_2^0 + z^2\kappa_2^2) \\
\varepsilon_3 &= 0 \\
\varepsilon_4 &= \varepsilon_4^0 + z^2\kappa_4^2 \\
\varepsilon_5 &= \varepsilon_5^0 + z^2\kappa_5^2 \\
\varepsilon_6 &= \varepsilon_6^0 + z(\kappa_6^0 + z^2\kappa_6^2)
\end{aligned} \tag{2.6}$$

where

$$
\begin{aligned}
\varepsilon_1^0 &= u_{,x} + \frac{1}{2} w_{,x}^2 \\
\kappa_1^0 &= \psi_{x,x} \\
\kappa_1^2 &= \frac{-4}{3h^2} (\psi_{x,x} + w_{,xx}) \\
\varepsilon_2^0 &= v_{,y} + \frac{1}{2} w_{,y}^2 \\
\kappa_2^0 &= \psi_{y,y} \\
\kappa_2^2 &= \frac{-4}{3h^2} (\psi_{y,y} + w_{,yy}) \\
\varepsilon_4^0 &= \psi_y + w_{,y} \\
\kappa_4^2 &= \frac{-4}{h^2} (\psi_y + w_{,y}) \\
\varepsilon_5^0 &= \psi_x + w_{,x} \\
\kappa_5^2 &= \frac{-4}{h^2} (\psi_x + w_{,x}) \\
\varepsilon_6^0 &= u_{,y} + v_{,x} + w_{,x} w_{,y} \\
\kappa_6^0 &= \psi_{x,y} + \psi_{y,x} \\
\kappa_6^2 &= \frac{-4}{3h^2} (\psi_{x,y} + \psi_{y,x} + 2w_{,xy})
\end{aligned}
\tag{2.7}
$$

In equations (2.7), the ε_i^0 represent the reference surface-strains at z = 0 (i.e., the mid-plane strains), the κ_i^0 represent the usual linear plate curvatures, and the κ_i^2 represent the additional linear curvature components associated with the higher-order shear-deformation formulation. It is interesting to point out that the expressions $\kappa_i^2 (i = 1,2,6)$ contain higher-order derivatives of the transverse deflection w. Such terms are completely absent in the classical and first-order shear-deformation theories.

2.4. Constitutive Relations

The plate (laminate) is assumed to be composed of N perfectly bonded, thin orthotropic layers (laminae). The total thickness of the laminate is h. An arbitrary mth layer (m = 1,2,...,N) is oriented at an angle θ_m with respect to the plate coordinate axes. The constitutive equations for the mth layer can be written in terms of the material principal directions as

$$\begin{bmatrix} \bar{\sigma}_1 \\ \bar{\sigma}_2 \\ \bar{\sigma}_6 \end{bmatrix}_{(m)} = \begin{bmatrix} \bar{Q}_{11} & \bar{Q}_{12} & 0 \\ \bar{Q}_{12} & \bar{Q}_{22} & 0 \\ 0 & 0 & \bar{Q}_{66} \end{bmatrix}_{(m)} \begin{bmatrix} \bar{\varepsilon}_1 \\ \bar{\varepsilon}_2 \\ \bar{\varepsilon}_6 \end{bmatrix}_{(m)}, \text{ and } \begin{bmatrix} \bar{\sigma}_4 \\ \bar{\sigma}_5 \end{bmatrix}_{(m)} = \begin{bmatrix} \bar{Q}_{44} & 0 \\ 0 & \bar{Q}_{55} \end{bmatrix}_{(m)} \begin{bmatrix} \bar{\varepsilon}_4 \\ \bar{\varepsilon}_5 \end{bmatrix}_{(m)} \tag{2.8}$$

where the $\bar{\sigma}_i^m$ and the $\bar{\varepsilon}_i^m$ are the components of stress and strain, respectively, and the $\bar{Q}_{ij}^m$ are the plane-stress reduced stiffness coefficients in the material axes of the layer and are given by

$$\begin{aligned} &\bar{Q}_{11} = \frac{E_1}{1 - \nu_{12}\nu_{21}}, \bar{Q}_{12} = \frac{\nu_{12}E_2}{1 - \nu_{12}\nu_{21}}, \bar{Q}_{22} = \frac{E_2}{1 - \nu_{12}\nu_{21}}, \\ &\bar{Q}_{44} = G_{23}, \bar{Q}_{55} = G_{13}, \text{ and } \bar{Q}_{66} = G_{12} \end{aligned} \tag{2.9}$$

in which the E_i, ν_{ij}, and G_{ij} are Young's moduli, Poisson's ratios, and shear moduli, respectively, in the principal directions (i,j) of elasticity. The lamina stress-strain relations can be written in terms of the stresses and strains in the laminate coordinates as:

$$\begin{bmatrix}\sigma_1\\ \sigma_2\\ \sigma_6\end{bmatrix}_{(m)} = \begin{bmatrix}Q_{11} & Q_{12} & Q_{16}\\ Q_{12} & Q_{22} & Q_{26}\\ Q_{16} & Q_{26} & Q_{66}\end{bmatrix}_{(m)} \begin{bmatrix}\bar{\varepsilon}_1\\ \bar{\varepsilon}_2\\ \bar{\varepsilon}_6\end{bmatrix}_{(m)}, \text{ and } \begin{bmatrix}\sigma_4\\ \sigma_5\end{bmatrix}_{(m)} = \begin{bmatrix}Q_{44} & Q_{45}\\ Q_{45} & Q_{55}\end{bmatrix}_{(m)} \begin{bmatrix}\bar{\varepsilon}_4\\ \bar{\varepsilon}_5\end{bmatrix}_{(m)} \tag{2.10}$$

where $Q_{ij}^{(m)}$ are the transformed stiffness coefficients (material constants) and are given by

$$\begin{aligned}
Q_{11} &= \bar{Q}_{11}\cos^4\theta + 2(\bar{Q}_{12} + 2\bar{Q}_{66})\sin^2\theta\cos^2\theta + \bar{Q}_{22}\sin^4\theta\\
Q_{12} &= (\bar{Q}_{11} + \bar{Q}_{22} - 4\bar{Q}_{66})\sin^2\theta\cos^2\theta + \bar{Q}_{12}(\sin^4\theta + \cos^4\theta)\\
Q_{22} &= \bar{Q}_{11}\sin^4\theta + 2(\bar{Q}_{12} + 2\bar{Q}_{66})\sin^2\theta\cos^2\theta + \bar{Q}_{22}\cos^4\theta\\
Q_{16} &= (\bar{Q}_{11} - \bar{Q}_{12} - 2\bar{Q}_{66})\sin\theta\cos^3\theta + (\bar{Q}_{12} - \bar{Q}_{22} + 2\bar{Q}_{66})\sin^3\theta\cos\theta\\
Q_{26} &= (\bar{Q}_{11} - \bar{Q}_{12} - 2\bar{Q}_{66})\sin^3\theta\cos\theta + (\bar{Q}_{12} - \bar{Q}_{22} + 2\bar{Q}_{66})\sin\theta\cos^3\theta\\
Q_{66} &= (\bar{Q}_{11} + \bar{Q}_{22} - 2\bar{Q}_{12} - 2\bar{Q}_{66})\sin^2\theta\cos^2\theta + \bar{Q}_{66}(\sin^4\theta + \cos^4\theta)\\
Q_{44} &= \bar{Q}_{44}\cos^2\theta + \bar{Q}_{55}\sin^2\theta\\
Q_{45} &= (\bar{Q}_{55} - \bar{Q}_{44})\cos\theta\sin\theta\\
Q_{55} &= \bar{Q}_{55}\cos^2\theta + \bar{Q}_{44}\sin^2\theta
\end{aligned} \tag{2.11}$$

and θ is the angle between the x- and $\bar{x}$ –axes as shown in Figure 2.3.

2.5. *The Lagrangian*

In this section, the Lagrangian for a general laminated rectangular plate is formulated. Lagrange's equations of motion are derived from Hamilton's principle in the next section. It is necessary at this stage to obtain the Lagrangian which will be the basis for more general treatments. The Lagrangian approach provides an elegant

and powerful technique for solving a variety of nonlinear physical systems, as we shall see in the succeeding chapters. The expression for the plate kinetic energy is

$$T = \frac{1}{2}\int_{-h/2}^{h/2}\int_{A}\rho\left[\dot{u}_1^2 + \dot{u}_2^2 + \dot{u}_3^2\right]dA\,dz \tag{2.12}$$

where ρ is the density of the plate and A is the area of the plate. Substituting the expressions for u_1, u_2, and u_3 from equations (2.5) into equation (2.12), integrating along the z-direction, and rearranging the result, we obtain

$$\begin{aligned} T = \frac{1}{2}\int_{A}\Big\{ & I_1(\dot{u}^2 + \dot{v}^2 + \dot{w}^2) + \bar{I}_3\,(\dot{\psi}_x^2 + \dot{\psi}_y^2) \\ & + 2\bar{I}_2(\dot{u}\dot{\psi}_x + \dot{v}\dot{\psi}_y) - \frac{8}{3h^2}I_4(\dot{u}\dot{w}_{,x} + \dot{v}\dot{w}_{,y}) \\ & - \frac{8}{3h^2}\bar{I}_5(\dot{\psi}_x\dot{w}_{,x} + \dot{\psi}_y\dot{w}_{,y}) + \frac{16}{9h^4}\,I_7(\dot{w}_{,x}^2 + \dot{w}_{,y}^2)\Big\}dA \end{aligned} \tag{2.13}$$

where the I_i are generalized inertias and are defined as

$$I_i = \int_{-h/2}^{h/2}\rho z^{i-1}dz \quad i = 1,2,\ldots,7 \tag{2.14}$$

and

$$\begin{aligned} \bar{I}_2 &= I_2 - \frac{4}{3h^2}I_4 \\ \bar{I}_5 &= I_5 - \frac{4}{3h^2}I_7 \\ \bar{I}_3 &= I_3 - \frac{8}{3h^2}I_5 + \frac{16}{9h^4}I_7 \end{aligned} \tag{2.15}$$

The total potential energy consists of the strain energy of the elastic plate and the work done by the specified external transverse load denoted by Q. The potential energy is

$$V = \frac{1}{2}\int_{-h/2}^{h/2}\int_A (\sigma_1\varepsilon_1 + \sigma_2\varepsilon_2 + \sigma_6\varepsilon_6 + \sigma_4\varepsilon_4 + \sigma_5\varepsilon_5)dAdz - \int_A QwdA \tag{2.16}$$

Substituting equations (2.6) and (2.7) into equation (2.16) and integrating over the thickness of the plate, we obtain the following expression for the potential energy:

$$\begin{aligned} V = \frac{1}{2}\int_A \Big\{ & N_1(u_{,x} + \frac{1}{2}w_{,x}^2) + N_2(v_{,y} + \frac{1}{2}w_{,y}^2) + N_6(u_{,y} + v_{,x} + w_{,x}w_{,y}) \\ & + M_1\psi_{x,x} + M_2\psi_{y,y} + M_6(\psi_{x,y} + \psi_{y,x}) \\ & - \frac{4}{3h^2}[P_1(\psi_{x,x} + w_{,xx}) + P_2(\psi_{y,y} + w_{,yy}) + P_6(\psi_{x,y} + \psi_{y,x} + 2w_{,xy})] \\ & + (Q_2 - \frac{4}{h^2}R_2)(\psi_y + w_{,y}) + (Q_1 - \frac{4}{h^2}R_1)(\psi_x + w_{,x}) \Big\} - Q\,w\Big\}dA \end{aligned} \tag{2.17}$$

where the N_i, M_i, P_i, Q_i, and R_i are the stress resultants (see Figure 2.4) defined as

$$\begin{aligned} (N_i, M_i, P_i) &= \int_{-h/2}^{h/2} \sigma_i(1, z, z^3)dz \quad (i = 1,2,6) \\ (Q_2, R_2) &= \int_{-h/2}^{h/2} \sigma_4(1, z^2)dz \\ (Q_1, R_1) &= \int_{-h/2}^{h/2} \sigma_5(1, z^2)dz \end{aligned} \tag{2.18}$$

Here, the N_i are inplane (membrane) forces, M_1 and M_2 are bending moments, M_6 is a twisting moment, the Q_i are transverse shear forces, and the P_i and R_i are higher-order stress couples associated with the higher-order shear-deformation

formulation and cannot be physically interpreted. The stress resultants in equations (2.18) are related to the strains and curvatures in equations (2.7) by the following plate constitutive equations:

$$\begin{bmatrix} N_1 \\ N_2 \\ N_6 \\ M_1 \\ M_2 \\ M_6 \\ P_1 \\ P_2 \\ P_6 \end{bmatrix} = \begin{bmatrix} A_{11} & A_{12} & A_{16} & B_{11} & B_{12} & B_{16} & E_{11} & E_{12} & E_{16} \\ & A_{22} & A_{26} & & B_{22} & B_{26} & & E_{22} & E_{26} \\ sym & & A_{66} & sym & & B_{66} & sym & & E_{66} \\ & & & D_{11} & D_{12} & D_{16} & F_{11} & F_{12} & F_{16} \\ & & & & D_{22} & D_{26} & & F_{22} & F_{26} \\ & & & sym & & D_{66} & sym & & F_{66} \\ & & & & & & H_{11} & H_{12} & H_{16} \\ & & & & & & & H_{22} & H_{26} \\ sym & & & & & & sym & & H_{66} \end{bmatrix} \begin{bmatrix} \varepsilon_1^0 \\ \varepsilon_2^0 \\ \varepsilon_6^0 \\ \kappa_1^0 \\ \kappa_2^0 \\ \kappa_6^0 \\ \kappa_1^2 \\ \kappa_2^2 \\ \kappa_6^2 \end{bmatrix} \tag{2.19}$$

$$\begin{bmatrix} Q_2 \\ Q_1 \\ R_2 \\ R_1 \end{bmatrix} = \begin{bmatrix} A_{44} & A_{45} & D_{44} & D_{45} \\ sym & A_{55} & sym & D_{55} \\ & & F_{44} & F_{45} \\ sym & & sym & F_{55} \end{bmatrix} \begin{bmatrix} \varepsilon_4^0 \\ \varepsilon_5^0 \\ \kappa_4^2 \\ \kappa_5^2 \end{bmatrix} \tag{2.20}$$

where the plate stiffness values are defined by

$$\begin{aligned} (A_{ij}, B_{ij}, D_{ij}, E_{ij}, F_{ij}, H_{ij}) &= \int_{-h/2}^{h/2} Q_{ij}(1, z, z^2, z^3, z^4, z^6)dz \\ &= \sum_{m=1}^{N} \int_{z_m}^{z_{m+1}} Q_{ij}^{(m)}(1, z, z^2, z^3, z^4, z^6)dz \quad (i,j = 1,2,6) \end{aligned} \tag{2.21}$$

$$(A_{ij}, D_{ij}, F_{ij}) = \int_{-h/2}^{h/2} Q_{ij}(1, z^2, z^4)dz$$
$$= \sum_{m=1}^{N} \int_{z_m}^{z_{m+1}} Q_{ij}^{(m)}(1, z^2, z^4)dz \quad (i,j = 4,5) \tag{2.22}$$

or

$$A_{ij} = \sum_{m=1}^{N} Q_{ij}^{(m)}(z_{m+1} - z_m) \quad (i,j = 1,2,6 \text{ and } i,j = 4,5) \tag{2.23a}$$

$$B_{ij} = \frac{1}{2} \sum_{m=1}^{N} Q_{ij}^{(m)}(z_{m+1}^2 - z_m^2) \quad (i,j = 1,2,6) \tag{2.23b}$$

$$D_{ij} = \frac{1}{3} \sum_{m=1}^{N} Q_{ij}^{(m)}(z_{m+1}^3 - z_m^3) \quad (i,j = 1,2,6 \text{ and } i,j = 4,5) \tag{2.23c}$$

$$E_{ij} = \frac{1}{4} \sum_{m=1}^{N} Q_{ij}^{(m)}(z_{m+1}^4 - z_m^4) \quad (i,j = 1,2,6) \tag{2.23d}$$

$$F_{ij} = \frac{1}{5} \sum_{N}^{m=1} Q_{ij}^{(m)}(z_{m+1}^5 - z_m^5) \quad (i,j = 1,2,6 \text{ and } i,j = 4,5) \tag{2.23e}$$

$$H_{ij} = \frac{1}{7} \sum_{m=1}^{N} Q_{ij}^{(m)}(z_{m+1}^7 - z_m^7) \quad (i,j = 1,2,6) \tag{2.23f}$$

where N is the total number of layers in the laminate and (z_m, z_{m+1}) are the z-coordinates of the bottom and top of the mth layer (see Figure 2.5). The Lagrangian L is the difference between the kinetic and potential energies given in equations (2.13) and (2.17), respectively; that is,

$$L = T - V \tag{2.24}$$

2.6. Equations of Motion

Hamilton's principle (see, e.g., Meirovitch, 1980) is used to derive the general nonlinear equations of motion and boundary conditions of the plate. The principle is stated in mathematical form as

$$\int_0^{t_1} \delta L dt = 0 \quad \text{for } 0 \leq x \leq a, 0 \leq y \leq b \tag{2.25}$$

where δL is a function of $\delta u, \delta v, \delta w, \delta \psi_x$, and $\delta \psi_y$, which are arbitrary virtual displacements and should be set equal to zero at times $t = 0$ and $t = t_1$ in the domain (i.e., the mid-plane) of the plate. Substituting for L in equation (2.25), we obtain

$$
\begin{aligned}
0 = -\int_0^t \int_A \{ & N_1(\delta u_{,x} + w_{,x}\delta w_{,x}) + N_2\,(\delta v_{,y} + w_{,y}\delta w_{,y}) \\
& + N_6(\delta u_{,y} + \delta v_{,x} + w_{,x}\delta w_{,y} + \delta w_{,x} w_{,y}) \\
& + M_1 \delta\psi_{x,x} + M_2 \delta\psi_{y,y} + M_6(\delta\psi_{x,y} + \delta\psi_{y,x}) \\
& - \frac{4}{3h^2}\,[P_1(\delta\psi_{x,x} + \delta w_{,xx}) + P_2(\delta\psi_{y,y} + \delta w_{,yy}) \\
& + P_6\,(\delta\psi_{x,y} + \delta\psi_{y,x} + 2\delta w_{,xy})] \\
& + (Q_2 - \frac{4}{h^2} R_2)(\delta\psi_y + \delta w_{,y}) \\
& + (Q_1 - \frac{4}{h^2} R_1)\,(\delta\psi_x + \delta w_{,x}) + Q\delta w\} dx dy dt \\
& - \int_0^t \int_A \Big\{ \delta u \Big[I_1 \ddot{u} + \bar{I}_2 \ddot{\psi}_x - \frac{4}{3h^2} I_4 \ddot{w}_{,x} \Big] \\
& + \delta v \Big[I_1 \ddot{v} + \bar{I}_2 \ddot{\psi}_y - \frac{4}{3h^2} I_4 \ddot{w}_{,y} \Big] \\
& + \delta w \Big[I_1 \ddot{w} - \frac{16}{9h^4} I_7 (\ddot{w}_{,xx} + \ddot{w}_{,yy}) \\
& + \frac{4}{3h^2} I_4 (\ddot{u}_{,x} + \ddot{v}_{,y}) + \frac{4}{3h^2} \bar{I}_5 (\ddot{\psi}_{x,x} + \ddot{\psi}_{y,y}) \Big] \\
& + \delta\psi_x \Big[\bar{I}_2 \ddot{u} + \bar{I}_3 \ddot{\psi}_x - \frac{4}{3h^2} \bar{I}_5 \ddot{w}_{,x} \Big] \\
& + \delta\psi_y \Big[\bar{I}_2 \ddot{v} + \bar{I}_3 \ddot{\psi}_y - \frac{4}{3h^2} \bar{I}_5 \ddot{w}_{,y} \Big] \Big\} dx dy dt
\end{aligned}
\tag{2.26}
$$

Carrying out the integration by parts and setting each of the coefficients of $\delta u, \delta v, \delta w, \delta\psi_x$, and $\delta\psi_y$ independently equal to zero, we obtain the following equations of motion

$$
\delta u\colon\ N_{1,x} + N_{6,y} = I_1 \ddot{u} + \bar{I}_2 \ddot{\psi}_x - \frac{4}{3h^2} I_4 \ddot{w}_{,x} \tag{2.27}
$$

$$
\delta v\colon\ N_{6,x} + N_{2,y} = I_1 \ddot{v} + \bar{I}_2 \ddot{\psi}_y - \frac{4}{3h^2} I_4 \ddot{w}_{,y} \tag{2.28}
$$

$$
\begin{aligned}
\delta w:\ & Q_{1,x} + Q_{2,y} + N_{1,x}w_{,x} + N_1 w_{,xx} + N_{6,x}w_{,y} \\
& + 2N_6 w_{,xy} + N_{6,y}w_{,x} + N_{2,y}w_{,y} + N_2 w_{,yy} \\
& - \frac{4}{h^2}(R_{1,x} + R_{2,y}) + \frac{4}{3h^2}(P_{1,xx} + 2P_{6,xy} + P_{2,yy}) - Q \\
& = I_1 \ddot{w} - \frac{16}{9h^4} I_7(\ddot{w}_{,xx} + \ddot{w}_{,yy}) + \frac{4}{3h^2} I_4(\ddot{u}_{,x} + \ddot{v}_{,y}) \\
& + \frac{4}{3h^2} \bar{I}_5(\ddot{\psi}_{x,x} + \ddot{\psi}_{y,y})
\end{aligned}
\tag{2.29}
$$

$$
\begin{aligned}
\delta\psi_x:\ & M_{1,x} + M_{6,y} - Q_1 + \frac{4}{h^2} R_1 - \frac{4}{3h^2}(P_{1,x} + P_{6,y}) \\
& = \bar{I}_2 \ddot{u} + \bar{I}_3 \ddot{\psi}_x - \frac{4}{3h^2} \bar{I}_5 \ddot{w}_{,x}
\end{aligned}
\tag{2.30}
$$

$$
\begin{aligned}
\delta\psi_y:\ & M_{6,x} + M_{2,y} - Q_2 + \frac{4}{h^2} R_2 - \frac{4}{3h^2}(P_{6,x} + P_{2,y}) \\
& = \bar{I}_2 \ddot{u} + \bar{I}_3 \ddot{\psi}_y - \frac{4}{3h^2} \bar{I}_5 \ddot{w}_{,y}
\end{aligned}
\tag{2.31}
$$

The general boundary conditions are to be specified as only one of each of the following pairs (see Figure 2.4):

$$
\begin{aligned}
& u_n = un_x + vn_y \ \text{ or } \ N_n = N_1 n_x^2 + N_2 n_y^2 + 2N_6 n_x n_y \\
& u_{ns} = -un_y + vn_x \ \text{ or } \ N_{ns} = (N_2 - N_1) n_x n_y + N_6(n_x^2 - n_y^2) \\
& w \ \text{ or } \ Q_n = \hat{Q}_1 n_x + \hat{Q}_2 n_y + \frac{4}{3h^2}(P_{ns,s} + P_{n,n}) \\
& w_{,n} \ \text{ or } \ P_n \\
& \psi_n \ \text{ or } \ M_n = \hat{M}_1 n_x^2 + \hat{M}_2 n_y^2 + 2\hat{M}_6 n_x n_y \\
& \psi_{ns} \ \text{ or } \ M_{ns} = (\hat{M}_2 - \hat{M}_1) n_x n_y + \hat{M}_6(n_x^2 - n_y^2)
\end{aligned}
\tag{2.32}
$$

where

$$\hat{M}_i = M_i - \frac{4}{3h^2} P_i \quad (i = 1,2,6),$$
$$\hat{Q}_i = Q_i - \frac{4}{3h^2} R_i \quad (i = 1,2), \tag{2.33}$$
$$\frac{\partial}{\partial n} = n_x \frac{\partial}{\partial x} + n_y \frac{\partial}{\partial y}, \frac{\partial}{\partial s} = n_x \frac{\partial}{\partial y} + n_y \frac{\partial}{\partial x}$$

The expressions for P_n and P_{ns} are similar to those of N_n and N_{ns}.

In equations (2.27)-(2.31), the terms containing $\ddot{u}$ and $\ddot{v}$ arise from the inplane inertia forces and those containing $\ddot{\psi}_x$ and $\ddot{\psi}_y$ arise from the shear-deformation inertia forces, which do not have counterparts in the classical plate theory. The term $I_1\ddot{w}$ in equation (2.29) is the transverse inertia term which also exists in the classical plate theory. The terms containing $\ddot{w}_{,x}$, $\ddot{w}_{,y}$ arise from the rotary-inertia effects and are analogous to those in the classical plate theory, and those of the form $\ddot{\psi}_{x,x}$ and $\ddot{\psi}_{y,y}$ arise from the shear-deformation rotary-inertia effects and are absent in the classical plate theory. The terms $\ddot{u}_{,x}$ and $\ddot{v}_{,y}$ in equation (2.29) are new inplane rotary inertia terms that add more to the dynamic coupling of equations (2.27)-(2.31). The higher-order rotary-inertia terms in equation (2.29), namely $\ddot{w}_{,xx}$ and $\ddot{w}_{,yy}$, are also new and important additional terms that the higher-order shear-deformation theory accounts for.

In equation (2.29), the terms $N_1w_{,xx}$, $N_2w_{,yy}$, and $2N_6w_{,xy}$ are curvature terms (Hermann, 1955) that account for the change of direction of an element due to curvature effects while the terms $N_{1,x}w_{,x}$, $N_{2,y}w_{,y}$, $N_{6,x}w_{,y}$, and $N_{6,y}w_{,x}$ can be identified as buoyancy terms (Biot, 1939) due to the "deformation of an element in its own stress field and depend on the stress gradient". Many of the inertia terms in equations (2.27)-(2.31) vanish for certain types of laminates in which the coefficients $\bar{I}_2$ and I_4 are identically zero as, e.g., in the case of antisymmetric cross-ply laminates.

2.7. The Case of Cylindrical Bending

Here, we follow Whitney and Pagano (1970) and consider a laminate composed of an arbitrary number of orthotropic layers such that their various axes of material symmetry form angles θ_m with the x-y axes of the plate. In addition, we assume a state of plane strain in which the plate is of infinite length in the y-direction (see Figure 2.6), uniformly supported along the edges x = 0 and a, and subjected to the transverse loading Q = Q (x). Under these conditions, the deformed surface of the plate is cylindrical. These conditions reduce the number of equations of motion from five (unknowns: u,v, w, ψ_x, and ψ_y) to only three (unknowns: u,w, and ψ_x). In essence the cylindrical-bending assumption reduces the governing equations to those of a beam-type structure and hence the term "plate strips in cylindrical bending" is widely used in the literature.

The displacements of the plate strip are functions of x only; that is,

$$v = \psi_y = 0,\ u = u(x),\ \psi_x = \psi_x(x),\ \text{and}\ w = w(x) \tag{2.34}$$

We now write the Lagrangian as

$$\begin{aligned} L = \frac{1}{2}\int_x \Big\{ & I_1(\dot{u}^2 + \dot{w}^2) + \bar{I}_3\dot{\psi}_x^2 + 2\bar{I}_2\dot{u}\dot{\psi}_x - \frac{8}{3h^2} I_4\dot{u}\dot{w}_{,x} \Big] \\ & - \frac{8}{3h^2}\ \bar{I}_5\dot{\psi}_x\dot{w}_{,x} + \frac{16}{9h^4} I_7\dot{w}_{,x}^2 \Big\} dx \\ & - \frac{1}{2}\int \Big\{ N_1(u_{,x} + \frac{1}{2} w_{,x}^2) + M_1\psi_{x,x} - \frac{4}{3h^2} P_1(\psi_{x,x} + w_{,xx}) \\ & + (Q_1 - \frac{4}{h^2} R_1)(\psi_x + w_{,x}) - Qw \} dx \end{aligned} \tag{2.35}$$

Equations (2.27)-(2.31) reduce to the following:

$$\delta u\colon\ N_{1,x} = I_1\ddot{u} + \bar{I}_2\ddot{\psi}_x - \frac{4}{3h^2} I_4\ddot{w}_{,x} \tag{2.36}$$

$$\begin{aligned}\delta w\colon\ & Q_{1,x} + N_{1,x}w_{,x} + N_1 w_{,xx} - \frac{4}{h^2} R_{1,x} + \frac{4}{3h^2} P_{1,xx} + Q \\ & = I_1\ddot{w} - \frac{16}{9h^4} I_7\ddot{w}_{,xx} + \frac{4}{3h^2} I_4\ddot{u}_{,x} + \frac{4}{3h^2}\bar{I}_5\ddot{\psi}_{x,x}\end{aligned} \tag{2.37}$$

$$\delta\psi_x\colon\ M_{1,x} - Q_1 + \frac{4}{h^2} R_1 - \frac{4}{3h^2} P_{1,x} = \bar{I}_2\ddot{u} + \bar{I}_3\ddot{\psi}_x - \frac{4}{3h^2}\bar{I}_5\ddot{w}_{,x} \tag{2.38}$$

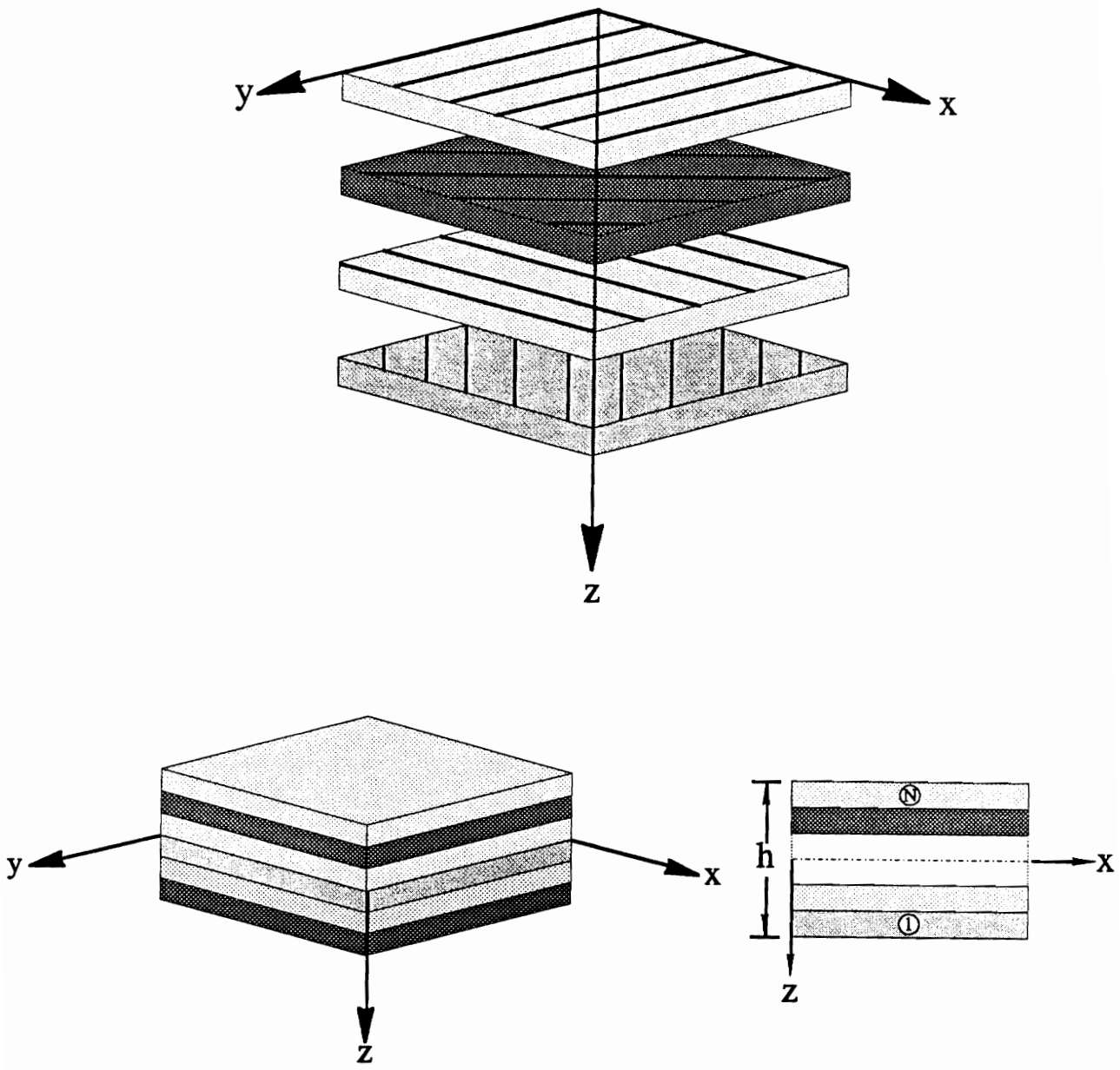

Figure 2.1. Laminated plate construction: layers lay out, geometry, and coordinate system.

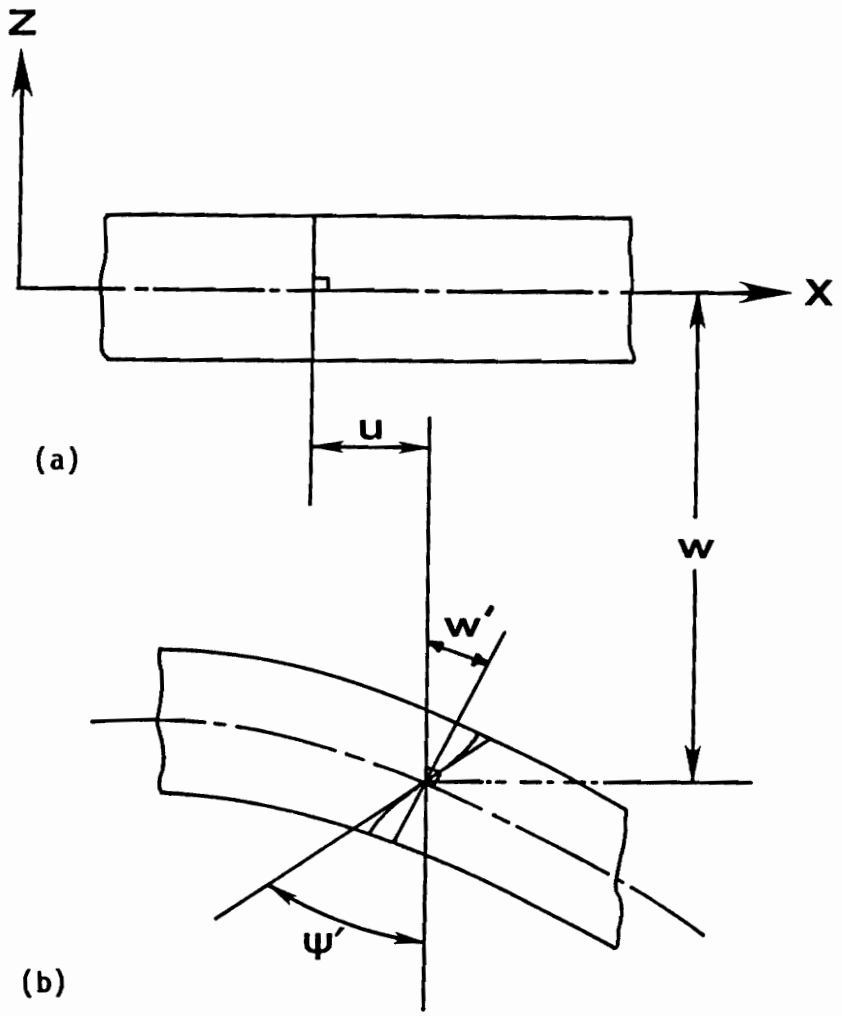

Figure 2.2. Geometry of deformation of a typical cross-section of the plate at y = constant (i.e., the x-z plane); (a) undeformed cross-section and (b) deformed cross-section.

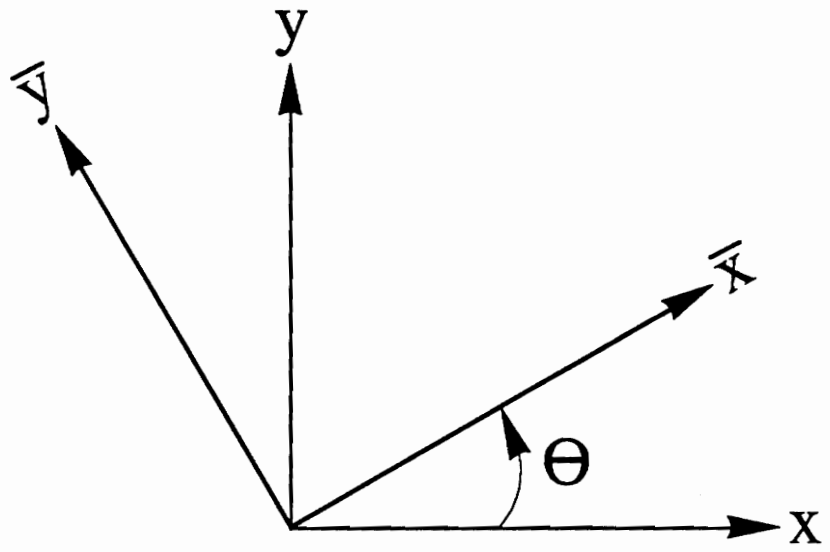

Figure 2.3. Coordinate transformation in the x-y plane due to a $\theta°$ rotation about the z-axis: x and y are the laminate coordinates and $\bar{x}$ and $\bar{y}$ are the lamina (or material) coordinates.

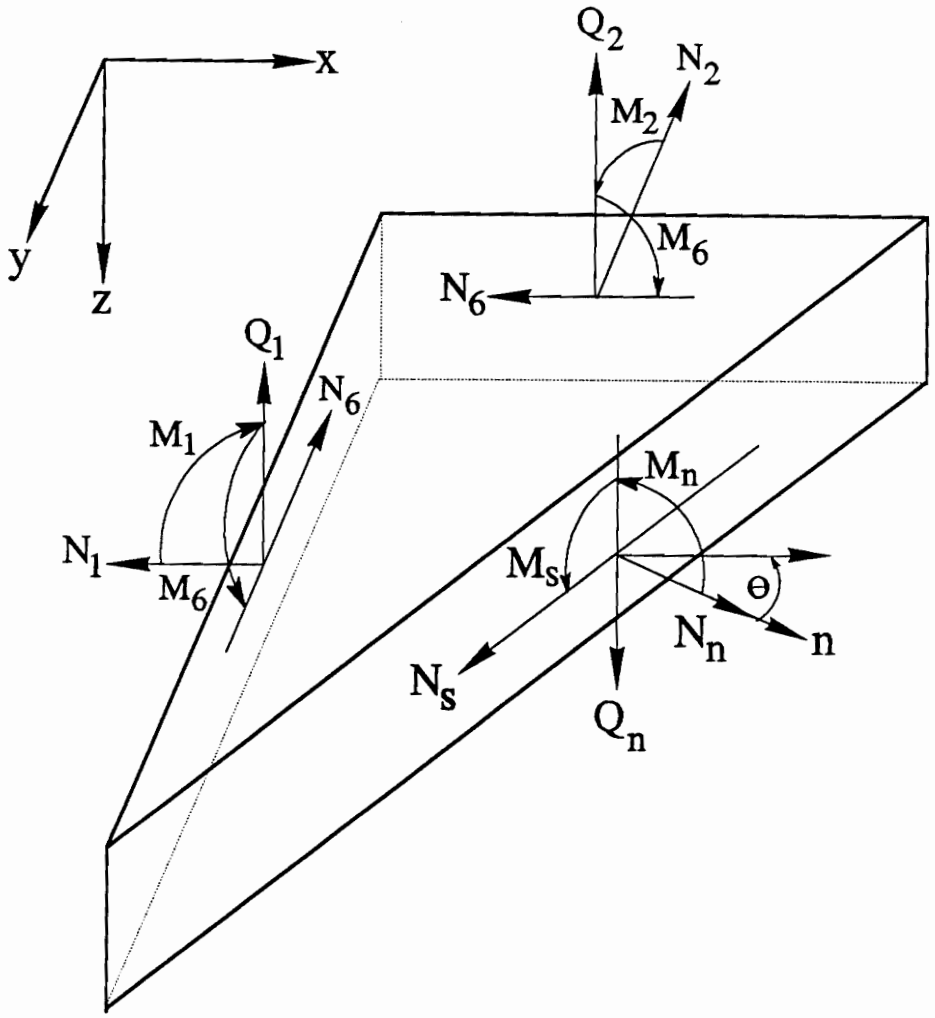

Figure 2.4. General natural boundary conditions (force and moment resultants): (1) at a point located on an edge whose normal is oriented at an angle θ to the x-axis and (2) at a point located on an edge whose normal is at a right angle to either the x-axis or the y-axis.

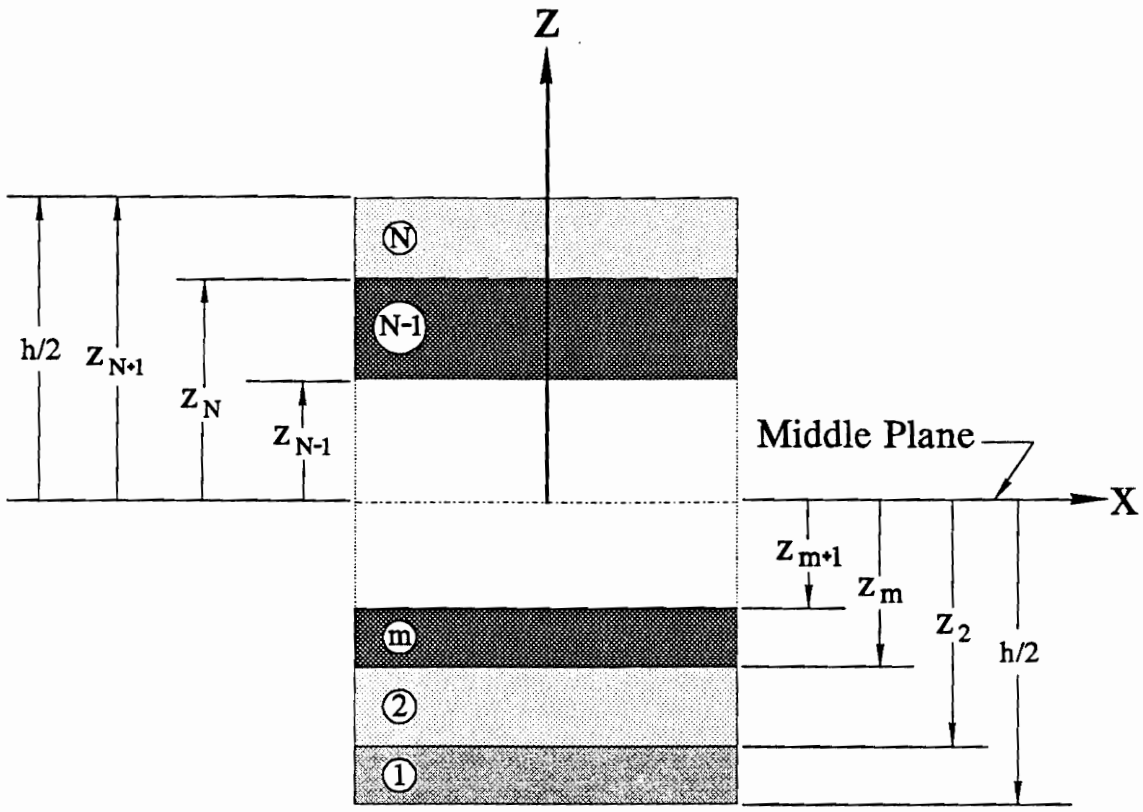

Figure 2.5. Thickness-geometry of a laminate consisting of N layers: layer coordinates in the laminate coordinate system.

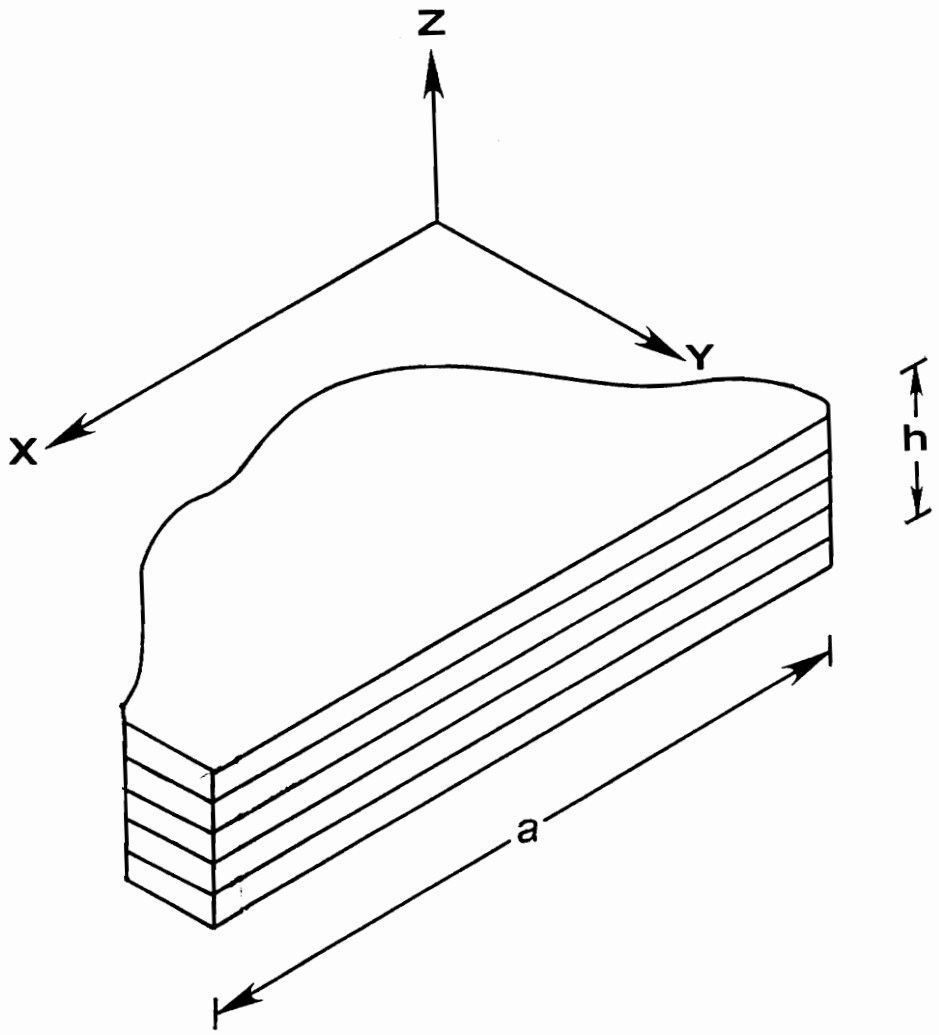

Figure 2.6. Geometry and coordinate system of a laminated plate strip in cylindrical bending.

3. LINEAR ANALYSIS

In the previous chapter, the nonlinear equations of motion of arbitrarily laminated plates have been derived by using a higher-order shear-deformation theory. In this chapter, we perform a linear analysis of the free vibrations of such laminates. This analysis will be used in Chapter 5 where a nonlinear study of the vibration characteristics is performed. We shall confine ourselves to the case of antisymmetric cross-ply laminates. The types of loads under consideration are uniform transverse harmonic loads. The boundary conditions are assumed to be simply supported. Attention is paid to the solutions for the case of plate strips in cylindrical bending. The free-vibration problem is first solved by using a Navier's type solution and the natural undamped frequencies and mode shapes are calculated. At the end of the chapter, we use the state-space concept to solve exactly the linear dynamic equations for the case of cylindrical bending.

3.1. Antisymmetric Cross-Ply Plates

An antisymmetric cross-ply laminate consists of an even number of orthotropic layers with orthotropic axes of symmetry in each layer alternately oriented at angles of 0° and 90° with the plate axes. The orientation of the fibers in the odd layers coincides with the x-axis while the orientation of those in the even layers coincides with the y-axis. All the layers, odd and even, have the same thickness and are made of the same orthotropic material. Because of this special stacking sequence, some of the plate inertias and stiffness coefficients vanish, namely,

$$I_2 = I_4 = \bar{I}_2 = 0 \tag{3.1a}$$

$$\begin{aligned} A_{16} = A_{26} = A_{45} = B_{12} = B_{16} = B_{26} = B_{66} = D_{16} = D_{26} = D_{45} \\ = E_{12} = E_{16} = E_{26} = E_{66} = F_{16} = F_{26} = F_{45} = H_{16} = H_{26} = 0 \end{aligned} \tag{3.1b}$$

Moreover, the following relations exist

$$\begin{aligned} A_{11} = A_{22}\,,\ A_{44} = A_{55}\,,\ B_{22} = -B_{11}\,,\ D_{11} = D_{22}\,,\ D_{44} = D_{55}, \\ E_{22} = -E_{11}\,,\ F_{11} = F_{22}\,,\ F_{44} = F_{55}\,,\ H_{11} = H_{22} \end{aligned} \tag{3.2}$$

3.2. Plate Equations in Terms of Displacements

The differential equations governing the vibrations of a general laminated plate were derived in Chapter 2. They were expressed in terms of force, moment, and shear resultants which can be subsequently expressed in terms of the displacements

u, v, w, ψ_x, and ψ_y and the plate stiffnesses A_{ij}, B_{ij}, E_{ij}, D_{ij}, F_{ij}, and H_{ij}. This alternative form of the equations is easily generated by using the MACSYMA code that we developed and is very convenient for obtaining exact closed-form solutions to certain lamination schemes.

For the case of antisymmetric cross-ply laminates, we obtain the following system of nonlinear governing equations:

$$\begin{aligned} &-A_{11}u_{,xx} - A_{66}u_{,yy} - (A_{12}+A_{66})v_{,xy} + c_1E_{11}w_{,xxx} - (B_{11}-c_1E_{11})\psi_{x,xx} \\ &\qquad = -I_1\ddot{u} + A_{11}w_{,x}w_{,xx} + (A_{12}+A_{66})w_{,y}w_{,xy} + A_{66}w_{,x}w_{,yy} \end{aligned} \tag{3.3}$$

$$\begin{aligned} &-A_{11}v_{,yy} - A_{66}v_{,xx} - (A_{12}+A_{66})u_{,xy} - c_1E_{11}w_{,yyy} + (B_{11}-c_1E_{11})\psi_{y,yy} \\ &\qquad = -I_1\ddot{v} + A_{11}w_{,y}w_{,yy} + (A_{12}+A_{66})w_{,x}w_{,xy} + A_{66}w_{,y}w_{,xx} \end{aligned} \tag{3.4}$$

$$\begin{aligned} &c_1^2H_{11}(w_{,xxxx}+w_{,yyyy}) + 2c_1^2(H_{12}+2H_{66})w_{,xxyy} + c_1E_{11}(u_{,xxx}+v_{,yyy}) \\ &\quad - c_1(F_{11}-c_1H_{11})(\psi_{x,xxx}+\psi_{y,yyy}) \\ &\quad - c_1(F_{12}+2F_{66}-c_1H_{12}-2c_1H_{66})(\psi_{x,xyy}+\psi_{y,xxy}) \\ &\quad - (A_{44}-2c_2D_{44}+c_2^2F_{44})(w_{,xx}+w_{,yy}+\psi_{x,x}+\psi_{y,y}) \\ &\quad = Q - I_1\ddot{w} + c_1^2I_7(\ddot{w}_{,xx}+\ddot{w}_{,yy}) - c_1\bar{I}_5(\ddot{\psi}_{x,x}+\ddot{\psi}_{y,y}) \\ &\quad + A_{11}(v_{,y}w_{,yy} + w_{,y}v_{,yy} + u_{,x}w_{,xx} + w_{,x}u_{,xx}) \\ &\quad + A_{12}(u_{,x}w_{,yy} + u_{,xy}w_{,y} + v_{,y}w_{,xx} + v_{,xy}w_{,x}) \\ &\quad + A_{66}(v_{,xx}w_{,y} + u_{,xy}w_{,y} + 2v_{,x}w_{,xy} + 2u_{,y}w_{,xy} + v_{,xy}w_{,x} + u_{,yy}w_{,x}) \\ &\quad + (B_{11}-c_1E_{11})(-\psi_{y,y}w_{,yy} - \psi_{y,yy}w_{,y} + \psi_{x,x}w_{,xx} + \psi_{x,xx}w_{,x}) \\ &\quad + \frac{3}{2}A_{11}(w_{,xx}w_{,x}^2 + w_{,yy}w_{,y}^2) \\ &\quad + (\frac{1}{2}A_{11} + A_{66})(w_{,xx}w_{,y}^2 + w_{,yy}w_{,x}^2) \\ &\quad + 2(A_{12}+2A_{66})w_{,x}w_{,y}w_{,xy} \end{aligned} \tag{3.5}$$

$$
\begin{aligned}
&- c_1(F_{11} - c_1H_{11})w_{,xxx} - c_1(F_{12} + 2F_{66} - c_1H_{12} - 2c_1H_{66})w_{,xyy} \\
&\quad - (A_{44} - 2c_2D_{44} + c_2^2F_{44})(w_{,x} + \psi_x) + (B_{11} - c_1E_{11})u_{,xx} \\
&\quad + (D_{12} + D_{66} + c_1^2H_{12} + c_1^2H_{66} - 2c_1F_{12} - 2c_1F_{66})\psi_{y,xy} \\
&\quad + (D_{66} + c_1^2H_{66} - 2c_1F_{66})\psi_{x,yy} + (D_{11} + c_1^2H_{11} - 2c_1F_{11})\psi_{x,xx} \\
&\quad = -\bar{I}_3\ddot{\psi}_x + c_1\bar{I}_5\ddot{w}_{,x} - (B_{11} - c_1E_{11})w_{,x}w_{,xx}
\end{aligned}
\tag{3.6}
$$

$$
\begin{aligned}
&c_1(F_{11} - c_1H_{11})w_{,yyy} + c_1(F_{12} + 2F_{66} - c_1H_{12} - 2c_1H_{66})w_{,xxy} \\
&\quad + (A_{44} - 2c_2D_{44} + c_2^2F_{44})(w_{,y} - \psi_y) + (B_{11} - c_1E_{11})v_{,yy} \\
&\quad - (D_{12} + D_{66} + c_1^2H_{12} + c_1^2H_{66} - 2c_1F_{12} - 2c_1F_{66})\psi_{x,xy} \\
&\quad - (D_{66} - c_1^2H_{66} - 2c_1F_{66})\psi_{y,xx} - (D_{11} - 2c_1F_{11} + c_1^2H_{11})\psi_{y,yy} \\
&\quad = \bar{I}_3\ddot{\psi}_y + c_1\bar{I}_5\ddot{w}_{,y} - (B_{11} - c_1E_{11})w_{,y}w_{,yy}
\end{aligned}
\tag{3.7}
$$

where

$$
c_1 = \frac{4}{3h^2} \quad \text{and} \quad c_2 = \frac{4}{h^2} \tag{3.8}
$$

For the case of simply-supported edge conditions (see Figure 3.1), the following boundary conditions are applicable:

$$
v = w = \psi_y = N_1 = M_1 = P_1 = 0 \quad \text{at} \quad x = 0,a \tag{3.9}
$$

$$
u = w = \psi_x = N_2 = M_2 = P_2 = 0 \quad \text{at} \quad y = 0,b \tag{3.10}
$$

The force and moment resultants can be expressed in terms of the five displacements and the plate stiffnesses as

$$
N_1 = A_{11}(u_{,x} + \frac{1}{2}w_{,x}^2) + A_{12}(v_{,y} + \frac{1}{2}w_{,y}^2) + B_{11}\psi_{x,x} - c_1E_{11}(w_{,xx} + \psi_{x,x}) \tag{3.11}
$$

$$M_1 = B_{11}(u_{,x} + \frac{1}{2} w_{,x}^2) + D_{11}\psi_{x,x} + D_{12}\psi_{y,y} - c_1 F_{11}(w_{,xx} + \psi_{x,x}) - c_1 F_{12}(w_{,yy} + \psi_{y,y}) \quad (3.12)$$

$$P_1 = E_{11}(u_{,x} + \frac{1}{2} w_{,x}^2) - c_1 H_{11}(w_{,xx} + \psi_{x,x}) - c_1 H_{12}(w_{,yy} + \psi_{y,y}) + F_{11}\psi_{x,x} + F_{12}\psi_{y,y} \quad (3.13)$$

$$N_2 = A_{11}(v_{,y} + \frac{1}{2} w_{,y}^2) + A_{12}(u_{,x} + \frac{1}{2} w_{,x}^2) - B_{11}\psi_{y,y} + c_1 E_{11}(w_{,yy} + \psi_{y,y}) \quad (3.14)$$

$$M_2 = -B_{11}(v_{,y} + \frac{1}{2} w_{,y}^2) + D_{11}\psi_{y,y} + D_{12}\psi_{x,x} - c_1 F_{11}(w_{,yy} + \psi_{y,y}) - c_1 F_{12}(w_{,xx} + \psi_{x,x}) \quad (3.15)$$

$$P_2 = -E_{11}(v_{,y} + \frac{1}{2} w_{,y}^2) - c_1 H_{11}(w_{,yy} + \psi_{y,y}) - c_1 H_{12}(w_{,xx} + \psi_{x,x}) + F_{11}\psi_{y,y} + F_{12}\psi_{x,x} \quad (3.16)$$

3.3. Cylindrical Bending

For antisymmetric cross-ply laminates, equations (3.3)-(3.7) become

$$-A_{11}u_{,xx} + c_1 E_{11} w_{,xxx} - (B_{11} - c_1 E_{11})\psi_{x,xx} = -I_1 \ddot{u} + A_{11} w_{,x} w_{,xx} \quad (3.17)$$

$$\begin{aligned} & c_1^2 H_{11} w_{,xxxx} + c_1 E_{11} u_{,xxx} - c_1 (F_{11} - c_1 H_{11})\psi_{x,xxx} \\ & \quad - (A_{44} - 2c_2 D_{44} + c_2^2 F_{44})(w_{,xx} + \psi_{x,x}) - Q \\ & \quad = -I_1 \ddot{w} + c_1^2 I_7 \ddot{w}_{,xx} - c_1 \bar{I}_5 \ddot{\psi}_{x,x} \\ & \quad + A_{11}(u_{,x} w_{,xx} + w_{,x} u_{,xx}) \\ & \quad + (B_{11} - c_1 E_{11})(\psi_{x,x} w_{,xx} + \psi_{x,xx} + w_{,x}) \\ & \quad + \frac{3}{2} A_{11} w_{,xx} w_{,x}^2 \end{aligned} \quad (3.18)$$

$$
\begin{aligned}
&- c_1(F_{11} - c_1H_{11})w_{,xxx} - (A_{44} - 2c_2D_{44} + c_2^2F_{44})(w_{,x} + \psi_x) \\
&\quad + (B_{11} - c_1E_{11})u_{,xx} + (D_{11} + c_1^2H_{11} - 2c_1F_{11})\psi_{x,xx} \\
&\quad = -\bar{I}_3\ddot{\psi}_x + c_1\bar{I}_5\ddot{w}_{,x} - (B_{11} - c_1E_{11})w_{,x}w_{,xx}
\end{aligned} \tag{3.19}
$$

Again, for simple supports the boundary conditions that should be considered are

$$
w = N_1 = M_1 = P_1 = 0 \quad \text{at} \quad x = 0,\ a \tag{3.20}
$$

The stress resultants in equations (3.11)-(3.16) reduce to the following:

$$
N_1 = A_{11}(u_{,x} + \frac{1}{2}w_{,x}^2) + B_{11}\psi_{x,x} - c_1E_{11}(w_{,xx} + \psi_{x,x}) \tag{3.21}
$$

$$
M_1 = B_{11}(u_{,x} + \frac{1}{2}w_{,x}^2) + D_{11}\psi_{x,x} - c_1F_{11}(w_{,xx} + \psi_{x,x}) \tag{3.22}
$$

$$
P_1 = E_{11}(u_{,x} + \frac{1}{2}w_{,x}^2) - c_1H_{11}(w_{,xx} + \psi_{x,x}) + F_{11}\psi_{x,x} \tag{3.23}
$$

3.4. Dynamic Response

In the foregoing developments, it is assumed that the plate (plate-strip) is restrained against rigid-body motion and that an external transverse load per unit area $Q(x,y,t)$ is applied at the top surface of the plate (plate-strip). Moreover, the load $Q(x,y,t)$ is assumed to be given explicitly in terms of its spatial and temporal variation. The case in which the plate is subjected to uniform in-plane edge-loads T_{xx} and T_{yy} applied in the directions x and y, respectively, can be easily considered by adding to Q the following extra terms:

$$\hat{Q} = T_{xx}w_{,xx} + T_{yy}w_{,yy} \tag{3.24}$$

The inclusion of the above terms is essential to the study of buckling of plates, which is not considered in this dissertation.

In this chapter (and also in Chapter 5), the numerical results are carried out for antisymmetric cross-ply laminates (0°/90°/0°/90°/...). The geometrical and material properties are the same for all layers. The following material properties are used:

$E_1 = 19.260 \times 10^6$ psi
$E_2 = 1.560 \times 10^6$ psi
$G_{12} = 0.820 \times 10^6$ psi
$G_{13} = 0.820 \times 10^6$ psi
$G_{23} = 0.523 \times 10^6$ psi
$\nu_{12} = 0.244$
$\rho = 0.00012\ \text{lb} - \text{s}^2/\text{in}^4$

(Khdeir, 1986)

3.4.1. Free vibrations

The free-vibration solutions are obtained by using the Navier solution procedure (Reddy, 1984c). According to this procedure, appropriate forms of the solutions (with arbitrary coefficients) that identically satisfy the boundary conditions are assumed. The coefficients in the assumed solution are calculated by substituting the assumed displacement functions into the linear undamped equations of motion. This procedure yields exact solutions for antisymmetric cross-ply composite rectangular plates and plate strips for the case of simply-supported boundary conditions.

3.4.1.1. Rectangular plates

In this case, the free-vibration solutions are expanded in terms of double Fourier series in the space variables x and y and the motion is assumed to be harmonic in time; that is,

$$u = \sum_{m,n=1}^{\infty} U_{mn} \cos \alpha_m x \ \sin \beta_n y \ e^{i\omega_{mn} t} \tag{3.25}$$

$$v = \sum_{m,n=1}^{\infty} V_{mn} \sin \alpha_m x \ \cos \beta_n y \ e^{i\omega_{mn} t} \tag{3.26}$$

$$w = \sum_{m,n=1}^{\infty} W_{mn} \sin \alpha_m x \ \sin \beta_n y \ e^{i\omega_{mn} t} \tag{3.27}$$

$$\psi_x = \sum_{m,n=1}^{\infty} \psi_{xmn} \cos \alpha_m x \ \sin \beta_n y \ e^{i\omega_{mn} t} \tag{3.28}$$

$$\psi_y = \sum_{m,n=1}^{\infty} \psi_{ymn} \sin \alpha_m x \ \cos \beta_n y \ e^{i\omega_{mn} t} \tag{3.29}$$

where

$$\alpha_m = \frac{m\pi}{a} \quad \text{and} \quad \beta_n = \frac{n\pi}{b} \quad (m,n = 1,2,3,...) \tag{3.30}$$

and the ω_{mn} are the undamped natural vibration frequencies of the plate. The form of the solution in (3.25)-(3.29) satisfies the linearized boundary conditions (3.9) and (3.10) and the constants U_{mn}, V_{mn}, W_{mn}, ψ_{xmn}, and ψ_{ymn} are to be determined by substituting (3.25)-(3.29) into the linearized equations of motion (3.3)-(3.7). To this end, we transform the system of partial-differential equations (3.3)-(3.7) into a system of algebraic equations that can can be expressed in the following compact matrix form:

$$[K]\{\xi\} = \omega_{mn}^2[M]\{\xi\} + \{F\} \tag{3.31}$$

Here, $\{\xi\}$ is 5×1 column vector that contains the free-vibration amplitudes defined as

$$\{\xi\}^T = \{U_{mn}, V_{mn}, W_{mn}, \psi_{xmn}, \psi_{ymn}\} \tag{3.32}$$

[K] is a 5×5 stiffness matrix whose elements are given in Appendix A, [M] is a 5×5 mass matrix whose elements are also given in Appendix A, and {F} is a 5×1 column vector that contains the force components and is given by

$$\{F\}^T = \{0, 0, Q_{mn}, 0, 0\} \tag{3.33}$$

The loading Q is expanded in terms of the double Fourier series as

$$Q = \sum_{m,n=1}^{\infty} Q_{mn} \sin \alpha_m x \sin \beta_n y \tag{3.34}$$

It should be pointed out that static bending can be investigated by setting ω_{mn}^2 equal to zero and letting Q_{mn} be a constant. In this dissertation, static bending is not addressed. For free vibrations we set the vector {F} equal to zero and solve the

resulting eigenvalue problem. The eigenvalues determine the natural frequencies of the structure and the eigenfunctions describe the linear mode shapes. Because the stiffness K and mass M matrices in (3.31) are real and symmetric, the eigenvalues and eigenvectors of the system (3.31) are real. Moreover, for all cases the calculations show that the eigenvalues are distinct and hence the eigenvectors are orthogonal.

In solving the eigenvalue problem in (3.31), we use the IMSL subroutine DGVCRG. Table 3.1 lists the natural frequencies and the corresponding eigenvectors (modes) for each pair of the mode numbers m and n as a function of the number of laminae for the case $L/h = 10$.

3.4.1.2. Plate strips

Following the same procedure given in the previous section, we expand the free-vibration solutions in terms of single Fourier series in the space variable x and assume the motion to be harmonic in time. Accordingly, (3.25)-(3.29) reduce to the following equations:

$$u = \sum_{m=1}^{\infty} U_m \cos \alpha_m x \, e^{i\omega_m t} \tag{3.35}$$

$$w = \sum_{m=1}^{\infty} W_m \sin \alpha_m x \, e^{i\omega_m t} \tag{3.36}$$

$$\psi_x = \sum_{m=1}^{\infty} \psi_{xm} \cos \alpha_m x \, e^{i\omega_m t} \tag{3.37}$$

The system of algebraic equations in (3.31) reduces to a 3×3 system of algebraic equations in the variables U_m, W_m, and ψ_{xm}. The corresponding [K] and [M] matrices are given in Appendix A. A list of the natural frequencies and corresponding eigenvectors are listed in Table 3.2 for the mode number m and $a/h = 10$.

3.4.2. Forced vibrations

In this section, exact solutions for the dynamic response of antisymmetric cross-ply plate strips in cylindrical bending subjected to harmonic transverse loads are developed. These solutions will be used later in Chapter 5 when we study the nonlinear vibrations of the plate strips in the presence of subharmonic and superharmonic resonances of different types.

In the literature, different researchers used a variety of techniques in dealing with the linear forced vibrations of composite laminates. The classical method of separation of variables and the method of orthogonality of principle modes in conjunction with the Mindlin-Goodman procedure were used by Sun and Whitney (1974, 1976), Whitney and Sun (1976), Sun and Chattopadhyay (1975), and Dobyns (1981) to determine linear forced response of plates described by the first-order theory. Chou (1971) employed the Laplace-transform method to study the dynamic response of orthotropic plates. Reddy (1982, 1983b, 1983c) and Bhimaraddi (1987a, 1987b) used the Newmark direct integration method in their dynamic analyses of plates described by first- and third-order theories. Khdeir and Reddy (1988, 1989)

used an exact approach based on the state-space technique to analyze the dynamic response of antisymmetric angle-ply and symmetric cross-ply laminates. In this section, we use the state-space technique as described by Khdeir and Reddy (1988, 1989) and consider the case of antisymmetric-cross ply plate strips.

3.4.2.1. State-space approach

The state-space representation of the dynamic equations (3.17)-(3.19) is used to analyze the linear forced dynamic response of an antisymmetric cross-ply plate strip that is simply-supported along its edges. Following the Navier-solution procedure, we assume the following solution form, which satisfies the boundary conditions in equations (3.20):

$$u = \sum_{m=1}^{\infty} U_m(t) \cos \alpha_m x \tag{3.38}$$

$$w = \sum_{m=1}^{\infty} W_m(t) \sin \alpha_m x \tag{3.39}$$

$$\psi_x = \sum_{m}^{\infty} \psi_{xm}(t) \cos \alpha_m x \tag{3.40}$$

where $\alpha_m = m\pi/a$. The transverse load $Q(x,t)$ is assumed to be expandable in terms of a Fourier series as

$$Q = \sum_{m=1}^{\infty} Q_m(t) \sin \alpha_m x \tag{3.41}$$

Substitution of (3.38)-(3.41) into (3.17)-(3.19) results in a system of second-order differential equations in the time domain, which can be written in the following form

$$\begin{Bmatrix} \ddot{U}_m \\ \ddot{W}_m \\ \ddot{\psi}_{xm} \end{Bmatrix} = \begin{bmatrix} C_1 & C_2 & C_3 \\ C_4 & C_5 & C_6 \\ C_7 & C_8 & C_9 \end{bmatrix} \begin{Bmatrix} U_m \\ W_m \\ \psi_{xm} \end{Bmatrix} + Q_m(t) \begin{Bmatrix} b_1 \\ b_2 \\ b_3 \end{Bmatrix} \tag{3.42}$$

The coefficients $C_i (i = 1,2,...,9)$ and $b_i (i = 1,2,3)$ in equation (3.42) are given in Appendix B.

In order to reduce the system of equations (3.42) to a state-space form, we transform it into a set of first-order differential equations. This is accomplished by defining the state vector $Z(t)$ according to

$$Z_1 = U_m, \quad Z_2 = \dot{U}_m, \quad Z_3 = W_m, \quad Z_4 = \dot{W}_m, \quad Z_5 = \psi_{xm}, \quad Z_6 = \dot{\psi}_{xm} \tag{3.43}$$

Hence, the system of equations (3.42) is converted to the form

$$\dot{Z} = AZ + b \tag{3.44}$$

where the matrix A and the load vector b are defined as:

$$A = \begin{bmatrix} 0 & 1 & 0 & 0 & 0 & 0 \\ C_1 & 0 & C_2 & 0 & C_3 & 0 \\ 0 & 0 & 0 & 1 & 0 & 0 \\ C_4 & 0 & C_5 & 0 & C_6 & 0 \\ 0 & 0 & 0 & 0 & 0 & 1 \\ C_7 & 0 & C_8 & 0 & C_9 & 0 \end{bmatrix} \tag{3.45}$$

and

$$b^T = Q_m(t)\{0, b_1, 0, b_2, 0, b_3\} \tag{3.46}$$

The solution of equation (3.44) is given by Franklin (1968) and Brogan (1985) and can be written as

$$Z(t) = e^{A(t-t_0)}Z(t_0) + \int_0^t e^{A(t-\tau)}b(\tau)d(\tau) \tag{3.47}$$

where t_0 is the starting time, $Z(t_0)$ is the input response, and $e^{A(t-\tau)}$ is evaluated according to

$$e^{A(t-\tau)} = [R]\begin{bmatrix} e^{\lambda_1(t-\tau)} & & 0 \\ & \ddots & \\ 0 & & e^{\lambda_6(t-\tau)} \end{bmatrix}[R]^{-1} \tag{3.48}$$

the $\lambda_i (i = 1,2,...,6)$ are the eigenvalues of A, and [R] is a 6×6 matrix containing the eigenvectors of A. It is noted that in the present study, all eigenvalues are distinct. If, in another case, the eigenvalues are repeated, then the Jordan canonical form associated with the matrix in equation (3.44) is to be used.

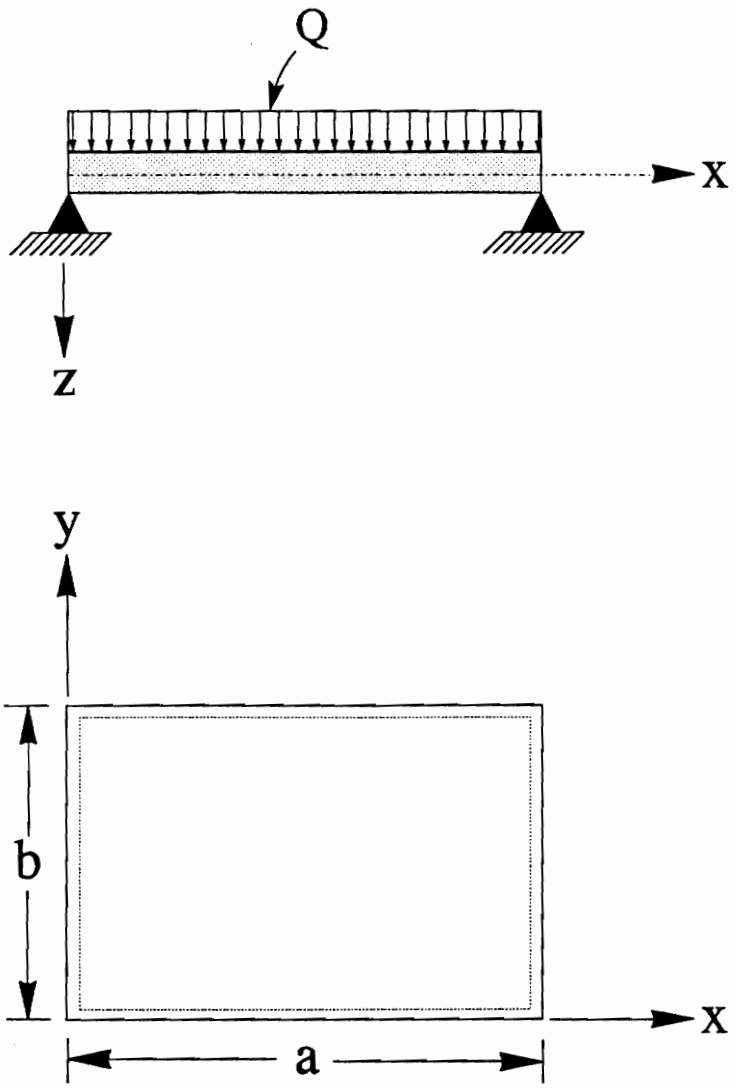

Figure 3.1. Geometry and coordinate system of a uniformly loaded simply supported rectangular plate.

Table 3.1. Antisymmetric cross-ply plate: Nondimensionalized undamped linear natural frequencies ($\hat{\omega}_{mn} = \omega_{mn} ab\sqrt{\rho/h^2 E_2}$) and mode shapes of simply supported rectangular panels (a = 10 in, b = 8 in, h = 1 in).

# Of Layers	m	n	Frequency	Mode Shape
2	1	1	8.0071485014	-0.0641951662
				0.0763958926
				1.0000000000
				-0.2769782311
				-0.3372674722
2	1	2	22.0225133322	-0.0647865520
				0.1190435071
				1.0000000000
				-0.2481355616
				-0.4947063058
2	1	3	40.9874899389	-0.0623785107
				0.1321582806
				1.0000000000
				-0.2178702506
				-0.4832154815
2	2	1	16.6479976947	-0.1058150683
				0.0765484814
				1.0000000000
				-0.4496359750
				-0.3130615999
2	2	2	27.4862437490	-0.1032746348
				0.1170037777
				1.0000000000
				-0.4085504583
				-0.4646810345

Table 3.1 - Continued

# of Layers		m	Frequency	Mode Shape
2	2	3	44.7079770808	-0.0990339385
				0.1301894821
				1.0000000000
				-0.3640575358
				-0.4572894223
2	3	1	29.9822841741	-0.1267727335
				0.0752752559
				1.0000000000
				-0.5001556558
				-0.2842049431
2	3	2	37.8750587247	-0.1234794322
				0.1138156549
				1.0000000000
				-0.4593420043
				-0.4277062927
2	3	3	52.2198711379	-0.1187392008
				0.1271167822
				1.0000000000
				-0.4135853047
				-0.4240731451
4	1	1	9.9789665517	-0.0310989075
				0.0362617941
				1.0000000000
				-0.2559314523
				-0.2993329435

Table 3.1 - Continued

# of Layers		m	Frequency	Mode Shape
4	1	2	26.1241174947	-0.0317920342
				0.0520631135
				1.0000000000
				-0.2341487501
				-0.3400328733
4	1	3	45.7259406304	-0.0313235702
				0.0571543565
				1.0000000000
				-0.2144377975
				-0.2393452134
4	2	1	20.0852871688	-0.0477445106
				0.0368480611
				1.0000000000
				-0.3451116530
				-0.2802533913
4	2	2	31.9711046692	-0.0478764508
				0.0521732965
				1.0000000000
				-0.3178877800
				-0.3197211387
4	2	3	49.5607600046	-0.0476076052
				0.0572768051
				1.0000000000
				-0.2932416463
				-0.2230354423

Table 3.1 - Continued

# of Layers		m	Frequency	Mode Shape
4	3	1	34.5432385078	-0.0548249087
				0.0368697393
				1.0000000000
				-0.3042853481
				-0.2610867626
4	3	2	42.9065053326	-0.0549076182
				0.0521365325
				1.0000000000
				-0.2799980778
				-0.2992585964
4	3	3	57.4011228080	-0.0548640188
				0.0573724878
				1.0000000000
				-0.2581937532
				-0.2066281920
6	1	1	10.2988842970	-0.0206996054
				0.0240859536
				1.0000000000
				-0.2528229190
				-0.2938630170
6	1	2	26.8188748222	-0.0213116599
				0.0345099088
				1.0000000000
				-0.2320006182
				-0.3198410433

Table 3.1 - Continued

# of Layers		m	Frequency	Mode Shape
6	1	3	46.7122686299	-0.0212772009
				0.0382019087
				1.0000000000
				-0.2138285222
				-0.2081529204
6	2	1	20.6554515563	-0.0316515130
				0.0245690948
				1.0000000000
				-0.3309440059
				-0.2754330437
6	2	2	32.7672509768	-0.0318945464
				0.0346755824
				1.0000000000
				-0.3052038209
				-0.3004137741
6	2	3	50.5979636148	-0.0319862392
				0.0383554893
				1.0000000000
				-0.2828863137
				-0.1925309223
6	3	1	35.3721712929	-0.0364374822
				0.0247608364
				1.0000000000
				-0.2791244862
				-0.2575414437

Table 3.1 - Continued

# of Layers		m	Frequency	Mode Shape
6	3	2	43.8742327207	-0.0366253971
				0.0348091940
				1.0000000000
				-0.2562687770
				-0.2816020769
6	3	3	58.5600309724	-0.0368200836
				0.0385383627
				1.0000000000
				-0.2367478642
				-0.1774961769
8	1	1	10.4090719330	-0.0155202217
				0.0180478887
				1.0000000000
				-0.2517850052
				-0.2920414398
8	1	2	27.0638578830	-0.0160230638
				0.0258561463
				1.0000000000
				-0.2312787274
				-0.3131401725
8	1	3	47.0765609726	-0.0160796281
				0.0287148015
				1.0000000000
				-0.2136308769
				-0.1976911685

Table 3.1 - Continued

# of Layers		m	Frequency	Mode Shape
8	2	1	20.8542619286	-0.0237098471
				0.0184358587
				1.0000000000
				-0.3262405364
				-0.2738211780
8	2	2	33.0496012866	-0.0239328429
				0.0260036347
				1.0000000000
				-0.3009689196
				-0.2939851850
8	2	3	50.9814347865	-0.0240754271
				0.0288477022
				1.0000000000
				-0.2794063201
				-0.1822739018
8	3	1	35.6695368585	-0.0273303960
				0.0186304497
				1.0000000000
				-0.2707472229
				-0.2563494428
8	3	2	44.2238724696	-0.0275046896
				0.0261450490
				1.0000000000
				-0.2483314719
				-0.2756925113

Table 3.1 - Continued

# of Layers		m	Frequency	Mode Shape
8	3	3	58.9911149477	-0.0277089067
				0.0290148224
				1.0000000000
				-0.2295279232
				-0.1676605169
10	1	1	10.4598014822	-0.0124150846
				0.0144330715
				1.0000000000
				-0.2513131666
				-0.2912140328
10	1	2	27.1777285242	-0.0128341946
				0.0206785792
				1.0000000000
				-0.2309497770
				-0.3100974147
10	1	3	47.2488050765	-0.0129113613
				0.0230001653
				1.0000000000
				-0.2135423315
				-0.1929187486
10	2	1	20.9462567880	-0.0189595984
				0.0147531271
				1.0000000000
				-0.3241053041
				-0.2730878742

Table 3.1 - Continued

# of Layers		m	Frequency	Mode Shape
10	2	2	33.1811007314	-0.0191531018
				0.0208050643
				1.0000000000
				-0.2990423313
				-0.2910625124
10	2	3	51.1627932655	-0.0192949296
				0.0231129130
				1.0000000000
				-0.2778193853
				-0.1775906313
10	3	1	35.8086504333	-0.0218693100
				0.0149282098
				1.0000000000
				-0.2669373672
				-0.2558061131
10	3	2	44.3878470255	-0.0220209340
				0.0209334492
				1.0000000000
				-0.2447156024
				-0.2730006619
10	3	3	59.1954259455	-0.0222058519
				0.0232575716
				1.0000000000
				-0.2262310831
				-0.1631630274

Table 3.2. Antisymmetric cross-ply plate strip: Nondimensionalized undamped linear natural frequencies ($\hat{\omega}_m = \omega_m a^2 \sqrt{\rho/h^2 E_2}$) and mode shapes of simply supported plate strips in cylindrical bending (a = 10 in, h = 1 in).

# of Layers	m	Frequency	Mode Shape
2	1	4.889958	-0.0649905511 1.0000000000 -0.3029679256
2	2	18.541326	-0.1208652135 1.0000000000 -0.5482077044
2	3	38.734213	-0.1633355550 1.0000000000 -0.7108712067
4	1	6.622442	-0.0319250965 1.0000000000 -0.2921590514
4	2	24.272238	-0.0569030120 1.0000000000 -0.4807356732
4	3	48.680568	-0.0733225395 1.0000000000 -0.5476097807
6	1	6.893091	-0.0212521582 1.0000000000 -0.2905333517
6	2	25.168289	-0.0377697975 1.0000000000 -0.4711071351

Table 3.2 - Continued

# of Layers	m	Frequency	Mode Shape
6	3	50.267714	-0.0485781673 1.0000000000 -0.5256153094
8	1	6.985390	-0.0159327988 1.0000000000 -0.2899901323
8	2	25.475685	-0.0282957740 1.0000000000 -0.4679047840
8	3	50.818581	-0.0363827082 1.0000000000 -0.5183226080
10	1	7.027717	-0.0127441550 1.0000000000 -0.2897431667
10	2	25.617023	-0.0226265257 1.0000000000 -0.4664508155
10	3	51.073087	-0.0290911292 1.0000000000 -0.5150134720

4. THE SOLUTION PROCEDURE

In using perturbation methods to determine the responses of weakly nonlinear distributed-parameter systems, one can either apply his favorite perturbation method directly to the partial-differential equations and boundary conditions or discretize the system first and then apply his favorite perturbation method. In this chapter, we use a simple example to demonstrate that the latter approach might lead to erroneous results for systems with quadratic and cubic nonlinearities. Then, we describe a perturbation technique that avoids the pitfalls of discretized nonlinear physical systems with quadratic and cubic nonlinearities. The technique applies either the method of multiple scales or the method of averaging to the Lagrangian of the system rather than the partial-differential equations of motion and boundary conditions. Following this approach, one averages the Lagrangian over the fast-time scale and obtains the ordinary-differential equations that govern the modulation of the amplitudes and phases of the response directly.

4.1. A Simple Example

In this section, we consider a simple example that serves to illustrate how to apply the perturbation procedure to the Lagrangian. The resulting solutions are in full agreement with those obtained by attacking the original differential equation. The power and simplicity of the technique are more evident when treating nonlinear partial-differential equations and boundary conditions. An appealing feature of the technique is that it requires less algebra than attacking the partial-differential equations and their associated boundary conditions.

To demonstrate the procedure, we consider the free oscillations of systems governed by the following equation of motion:

$$\ddot{u} + \omega^2 u + \delta u^2 + \alpha u^3 = 0 \tag{4.1}$$

Equation (4.1) represents the motion of a mass restrained by a nonlinear spring in the presence of gravity force (Nayfeh and Mook, 1979). Because there are quadratic and cubic nonlinear terms in (4.1), one needs to exercise care in obtaining an approximate solution that correctly accounts for the effect of the quadratic nonlinearity. It is worth mentioning here that the ordinary method of averaging yields an incomplete (incorrect) solution because it does not capture the interaction between the first and second harmonics. On the other hand, a correct second-order uniform expansion can be obtained by using one of the following: the method of multiple scales, the generalized method of averaging, the Krylov-Bogoliubov-Mitropolski technique, or the method of normal forms.

In order to fix our ideas, we present the details of solving equation (4.1) by using the method of multiple scales (Nayfeh, 1973, 1981; Nayfeh and Mook, 1979). As we

shall see, we need at least a two-term expansion to obtain a first approximation that correctly accounts for the nonlinearity; accordingly, we need at least three time scales: $T_0 = t$, $T_1 = \varepsilon t$, and $T_2 = \varepsilon^2 t$. Then, the time derivatives become

$$\frac{d}{dt} = D_0 + \varepsilon D_1 + \varepsilon^2 D_2 + \ldots \tag{4.2}$$

$$\frac{d^2}{dt^2} = D_0^2 + 2\varepsilon D_0 D_1 + \varepsilon^2 (D_1^2 + 2D_0 D_2) + \ldots \tag{4.3}$$

where ε is a small dimensionless bookkeeping device and $D_n = \frac{\partial}{\partial T_n}$. Next, we seek an approximate solution of (4.1) in the form

$$u \simeq \varepsilon u_1 + \varepsilon^2 u_2 + \varepsilon^3 u_3 \text{ where } u_i = u_i(T_0, T_1, T_2) \text{ for } i = 1,2, \text{ and } 3 \tag{4.4}$$

Substituting (4.3) and (4.4) into (4.1) and equating coefficients of like powers of ε to zero, we obtain

$$\varepsilon: D_0^2 u_1 + \omega^2 u_1 = 0 \tag{4.5}$$

$$\varepsilon^2: D_0^2 u_2 + \omega^2 u_2 = -2D_0 D_1 u_1 - \delta u_1^2 \tag{4.6}$$

$$\varepsilon^3: D_0^2 u_3 + \omega^2 u_3 = -2D_0 D_1 u_2 - (D_1^2 + 2D_0 D_2) u_1 - 2\delta u_1 u_2 - \alpha u_1^3 \tag{4.7}$$

The solution of (4.5) can be expressed in the following form:

$$u_1 = A(T_1, T_2) e^{i\omega T_0} + \bar{A}(T_1, T_2) e^{-i\omega T_0} \tag{4.8}$$

where A is, at this point, an arbitrary complex function and the overbar denotes the complex conjugate. Substituting (4.8) into (4.6) yields

$$D_0^2 u_2 + \omega^2 u_2 = -2i\omega D_1 A e^{i\omega T_0} + 2i\omega D_1 \bar{A} e^{-i\omega T_0} - \delta(A^2 e^{2i\omega T_0} + 2A\bar{A} + \bar{A}^2 e^{-2i\omega T_0}) \tag{4.9}$$

In order to eliminate secular terms from u_2, we must put

$$D_1 A = 0 \quad \text{or} \quad A = A(T_2) \tag{4.10}$$

Then, the solution of (4.9) can be expressed as

$$u_2 = \frac{\delta}{3\omega^2} A^2 e^{2i\omega T_0} + \frac{\delta}{3\omega^2} \bar{A}^2 e^{-2i\omega T_0} - \frac{2\delta}{\omega^2} A\bar{A} \tag{4.11}$$

Because A is a function of T_2 and not T_1, as indicated in (4.10), it is now apparent that we must at least consider u_3 in order to capture the influence of the nonlinearity.

Substituting (4.8), (4.10), and (4.11) into (4.7) yields

$$D_0^2 u_3 + \omega^2 u_3 = -2i\omega A' e^{i\omega T_0} + 2i\omega \bar{A}' e^{-i\omega T_0} - \alpha(A e^{i\omega T_0} + \bar{A} e^{-i\omega T_0})^3 - \frac{2\delta^2}{3\omega^2}\left(A e^{i\omega T_0} + \bar{A} e^{-i\omega T_0}\right)\left(A^2 e^{2i\omega T_0} + \bar{A}^2 e^{-2i\omega T_0} - 6A\bar{A}\right) \tag{4.12}$$

where the prime indicates the derivative with respect to T_2. Collecting terms in (4.12), we obtain

$$D_0^2 u_3 + \omega^2 u_3 = \left[-2i\omega A' + \left(\frac{10}{3\omega^2}\delta^2 - 3\alpha \right) A^2 \bar{A} \right] e^{i\omega T_0} + cc + NST \tag{4.13}$$

where NST stands for the terms that are not responsible for secular terms in u_3 and cc stands for the complex conjugate of the preceding term. To eliminate the secular terms from u_3, we must put

$$-2i\omega A' + \left(\frac{10}{3\omega^2}\delta^2 - 3\alpha\right)A^2\bar{A} = 0 \tag{4.14}$$

Expressing A in the polar form

$$A = \frac{1}{2}a(T_2)e^{i\beta(T_2)} \tag{4.15}$$

where a and β are real, we rewrite (4.14) as

$$-i\omega a' + \omega a\beta' + \frac{a^2}{8}\left(\frac{10\delta^2}{\omega^2} - 3\alpha\right) = 0 \tag{4.16}$$

Separating real and imaginary parts in (4.16) yields

$$a' = 0 \tag{4.17}$$

$$a\beta' = \frac{a^3}{\omega}\left(\frac{3\alpha}{8} - \frac{5\delta^2}{12\omega^2}\right) \tag{4.18}$$

It follows from (4.17) that $a = a_0 =$ a constant. Integrating (4.18) and recalling that $T_2 = \varepsilon^2 t$, we have

$$\beta = \frac{\varepsilon^2}{\omega}\left(\frac{3\alpha}{8} - \frac{5\delta^2}{12\omega^2}\right)a_0^2 t + \beta_0 \tag{4.19}$$

where β_0 is a constant and $a_0 \neq 0$.

Substituting (4.15) into (4.8) and (4.11) and recalling that $T_0 = t$, we obtain

$$u_1 = a\cos(\omega t + \beta) \tag{4.20}$$

$$u_2 = \frac{\delta a^2}{6\omega^2}[\cos(2\omega t + 2\beta) - 3] \tag{4.21}$$

Then, (4.4) becomes

$$u \simeq \varepsilon a \cos(\omega t + \beta) + \frac{\varepsilon^2 \delta a^2}{6\omega^2} [\cos(2\omega t + 2\beta) - 3] \tag{4.22}$$

Substituting (4.19) into (4.22) and recalling that $a = a_0$, we rewrite (4.22) as

$$u \simeq \varepsilon a_0 \cos(\Omega t + \beta_0) + \frac{\varepsilon^2 a_0^2 \delta}{6\omega^2} [\cos(2\Omega t + 2\beta_0) - 3] \tag{4.23}$$

where

$$\Omega \simeq \omega + \frac{1}{\omega}\left(\frac{3\alpha}{8} - \frac{5\delta^2}{12\omega^2}\right)\varepsilon^2 a_0^2 \tag{4.24}$$

When the ordinary method of averaging is used, one does not get the second term in (4.23) and, more importantly, $5\delta^2/12\omega^2$ is missing from (4.24).

Next, we explain how the approximate solution of (4.1) can be obtained by applying the method of multiple scales to the Lagrangian rather than the differential equation. It can be easily shown that the Lagrangian corresponding to (4.1) is

$$L = \frac{1}{2}\dot{u}^2 - \frac{1}{2}\omega^2 u^2 - \frac{1}{3}\delta u^3 - \frac{1}{4}\alpha u^4 \tag{4.25}$$

To determine an approximate solution that captures the effect of the quadratic term, we need to supplement the linear solution with other terms. Thus, if the first (i.e., linear) term is $\varepsilon(Ae^{i\omega T_0} + \bar{A}e^{-i\omega T_0})$ where A is a complex function of T_2, then we need to add to it a term proportional to $A\bar{A}$ and another term proportional to $A^2e^{2i\omega T_0} + \bar{A}^2e^{-2i\omega T_0}$. Thus, we let

$$u \simeq \varepsilon(Ae^{i\omega T_0} + \bar{A}e^{-i\omega T_0}) + \varepsilon^2 JA\bar{A} + \varepsilon^2 K(A^2e^{2i\omega T_0} + \bar{A}^2e^{-2i\omega T_0}) \tag{4.26}$$

where J and K are constants to be determined from the analysis. Substituting (4.26) into (4.25), keeping terms up to $0(\varepsilon^4)$, and averaging over the period $2\pi/\omega$ while treating A as a constant, we obtain

$$<L> = i\varepsilon^4\omega(A\bar{A}' - \bar{A}A') + \varepsilon^4(3K^2\omega^2 - \frac{1}{2}J^2\omega^2 - 2\delta K - 2\delta J - \frac{3}{2}\alpha)A^2\bar{A}^2 \quad (4.27)$$

where the prime here indicates the derivative with respect to T_2. Requiring the averaged Lagrangian $<L>$ in (4.27) to be stationary with respect to J and K independently, we obtain the following equations for J and K:

$$\frac{\partial <L>}{\partial J} = 0 \Rightarrow J = \frac{-2\delta}{\omega^2} \quad (4.28)$$

$$\frac{\partial <L>}{\partial K} = 0 \Rightarrow K = \frac{\delta}{3\omega^2} \quad (4.29)$$

which agrees with the expression (4.11) for u_2 obtained by the method of multiple scales. We recall that (4.11) was the result of eliminating secular terms from u_2 (i.e., guaranteeing that u_2 is bounded). For any other choice of J and K, $<L>$ grows with time. Substituting the values of J and K into (4.27) yields

$$<L> = i\varepsilon^4\omega(A\bar{A}' - \bar{A}A') + \varepsilon^4\left(\frac{5\delta^2}{3\omega^2} - \frac{3}{2}\alpha\right)A^2\bar{A}^2 \quad (4.30)$$

Substituting (4.15) into (4.30) yields

$$<L> = \frac{1}{2}\varepsilon^4\omega a^2\beta' + \frac{\varepsilon^4}{32}\left(\frac{10\delta^2}{3\omega^2} - 3\alpha\right)a^4 \quad (4.31)$$

Clearly a and β are the generalized coordinates in (4.31) and hence the Euler-Lagrange equations can be written as

$$\frac{d}{dT_2}\left(\frac{\partial <L>}{\partial a'}\right) - \frac{\partial <L>}{\partial a} = 0 \tag{4.32}$$

$$\frac{d}{dT_2}\left(\frac{\partial <L>}{\partial \beta'}\right) - \frac{\partial <L>}{\partial \beta} = 0 \tag{4.33}$$

Substituting (4.31) into (4.33) and (4.32) yields, respectively,

$$a' = 0 \tag{4.34}$$

and

$$-\omega a\beta' + \varepsilon^2\left(\frac{3\alpha}{8} - \frac{5\delta^2}{12\omega^2}\right)a^3 = 0 \tag{4.35}$$

Equations (4.34) and (4.35) are the same as (4.17) and (4.18) obtained by attacking the differential equation. Moreover, it can be easily shown that (4.26), (4.34), and (4.35) yield (4.23) and (4.24).

4.2. Nonlinear Response of a Fluid Valve

We consider the nonlinear dynamic response of an experimental relief valve used to protect a fluid system from overpressure. A schematic representation is shown in Figure 4.1. The valve mechanism consists of a ball held by a uniform helical spring against a valve seat having nonlinear characteristics. The helical spring is considered a distributed-parameter system and its motion is governed by the wave equation subject to certain boundary conditions. One end of the spring is fixed and

the other end is restrained by a force induced by the valve seat. This end is also subjected to a constant static pressure and a sinusoidally varying dynamic pressure, resulting from vibrations in the pneumatic transmission lines.

The relief-valve mechanism is schematically represented in Figure 4.2 as a linear helical spring having mass M, length L, stiffness constant K, and viscous damping coefficient μ^*. The displacement at time t^* of the point on the axis of the helical spring originally at the position x^* is given by u^*. The ball has a concentrated mass m and is attached to the helical spring at $x^* = L$. The valve seat restrains the motion of the valve and is modeled as a spring having nonlinear characteristics. The ball is subject to a static pressure S^* and a dynamic pressure $F^* \cos \Omega^* t^*$ exerted by the fluid.

We consider the helical spring a distributed-parameter system and use the well known extended Hamilton's principle (e.g., Meirovitch, 1980) to derive the governing equations. The kinetic-energy density of the linear spring is

$$\hat{T} = \frac{1}{2} \frac{M}{L} u_{,t^*}^{*2} \tag{4.36}$$

Its potential-energy density is

$$\hat{V} = \frac{1}{2} KL u_{,x^*}^{*2} \tag{4.37}$$

Its Lagrangian-density function is

$$\hat{L} = \hat{T} - \hat{V} = \frac{1}{2} \frac{M}{L} u_{,t^*}^{*2} - \frac{1}{2} KL u_{,x^*}^{*2} \tag{4.38}$$

To account for the mass of the ball and the elasticity of the valve seat at the end $x^* = L$, we introduce what is called the discrete Lagrangian L_0 and write

$$L_0 = \frac{1}{2} m u_{,t^*}^{*2}(L,t^*) - \frac{1}{2}\alpha[u^*(L,t^*)]^2 - \frac{1}{4}\beta[u^*(L,t^*)]^4 \tag{4.39}$$

where the nonlinear character of the restoring force F_s generated by the valve seat is described as follows:

$$F_s = \alpha u^*(L,t) + \beta u^{*3}(L,t) \tag{4.40}$$

The virtual work done by the force exerted by the fluid pressure on the ball is given by

$$\delta\hat{W}_p = -(S^* + F^* \cos\Omega^* t^*)u^*(L,t^*) \tag{4.41}$$

where S^*, F^*, and Ω^* are constants. The extended Hamilton's principle can be expressed as

$$\int_{t_1}^{t_2}\left[\int_0^L \delta\hat{L}dx + \delta\hat{W}_p + \delta L_0\right]dt = 0 \quad \begin{cases}\delta u^* = 0, 0 \le x \le L \\ \text{at } t = t_1, t_2\end{cases} \tag{4.42}$$

where δu^* is a virtual displacement taken to be zero at times t_1 and t_2 along the entire length of the helical spring. Performing the first variation of equations (4.38)- (4.41), substituting the results into (4.42), integrating by parts, and setting the coefficient of δu^* equal to zero, we obtain the following equation of motion and boundary conditions:

$$u,^*_{t^*t^*} = \frac{KL^2}{M} u,^*_{x^*x^*} \tag{4.43}$$

$$u^* = 0 \quad \text{at} \quad x^* = 0 \tag{4.44}$$

$$mu,_{t^*t^*} + KLu,_{x^*} + \alpha u^* + \beta u^{*3} = -(S^* + F^* \cos \Omega^* t^*) \quad \text{at} \quad x^* = L \tag{4.45}$$

In the presence of linear viscous damping, equation (4.43) becomes

$$u^*_{,t^*t^*} + \frac{2\mu^*}{M} u^*_{,t^*} = \frac{KL^2}{M} u^*_{,x^*x^*} \tag{4.46}$$

Next, we introduce the dimensionless quantities

$$u = u^*/L^*, \; t = \sqrt{K/M}\, t^*, \; x = x^*/L, \; \text{and} \; \Omega^* t^* = \Omega \sqrt{k/M}\, t^* \tag{4.47}$$

and rewrite equations (4.46), (4.44), and (4.45) as

$$u_{,xx} = u_{,tt} + 2\hat{\mu} u_{,t} \tag{4.48}$$

$$u = 0 \quad \text{at} \quad x = 0 \tag{4.49}$$

$$u_{,tt} + \alpha_1 u_{,x} + ku + \alpha_3 u^3 = -(S + \hat{F} \cos \Omega t) \quad \text{at} \quad x = 1 \tag{4.50}$$

where

$$\hat{\mu} = \frac{\mu^*}{\sqrt{kM}}, \; \alpha_1 = \frac{M}{m}, \; k = \frac{M\alpha}{mK}, \; \alpha_3 = \frac{\beta L^{*2} M}{mK}, \; S = \frac{S^* M}{mKL^*}, \; \hat{F} = \frac{F^* M}{mKL^*} \tag{4.51}$$

We express the solution of equations (4.48)-(4.50) as the sum of a static component and a dynamic component:

$$u(x,t) = bx + w(x,t) \tag{4.52}$$

where b is a constant, the static equilibrium position of the valve. The first term in (4.52) satisfies (4.48) and (4.49), and b is determined according to

$$(\alpha_1 + k)b + \alpha_3 b^3 = -S \tag{4.53}$$

The second term $w(x,t)$ in (4.52) is the deviation from the static equilibrium position and is governed by

$$w_{,xx} = w_{,tt} + 2\hat{\mu}w_{,t} \tag{4.54}$$

$$w = 0 \quad \text{at} \quad x = 0 \tag{4.55}$$

$$w_{,tt} + \alpha_1 w_{,x} + \alpha_0 w + \alpha_2 w^2 + \alpha_3 w^3 = -\hat{F}\cos\Omega t \quad \text{at} \quad x = 1 \tag{4.56}$$

where

$$\alpha_0 = k + 3\alpha_3 b^2 \quad \text{and} \quad \alpha_2 = 3\alpha_3 b \tag{4.57}$$

In (4.52), b is not necessarily small. Now we consider small, but finite, motions around the static equilibrium position $u = bx$ (i.e, $|w| << b$).

It can be easily shown that in the absence of damping equation (4.54) and its associated boundary conditions (4.55) and (4.56) are derivable from the following Lagrangian:

$$\begin{aligned} L = {} & \frac{1}{2}\alpha_1 \int_0^1 \left[w_{,t}^2(x,t) - w_{,x}^2(x,t)\right]dx + \frac{1}{2}w_{,t}^2(1,t) - \frac{1}{2}\alpha_0 w^2(1,t) \\ & - \frac{1}{3}\alpha_2 w^3(1,t) - \frac{1}{4}\alpha_3 w^4(1,t) - \hat{F}\cos\Omega t \; w(1,t) \end{aligned} \tag{4.58}$$

Next, we determine a second-order approximation to the response of the system for the cases of primary resonance, subharmonic resonance of order one-half, superharmonic resonance of order two, subharmonic resonance of order one-third,

and superharmonic resonance of order three. We assume that the directly excited mode is not involved in an internal (autoparametric) resonance with any other mode.

In each case, we use three methods to determine a second-order expansion. First, we apply the method of multiple scales directly to the original partial-differential equation (4.54) and its associated boundary conditions (4.55) and (4.56) and obtain equations describing the modulations of the amplitude and phase. Second, we derive a second-order nonlinear ordinary-differential equation that describes the time evolution of a single mode, the so-called single-mode discretization. Then, we use the method of multiple scales to determine second-order approximate solutions of this equation, thereby obtaining the equations that describe the modulations of the amplitude and phase of the response. We show that the results of the second approach are erroneous. Third, we postulate the form of the response, average the Lagrangian over the fast-time scale, and then obtain the equations that describe the modulations of the amplitude and phase as the Euler-Lagrange equations of the averaged Lagrangian. We show that, when the assumed form of the response is complete, the method is very attractive.

4.3. Case of Primary Resonance

4.3.1. Attacking the original problem

In this case, the excitation frequency Ω is near ω, where ω is one of the linear natural frequencies of the system. We introduce a small dimensionless measure ε

of the amplitude of w as a bookkeeping device. We use the method of multiple scales (Nayfeh, 1973, 1981) and seek a second-order approximation to the solution of (4.54)-(4.56) in the form

$$w(x,t;\varepsilon) \simeq \varepsilon w_1(x, T_0, T_1, T_2) + \varepsilon^2 w_2(x, T_0, T_1, T_2) + \varepsilon^3 w_3(x, T_0, T_1, T_2) \tag{4.59}$$

where $T_0 = t$ is a fast-time scale characterizing changes occurring at the frequencies Ω and ω, $T_1 = \varepsilon t$ and $T_2 = \varepsilon^2 t$ are slow-time scales characterizing the modulations of the amplitudes and phases due to damping, nonlinearity, and possible resonances, and the w_n are 0(1) as $\varepsilon \to 0$. The damping $\hat{\mu}$, excitation amplitude $\hat{F}$, and the nonlinearities are ordered in such a way that they balance each other. Thus, we put

$$\hat{\mu} = \varepsilon^2 \tilde{\mu} \text{ and } \hat{F} = \varepsilon^3 F \tag{4.60}$$

And we note that

$$\frac{\partial}{\partial t} = D_0 + \varepsilon D_1 + \varepsilon^2 D_2 + \ldots \tag{4.61}$$

and

$$\frac{\partial^2}{\partial t^2} = D_0^2 + 2\varepsilon D_0 D_1 + \varepsilon^2 (D_1^2 + 2D_0 D_2) + \ldots \tag{4.62}$$

Then we substitute (4.59)-(4.62) into (4.54)-(4.56), equate coefficients of like powers of ε, and obtain the following:

order ε:

$$w_{1,xx} = D_0^2 w_1 \tag{4.63}$$

$$w_1 = 0 \quad \text{at} \quad x = 0 \tag{4.64}$$

$$D_0^2 w_1 + \alpha_1 w_{1,x} + \alpha_0 w_1 = 0 \quad \text{at} \quad x = 1 \tag{4.65}$$

order ε^2:

$$w_{2,xx} = D_0^2 w_2 + 2D_0 D_1 w_1 \tag{4.66}$$

$$w_2 = 0 \quad \text{at} \quad x = 0 \tag{4.67}$$

$$D_0^2 w_2 + \alpha_1 w_{2,x} + \alpha_0 w_2 = -2D_0 D_1 w_1 - \alpha_2 w_1^2 \quad \text{at} \quad x = 1 \tag{4.68}$$

order ε^3:

$$w_{3,xx} = D_0^2 w_3 + 2D_0 D_1 w_2 + (2D_0 D_2 + D_1^2) w_1 + 2\tilde{\mu} D_0 w_1 \tag{4.69}$$

$$w_3 = 0 \quad \text{at} \quad x = 0 \tag{4.70}$$

$$\begin{aligned} D_0^2 w_3 + \alpha_1 w_{3,x} + \alpha_0 w_3 = & -2D_0 D_1 w_2 - (2D_0 D_2 + D_1^2) w_1 \\ & - 2\alpha_2 w_1 w_2 - \alpha_3 w_1^3 - F \cos \Omega T_0 \quad \text{at} \quad x = 1 \end{aligned} \tag{4.71}$$

The general solution of (4.63)-(4.65) has the form

$$w_1(x, T_0, T_1, T_2) = \sum_{n=1}^{\infty} \left[A_n(T_1, T_2) e^{i\omega_n T_0} + cc \right] \frac{\sin \omega_n x}{\sin \omega_n} \tag{4.72}$$

where the natural frequencies ω_n are the solutions of

$$\alpha_1 \omega_n + (\alpha_0 - \omega_n^2) \tan \omega_n = 0, \tag{4.73}$$

the complex functions A_n are arbitrary at this point, and as above cc denotes the complex conjugate of the preceding term. It is a linear combination of all modes. However, in the presence of damping, the modes that are not directly excited by the fluid vibrations or indirectly excited by an internal resonance decay with time. Because Ω is near one of the ω_n, only this mode is directly excited. We consider the case in which this mode is not involved in an internal resonance. Hence, the solution of (4.63)-(4.65) consists of only the mode corresponding to ω_n:

$$w_1 = A(T_1, T_2)\frac{\sin \omega x}{\sin \omega} e^{i\omega T_0} + cc \tag{4.74}$$

where the subscript n has been dropped.

Substituting (4.74) into (4.66)-(4.68) yields

$$w_{2,xx} = D_0^2 w_2 + 2i\omega D_1 A \frac{\sin \omega x}{\sin \omega} e^{i\omega T_0} + cc \tag{4.75}$$

$$w_2 = 0 \quad \text{at} \quad x = 0 \tag{4.76}$$

$$\begin{aligned} D_0^2 w_2 + \alpha_1 w_{2,x} + \alpha_0 w_2 = & -2i\omega D_1 A e^{i\omega T_0} \\ & - \alpha_2 \left[A^2 e^{2i\omega T_0} + A\bar{A} \right] + cc \quad \text{at} \quad x = 1 \end{aligned} \tag{4.77}$$

The solvability condition for (4.75)-(4.77), which is described below, demands that

$$D_1 A = 0 \tag{4.78}$$

Substituting (4.78) into (4.75)-(4.77) and solving for w_2 yields

$$w_2 = c_1 A\bar{A}x + c_2 A^2 \frac{\sin 2\omega x}{\sin 2\omega} e^{2i\omega T_0} + cc \tag{4.79}$$

where

$$c_1 = \frac{-\alpha_2}{\alpha_1 + \alpha_0} \quad \text{and} \quad c_2 = \frac{-\alpha_2}{\alpha_0 - 4\omega^2 + 2\omega\alpha_1 \cot 2\omega} \tag{4.80}$$

Because A is a function of T_2 we express the nearness of Ω to ω by introducing the detuning parameter σ defined by $\Omega = \omega + \varepsilon^2\sigma$. Then, substituting (4.74), (4.78), and (4.79) into (4.69)-(4.71) yields

$$w_{3,xx} = D_0^2 w_3 + 2i\omega(A' + \tilde{\mu}A)\frac{\sin \omega x}{\sin \omega} e^{i\omega T_0} + cc \tag{4.81}$$

$$w_3 = 0 \quad \text{at} \quad x = 0 \tag{4.82}$$

$$\begin{aligned} D_0^2 w_3 + \alpha_1 w_{3,x} + \alpha_0 w_3 = &-\frac{1}{2} F e^{i(\omega T_0 + \sigma T_2)} - 2i\omega A' e^{i\omega T_0} \\ &- [2\alpha_2(2c_1 + c_2) + 3\alpha_3]A^2\bar{A}e^{i\omega T_0} + NST + cc \quad \text{at} \quad x = 1 \end{aligned} \tag{4.83}$$

where the prime indicates the derivative with respect to T_2. Because the homogeneous equations related to (4.81)-(4.83) are the same as (4.63)-(4.65) and because the latter have a nontrivial solution, the former inhomogeneous equations have a solution only if a certain condition is satisfied (Nayfeh, 1981). To determine this solvability condition, we first write the solution in the form

$$w_3 = \phi(x, T_2)e^{i\omega T_0} + cc + W_3(x, T_0, T_2) \tag{4.84}$$

where W_3 is governed by equations (4.81)-(4.83) with the terms proportional to $\exp(i\omega T_0)$ being deleted. Therefore, W_3 exists, unique and free of small-divisor terms. Substituting (4.84) into (4.81)-(4.83) and equating the coefficients of $\exp(i\omega T_0)$ on both sides of each equation results in

$$\phi_{,xx} + \omega^2\phi = 2i\omega(A' + \tilde{\mu}A)\frac{\sin \omega x}{\sin \omega} = g(x, T_2) \tag{4.85}$$

$$\phi = 0 \quad \text{at} \quad x = 0 \tag{4.86}$$

$$\phi_{,x} + \alpha\phi = \frac{1}{\alpha_1}\left[-\frac{1}{2} F e^{i\sigma T_2} - 2i\omega A' - 2\alpha_2 B A^2 \bar{A} \right] = h(T_2) \quad \text{at} \quad x = 1 \tag{4.87}$$

where

$$\alpha = \frac{\alpha_0 - \omega^2}{\alpha_1} \quad \text{and} \quad B = 2c_1 + c_2 + \frac{3\alpha_3}{2\alpha_2} \tag{4.88}$$

Multiplying (4.85) by the adjoint function $\psi(x)$ and integrating the result by parts from $x = 0$ to $x = 1$ to transfer the derivatives from ϕ to ψ yields

$$[\phi_{,x}\psi - \phi\psi']_0^1 + \int_0^1 (\psi'' + \omega^2\psi)\phi dx = \int_0^1 \psi g dx \tag{4.89}$$

The equation governing the adjoint function is obtained by setting the coefficient of ϕ in the integrand in (4.89) equal to zero; that is,

$$\psi'' + \omega^2\psi = 0 \tag{4.90}$$

To determine the boundary conditions for the adjoint function, we consider the homogeneous problem. Thus, using (4.86) and (4.87) in (4.89) with g and h being zero yields

$$\phi(1, T_2)[\psi'(1) + \alpha\psi(1)] + \phi_{,x}(0, T_2)\psi(0) = 0$$

Setting each of the coefficients of $\phi(1, T_2)$ and $\phi_{,x}(0, T_2)$ equal to zero yields the boundary conditions

$$\psi(0) = 0, \quad \psi'(1) + \alpha\psi(1) = 0 \tag{4.91}$$

Having defined the adjoint problem, we return to the inhomogeneous problem, use (4.86), (4.87), (4.90), and (4.91) in (4.89), and obtain the following solvability condition:

$$h\psi(1) = \int_0^1 \psi g dx \tag{4.92}$$

The solution of (4.90) and (4.91) can be expressed as

$$\psi = \frac{\sin \omega x}{\sin \omega} \tag{4.93}$$

where ω is governed by (4.73). Substituting for h, g, and ψ in (4.92), we rewrite the solvability condition as

$$2i\omega(A' + \tilde{\mu}A) = \frac{-\Gamma}{\alpha_1}\left[2i\omega A' + 2\alpha_2 B A^2 \bar{A} + \frac{1}{2} F e^{i\sigma T_2}\right] \tag{4.94}$$

where

$$\Gamma = \left[\int_0^1 \frac{\sin^2 \omega x}{\sin^2 \omega} dx\right]^{-1} = \frac{4\omega \sin^2 \omega}{2\omega - \sin 2\omega} \tag{4.95}$$

Substituting the polar form (4.15) into (4.94) and separating the result into real and imaginary parts yields

$$a' = -\mu a - \frac{f}{2\omega} \sin \gamma \tag{4.96}$$

$$a\beta' = \alpha_e a^3 + \frac{f}{2\omega} \cos \gamma \tag{4.97}$$

$$\gamma = \sigma T_2 - \beta \tag{4.98}$$

where $\mu = \alpha_1\tilde{\mu}/(\alpha_1 + \Gamma)$,

$$\alpha_e = \frac{\Gamma\alpha_2 B}{4\omega(\alpha_1 + \Gamma)} = \frac{3\alpha}{8\omega} - \frac{\alpha_2\delta}{4\omega}\left[\frac{2}{\alpha_1 + \alpha_0} + \frac{1}{\alpha_0 - 4\omega^2 + 2\omega\alpha_1 \cot 2\omega}\right] \tag{4.99}$$

$$(\delta, \alpha, f) = \frac{\Gamma}{\Gamma + \alpha_1}(\alpha_2, \alpha_3, F) = \frac{4\omega \sin^2\omega}{\alpha_1(2\omega - \sin 2\omega) + 4\omega \sin^2\omega}(\alpha_2, \alpha_3, F) \tag{4.100}$$

Using (4.98) and (4.97) to eliminate β yields

$$a\gamma' = \sigma a - \alpha_e a^3 - \frac{f}{2\omega}\cos\gamma \tag{4.101}$$

Substituting (4.74) and (4.79) into (4.59), recalling that $\Omega = \omega + \varepsilon^2\sigma$, and using (4.15) and (4.98), we obtain to the second approximation

$$w \simeq a\cos(\Omega t - \gamma)\frac{\sin\omega x}{\sin\omega} - \frac{1}{2}\varepsilon^2\alpha_2 a^2\left[\frac{x}{\alpha_1 + \alpha_0} + \frac{\sin 2\omega x \cos(2\Omega t - 2\gamma)}{(\alpha_0 - 4\omega^2)\sin 2\omega + 2\omega\alpha_1 \cos 2\omega}\right] \tag{4.102}$$

where a and γ are defined by (4.96) and (4.101).

4.3.2. Attacking the discretized problem

One of the most commonly used procedures for obtaining approximate solutions of nonlinear distributed-parameter problems is to discretize the problem first. For the problem at hand, one assumes an approximate solution in the form

$$w \simeq \sum_{n=1}^{\infty} \eta_n(t)\phi_n(x) \tag{4.103}$$

Because (4.103) does not satisfy the partial-differential equation (4.54) and boundary conditions (4.55) and (4.56) exactly, one uses a weighted residual procedure, such as the Galerkin or Ritz procedure, to minimize the errors, thereby obtaining nonlinear coupled second-order ordinary-differential equations governing the η_n. These equations and the associated boundary conditions are called the discretized form of the distributed-parameter problem. Then, one can use either a perturbation or a numerical method to analyze the solutions of the resulting discretized form of the problem. In many instances, one chooses the $\phi_n(x)$ to be the mode shapes of the linear problem. Typically, N is taken to be unity and the result is called a single-mode approximation. Thus, for the present problem, one seeks an approximate solution of (4.54)-(4.56) in the form

$$w(x,t) \simeq \eta(t) \frac{\sin \omega x}{\sin \omega} \tag{4.104}$$

where ω is one of the linear frequencies that can be calculated from the transcendental equation (4.73) and $\eta(t)$ is a time-varying function to be determined.

Clearly, there is no two-term function $\eta(t)$ that will make it possible for the assumed approximation in (4.104) to match the correct approximation given in (4.102). The only possibility is that the first terms in the two expansions will match. But, as we show next, even this match does not occur.

Because one of the boundary conditions is nonlinear, it is more convenient to determine the equation governing $\eta(t)$ by using the Lagrangian. Substituting (4.104)

into (4.58) and integrating the result from $x = 0$ to $x = 1$ yields the following Lagrangian:

$$L = \frac{1}{2}\dot{\eta}^2 - \frac{1}{2}\omega^2\eta^2 - \frac{1}{3}\delta\eta^3 - \frac{1}{4}\alpha\eta^4 - f\eta\cos\Omega t \tag{4.105}$$

where

$$(\delta, \alpha, f) = \frac{\Gamma}{\Gamma + \alpha_1}(\alpha_2, \alpha_3, F) = \frac{4\omega\sin^2\omega}{\alpha_1(2\omega - \sin 2\omega) + 4\omega\sin^2\omega}(\alpha_2, \alpha_3, F) \tag{4.106}$$

Writing the Euler-Lagrange equation associated with the Lagrangian in (4.105) yields the following:

$$\ddot{\eta} + \omega^2\eta + 2\hat{\mu}\dot{\eta} + \delta\eta^2 + \alpha\eta^3 = -f\cos\Omega t \tag{4.107}$$

where damping was added. Nayfeh (1985) extensively studied the weakly nonlinear solutions of (4.107) by using different perturbation techniques. We summarize some of these solutions for comparison with solutions obtained by attacking the original problem. For the case of primary resonance, Nayfeh (1985) found that, to the second approximation,

$$\eta = \varepsilon a\cos(\Omega t - \gamma) + \frac{\varepsilon^2\delta a^2}{6\omega^2}[\cos(2\Omega t - 2\gamma) - 3] + \ldots \tag{4.108}$$

where f was replaced with $\varepsilon^3 f$ and a and β are governed by

$$a' = -\mu a - \frac{f}{2\omega}\sin\gamma \tag{4.109}$$

$$a\beta' = \hat{\alpha}_e a^3 + \frac{f}{2\omega}\cos\gamma \tag{4.110}$$

$$\gamma = \sigma T_2 - \beta, \quad \hat{\alpha}_e = \frac{9\alpha\omega^2 - 10\delta^2}{24\omega^3} \tag{4.111}$$

Therefore, to the second approximation,

$$w = \frac{\sin \omega x}{\sin \omega} \left\{ a \cos(\Omega t - \gamma) + \frac{\delta a^2}{6\omega^2} [\cos(2\Omega t - 2\gamma) - 3] + \ldots \right\} \tag{4.112}$$

where a and γ are given by (4.109)-(4.111). We note that (4.109) and (4.110) have the same form as (4.96) and (4.97), but that α_e in (4.97) is not the same as $\hat{\alpha}_e$ in (4.110). Therefore, we conclude that even the one-term result obtained by the single-mode discretization is wrong; it fails to capture the effect of the nonlinearity (manifested in the coefficients α_e and $\hat{\alpha}_e$) correctly.

4.3.3. Time-averaged Lagrangian

A quick inspection of the Lagrangian in (4.58) shows that the cubic term is the source of the quadratic nonlinearity in the boundary condition (4.56). Therefore, this term is responsible for the drift and second-harmonic components in the response (4.102).

Hence, to determine a uniform expansion, we express w to second order in ε as

$$w \simeq \varepsilon(Ae^{i\omega T_0} + \bar{A}e^{-i\omega T_0}) \frac{\sin \omega x}{\sin \omega} + \varepsilon^2 \phi_0(x) A\bar{A} + \varepsilon^2 \phi_1(x)(A^2 e^{2i\omega T_0} + \bar{A}^2 e^{-2i\omega T_0}) \tag{4.113}$$

where $\phi_0(x)$, $\phi_1(x)$, and $A(T_2)$ are to be determined from the analysis. We remark that the determination of ϕ_0 and ϕ_1 may require extensive algebra and numerical calculations in other physical problems when applying the time-averaged-Lagrangian

method; nevertheless, the neatness and the considerable reduction in the algebra are rather striking in comparison with attacking the nonlinear partial-differential equations and boundary conditions.

Substituting (4.113) into (4.58), replacing $\hat{F}$ by $\varepsilon^3 F$, keeping terms up to $0(\varepsilon^4)$, averaging with respect to T_0 over the period $2\pi/\omega$, considering T_2 to be constant, and recalling that $\Omega = \omega + \varepsilon^2\sigma$, we obtain

$$\begin{aligned} <L> = i\varepsilon^4\omega\left\{1 + \frac{\alpha_1}{\sin^2\omega}\int_0^1 \sin^2\omega x\, dx\right\}(A\bar{A}' - \bar{A}A') \\ + \varepsilon^4\left\{\alpha_1\int_0^1\left[4\omega^2\phi_1^2(x) - \phi_1'^2(x) - \frac{1}{2}\phi_0'^2(x)\right]dx\right. \\ - \frac{3}{2}\alpha_3 - 2\alpha_2[\phi_0(1) + \phi_1(1)] + (4\omega^2 - \alpha_0)\phi_1^2(1) \\ \left. - \frac{1}{2}\alpha_0\phi_0^2(1)\right\}A^2\bar{A}^2 - \frac{1}{2}\varepsilon^4 F(Ae^{-i\sigma T_2} + \bar{A}e^{i\sigma T_2}) \end{aligned} \tag{4.114}$$

To solve for ϕ_0 and ϕ_1, one can either use a finite-element method directly on the Lagrangian or solve the differential equations and boundary conditions governing them. In this work, we use the latter approach. To this end, we use the calculus of variations and focus our attention on the coefficient of $A^2\bar{A}^2$. Moreover, we define this coefficient as the functional I and write

$$\begin{aligned} I = 4\alpha_1\omega^2\int_0^1\phi_1^2(x)dx - \alpha_1\int_0^1\phi_1'^2(x)dx - \frac{1}{2}\alpha_1\int_0^1\phi_0'^2(x)dx \\ - \frac{3}{2}\alpha_3 - 2\alpha_2[\phi_0(1) + \phi_1(1)] + (4\omega^2 - \alpha_0)\phi_1^2(1) - \frac{1}{2}\alpha_0\phi_0^2(1) \end{aligned} \tag{4.115}$$

The functional I is obviously a function of ϕ_0, ϕ_1, and their first derivatives. Hence, the first variation of I is given by

$$\delta I = \frac{\partial I}{\partial \phi_1}\delta\phi_1 + \frac{\partial I}{\partial \phi_1'}\delta\phi_1' + \frac{\partial I}{\partial \phi_0}\delta\phi_0 + \frac{\partial I}{\partial \phi_0'}\delta\phi_0' \tag{4.116}$$

Substituting (4.115) into (4.116) and integrating the result by parts so that δI contains only $\delta\phi_0$ and $\delta\phi_1$ (i.e., δI free of $\delta\phi_0'$ and $\delta\phi_1'$) yields

$$\begin{aligned}\delta I = {} & 8\alpha_1\omega^2\int_0^1 \phi_1\delta\phi_1 dx - 2\alpha_1\left[\phi_1'\delta\phi_1\Big|_0^1 - \int_0^1 \delta\phi_1\phi_1'' dx\right] \\ & - \alpha_1\left[\phi_0'\delta\phi_0\Big|_0^1 - \int_0^1 \delta\phi_0\phi_0'' dx\right] - 2\alpha_2\delta\phi_0(1) \\ & - 2\alpha_2\delta\phi_1(1) + 2(4\omega^2 - \alpha_0)\phi_1(1)\delta\phi_1(1) - \alpha_0\phi_0(1)\delta\phi_0(1)\end{aligned} \tag{4.117}$$

Requiring that $\delta I = 0$ and that $\delta\phi_0$ and $\delta\phi_1$ be independent arbitrary functions, we arrive at the following Euler-Lagrange equations and associated boundary conditions:

$\delta\phi_0$:

$$\alpha_1\phi_0'' = 0 \quad 0 < x < 1 \tag{4.118}$$

$$\phi_0 = 0 \quad \text{at} \quad x = 0 \tag{4.119}$$

$$\alpha_1\phi_0' + \alpha_0\phi_0 = -2\alpha_2 \quad \text{at} \quad x = 1 \tag{4.120}$$

$\delta\phi_1$:

$$\phi_1'' + 4\omega^2\phi_1 = 0 \quad 0 < x < 1 \tag{4.121}$$

$$\phi_1 = 0 \quad \text{at} \quad x = 0 \tag{4.122}$$

$$\alpha_1\phi_1' + (\alpha_0 - 4\omega^2)\phi_1 = -\alpha_2 \quad \text{at} \quad x = 1 \tag{4.123}$$

Solving equations (4.118)-(4.120) and (4.121)-(4.123) yields

$$\phi_0 = \frac{-2\alpha_2 x}{\alpha_1 + \alpha_0} \tag{4.124}$$

$$\phi_1 = \frac{-\alpha_2 \sin 2\omega x}{(\alpha_0 - 4\omega^2)\sin 2\omega + 2\omega\alpha_1 \cos 2\omega} \tag{4.125}$$

which are in full agreement with (4.79) and (4.80) obtained by attacking the original problem.

Substituting (4.124) and (4.125) into (4.114) and simplifying, we rewrite the time-averaged Lagrangian as

$$\begin{aligned} <L> = \frac{\Gamma + \alpha_1}{\Gamma}\varepsilon^4\Big[& i(A\bar{A}' - \bar{A}A') \\ & - 4\alpha_e A^2\bar{A}^2 - \frac{f}{2\omega}\left(A\bar{e}^{i\sigma T_2} + \bar{A}e^{i\sigma T_2}\right)\Big] \end{aligned} \tag{4.126}$$

where α_e is defined in (4.99) and Γ is defined in (4.95). Introducing the polar form (4.15) into (4.126) and using (4.98), we obtain

$$\begin{aligned} <L> &= \frac{\Gamma + \alpha_1}{\Gamma}\varepsilon^4\left[\frac{1}{2}a^2\beta' - \frac{1}{4}\alpha_e a^4 - \frac{fa}{2\omega}\cos(\sigma T_2 - \beta)\right] \\ \text{or} \\ <L> &= \frac{\Gamma + \alpha_1}{\Gamma}\varepsilon^4\left[\frac{1}{2}a^2(\sigma - \gamma') - \frac{1}{4}\alpha_e a^4 - \frac{fa}{2\omega}\cos\gamma\right] \end{aligned} \tag{4.127}$$

where $\gamma = \sigma T_2 - \beta$ and the prime indicates the derivative with respect to T_2. Substituting (4.127) into (4.32) and (4.33) with β being replaced by γ yields after some algebra

$$a' = -\frac{f}{2\omega}\sin\gamma \tag{4.128}$$

and

$$a\gamma' = \sigma a - \alpha_e a^3 - \frac{f}{2\omega}\cos\gamma \tag{4.129}$$

where f, δ, and α are defined in (4.106). Equations (4.128) and (4.129) with the proper damping term added to (4.128) are in full agreement with (4.96) and (4.101) obtained by attacking the original problem.

4.4. Case of Subharmonic Resonance of Order One-Half

In this resonance, the excitation frequency Ω is approximately twice one of the linear natural frequencies ω of the system; that is, $\Omega = 2\omega + \varepsilon^2\sigma$. Again, any mode that is neither directly excited nor indirectly excited through an internal resonance will decay with time. If $w = 0(\varepsilon)$, then in order that the subharmonic resonance balances the effect of the nonlinearity, we put $\hat{F} = \varepsilon^2 F$. Attacking the original problem, Nayfeh and Bouguerra (1990) obtained the second-order uniform expansion

$$\begin{aligned} w \simeq \varepsilon a \frac{\sin\omega x}{\sin\omega}\cos\left(\frac{1}{2}\Omega t - \frac{1}{2}\gamma\right) - 2\varepsilon^2\Lambda\frac{\sin\Omega x}{\sin\Omega}\cos\Omega t \\ -\frac{1}{2}\varepsilon^2\alpha_2\chi(2\omega)a^2\frac{\sin 2\omega x}{\sin 2\omega}\cos(\Omega t - \gamma) - \frac{\varepsilon^2\alpha_2 a^2 x}{2(\alpha_0 + \alpha_1)} \end{aligned} \tag{4.130}$$

where

$$a' = -\mu a + \frac{\delta\Lambda}{\omega} a \sin\gamma \tag{4.131}$$

$$a\gamma' = \sigma a - 2\alpha_e a^3 + \frac{2\delta\Lambda}{\omega} a \cos\gamma \tag{4.132}$$

$$\Lambda = \frac{1}{2} F\chi(\Omega) \tag{4.133}$$

$$\chi(\Omega) = \frac{\sin\Omega}{\alpha_1\Omega\cos\Omega + (\alpha_0 - \Omega^2)\sin\Omega} \tag{4.134}$$

and α_e is defined in (4.99).

To determine a second-order uniform expansion by using the time-averaged Lagrangian, we postulate that

$$w \simeq \varepsilon A \frac{\sin\omega x}{\sin\omega} e^{i\omega T_0} + \varepsilon^2\left[-\Lambda \frac{\sin\Omega x}{\sin\Omega} e^{i\Omega T_0} + \frac{1}{2}\phi_0(x)A\bar{A} + \phi_1(x)A^2 e^{2i\omega T_0}\right] + cc \tag{4.135}$$

where Λ is defined by (4.133) and (4.134). Substituting (4.135) into the Lagrangian (4.58), averaging over the fast-time scale, and setting its variation with respect to ϕ_0 and ϕ_1 equal to zero, we obtain equations (4.118)-(4.123) whose solution is (4.124) and (4.125). Then, substituting the polar form (4.15) into the resulting Lagrangian, writing the Euler-Lagrange equations, and adding a linear damping term, we obtain (4.131) and (4.132), the solution obtained by attacking the original problem.

Attacking the single-mode discretized form (4.107), Nayfeh (1985) obtained the second-order expansion

$$\eta = \varepsilon a \cos\left(\frac{1}{2}\Omega t - \frac{1}{2}\gamma\right) - 2\varepsilon^2\hat{\Lambda}\cos\Omega t + \frac{\varepsilon^2\delta a^2}{6\omega^2}[\cos(\Omega t - \gamma) - 3] + \ldots \tag{4.136}$$

where

$$a' = -\mu a + \frac{\delta\hat{\Lambda}}{\omega} a \sin\gamma \tag{4.137}$$

$$a\gamma' = \sigma a - 2\hat{\alpha}_e a^3 + \frac{2\delta\hat{\Lambda}}{\omega} a \cos\gamma \tag{4.138}$$

$$\hat{\Lambda} = \frac{f}{2(\omega^2 - \Omega^2)} \tag{4.139}$$

and $\hat{\alpha}_e$ is defined in (4.111). It follows from (4.104) and (4.136) that

$$w = \frac{\sin\omega x}{\sin\omega}\left\{a\cos\left(\frac{1}{2}\Omega t - \frac{1}{2}\gamma\right) - 2\hat{\Lambda}\cos\Omega t + \frac{\delta a^2}{6\omega^2}[\cos(\Omega t - \gamma) - 3]\right\} + \ldots \tag{4.140}$$

Clearly, the single-mode discretization cannot produce the spatial variations of the drift and second-harmonic terms. Moreover, comparing (4.139) with (4.133) and (4.134), we conclude that the single-mode discretization does not produce the correct value for Λ. Finally, the effective nonlinearity $\hat{\alpha}_e$ predicted by the single-mode discretization is also wrong.

4.5. Case of Superharmonic Resonance of Order Two

In this resonance, the excitation frequency Ω is approximately one-half of one of the natural frequencies ω. We express the nearness of 2Ω to ω by introducing the detuning parameter σ defined according to

$$2\Omega = \omega + \varepsilon^2\sigma \tag{4.141}$$

As in the case of subharmonic resonance of order one-half, we put $\hat{F} = \varepsilon^{3/2}F$ so that the superharmonic resonance balances the effect of the nonlinearity. Attacking the original problem, Nayfeh and Bouguerra (1990) obtained the second-order expansion

$$\begin{aligned} w = {} & \varepsilon a \frac{\sin \omega x}{\sin \omega} \cos(2\Omega t - \gamma) - 2\varepsilon^{3/2}\Lambda \frac{\sin \Omega x}{\sin \Omega} \cos \Omega t \\ & - \frac{1}{2}\varepsilon^2\alpha_2\chi(2\omega)a^2 \frac{\sin 2\omega x}{\sin 2\omega} \cos(4\Omega t - 2\gamma) - \frac{\varepsilon^2\alpha_2 a^2 x}{2(\alpha_0 + \alpha_1)} + \ldots \end{aligned} \tag{4.142}$$

where Λ and χ are defined in (4.133) and (4.134) and

$$a' = -\mu a - \frac{\delta\Lambda^2}{\omega} \sin \gamma \tag{4.143}$$

$$a\gamma' = \sigma a - \alpha_e a^3 - \frac{\delta\Lambda^2}{\omega} \cos \gamma \tag{4.144}$$

Assuming the form

$$\begin{aligned} w = {} & \varepsilon A \frac{\sin \omega x}{\sin \omega} e^{i\omega T_0} - \varepsilon^{3/2}\Lambda \frac{\sin \Omega x}{\sin \Omega} e^{i\Omega T_0} \\ & + \varepsilon^2\left[\frac{1}{2}\phi_0(x)A\overline{A} + \phi_1(x)A^2 e^{2i\omega T_0} \right] + cc \end{aligned} \tag{4.145}$$

and using the time-averaged Lagrangian, we obtained (4.142)-(4.144) except for the damping term in (4.143).

Attacking the discretized form (4.107), Nayfeh (1985) obtained the second-order approximation

$$\eta = \varepsilon a \cos(2\Omega t - \gamma) - 2\varepsilon^{3/2}\hat{\Lambda} \cos \Omega t + \frac{\varepsilon^2\delta a^2}{6\omega^2}\left[\cos(4\Omega t - 2\gamma) - 3 \right] + \ldots \tag{4.146}$$

where

$$a' = -\mu a - \frac{\delta \hat{\Lambda}^2}{\omega} \sin \gamma \tag{4.147}$$

$$a\gamma' = \sigma a - \hat{\alpha}_e a^3 - \frac{\delta \hat{\Lambda}^2}{\omega} \cos \gamma \tag{4.148}$$

where $\hat{\Lambda}$ and $\hat{\alpha}_e$ are defined in (4.139) and (4.111). Therefore, to the second approximation

$$w = \frac{\sin \omega x}{\sin \omega} \left\{ \varepsilon a \cos(2\Omega t - \gamma) - 2\varepsilon^{3/2} \hat{\Lambda} \cos \Omega t + \frac{\varepsilon^2 \delta a^2}{6\omega^2} [\cos(4\Omega t - 2\gamma) - 3] \right\} + \ldots \tag{4.149}$$

Again, the single-mode discretization (a) cannot produce the correct spatial variations of the drift, first-harmonic, and fourth-harmonic terms, (b) produces the wrong effective nonlinearity, and (c) produces the wrong value of Λ.

4.6. Case of Subharmonic Resonance of Order One-Third

In this case, we put

$$\Omega = 3\omega + \varepsilon^2 \sigma \tag{4.150}$$

In order that the subharmonic resonance of order one-third balances the effect of nonlinearity, we put $\hat{F} = \varepsilon F$. Consequently, attacking the original problem, Nayfeh and Bouguerra (1990) found that

$$w_1 = A\frac{\sin \omega x}{\sin \omega} e^{i\omega T_0} - \Lambda \frac{\sin \Omega x}{\sin \Omega} e^{i\Omega T_0} + cc \tag{4.151}$$

where ω is defined by equation (4.73) and Λ is defined by (4.133) and (4.134). Carrying out the expansion to second order, they found that

$$\begin{aligned} w = \varepsilon\left(A\frac{\sin \omega x}{\sin \omega} e^{i\omega t} - \Lambda \frac{\sin \Omega x}{\sin \Omega} e^{i\Omega t}\right) - \varepsilon^2\alpha_2\Big\{\chi(2\omega)A^2 \frac{\sin 2\omega x}{\sin 2\omega} e^{2i\omega t} \\ + \chi(2\Omega)\Lambda^2 \frac{\sin 2\Omega x}{\sin 2\Omega} e^{2i\Omega t} - 2\Lambda A\chi(\Omega+\omega)\frac{\sin(\Omega+\omega)x}{\sin(\Omega+\omega)} e^{i(\omega+\Omega)t} \\ - 2\Lambda\bar{A}\chi(\Omega-\omega)\frac{\sin(\Omega-\omega)x}{\sin(\Omega-\omega)} e^{i(\Omega-\omega)t} + \frac{1}{\alpha_0+\alpha_1}(A\bar{A}+\Lambda^2)x\Big\} + cc \end{aligned} \tag{4.152}$$

where the function χ is defined in (4.134). Letting $a = \frac{1}{2}a\exp(i\beta)$, we find that

$$a' = -\mu a + \frac{\Gamma B_2 \Lambda}{\omega(\alpha_1+\Gamma)} a^2 \sin\gamma \tag{4.153}$$

$$a\beta' = \alpha_e a^3 + \frac{\Gamma}{\omega(\alpha_1+\Gamma)}\left[-B_2\Lambda a^2\cos\gamma + B_3\Lambda^2 a\right] \tag{4.154}$$

$$\gamma = \sigma T_2 - 3\beta \tag{4.155}$$

$$4B_2 = 3\alpha_3 - 2\alpha_2^2[\chi(2\omega) + 2\chi(\Omega-\omega)] \tag{4.156}$$

$$B_3 = 3\alpha_3 - 2\alpha_2^2\left[\chi(\Omega+\omega) + \chi(\Omega-\omega) + (\alpha_0+\alpha_1)^{-1}\right] \tag{4.157}$$

To determine a uniform expansion by using the time-averaged Lagrangian, we need to assume a form for the expansion that fully accounts for the influence of the quadratic nonlinearity. In this case, because the first-order expansion consists of two terms having the frequencies ω and Ω according to (4.151), the second-order term must contain all possible terms arising from the interaction of the first-order terms

due to the quadratic nonlinearity; that is, it must contain a drift term and terms having the frequencies 2ω, 2Ω, $\Omega + \omega$, and $\Omega - \omega$. Consequently, we assume a solution of the form

$$\begin{aligned} w = \varepsilon\left(A\frac{\sin \omega x}{\sin \omega}e^{i\omega T_0} - \Lambda\frac{\sin \Omega x}{\sin \Omega}e^{i\Omega T_0}\right) \\ + \varepsilon^2\left[\phi_0(x)A\bar{A} + \phi_1(x)\Lambda^2 + \phi_2(x)A^2e^{2i\omega T_0} + \phi_3(x)\Lambda^2e^{2i\Omega T_0}\right. \\ \left. + \phi_4(x)\ A\Lambda e^{i(\Omega+\omega)T_0} + \phi_5(x)\Lambda\bar{A}e^{i(\Omega-\omega)T_0}\right] + cc \end{aligned} \tag{4.158}$$

Substituting (4.158) into the Lagrangian, averaging it over the fast-time scale, and requiring the first variation of the averaged Lagrangian to vanish, we obtain the equations and boundary conditions governing the $\phi_n(x)$. Solving these problems, we find that the resulting expression for w in (4.158) is identical to (4.152) obtained by attacking the original problem. Expressing A in the polar form (4.15) and writing the Euler-Lagrange equations, we obtain (4.153)-(4.157) except for the damping term in (4.153).

Attacking the single-mode discretized form (4.107), Nayfeh (1985) obtained the second-order expansion

$$\begin{aligned} \eta = \varepsilon a\cos(\omega t + \beta) - 2\varepsilon\hat{\Lambda}\cos\Omega t - \varepsilon^2\left\{\frac{\delta}{2\omega^2}(a^2 + \hat{\Lambda}^2) - \frac{\delta a^2}{6\omega^2}\cos(2\omega t + 2\beta)\right. \\ + \frac{2\delta\hat{\Lambda}^2}{\omega^2 - 4\Omega^2}\cos\ 2\Omega t + \frac{2\delta\hat{\Lambda}a}{\Omega(\Omega + 2\omega)}\cos[(\omega + \Omega)t + \beta] \\ \left. + \ \frac{2\delta\hat{\Lambda}a}{\Omega(\Omega - 2\omega)}\cos[(\omega - \Omega)t + \beta]\right\} + \ldots \end{aligned} \tag{4.159}$$

where

$$a' = -\mu a + \left(\frac{3\alpha}{4\omega} + \frac{\delta^2}{2\omega^3}\right)\hat{\Lambda}a^2\sin\gamma \tag{4.160}$$

$$a\beta' = \left(\frac{3\alpha}{\omega} - \frac{6\delta^2}{5\omega^3} \right) \hat{\Lambda}^2 a + \hat{\alpha}_e a^3 - \left(\frac{3\alpha}{4\omega} + \frac{\delta^2}{2\omega^3} \right) \hat{\Lambda} a^2 \cos\gamma \tag{4.161}$$

$$\gamma = \sigma T_2 - 3\beta \tag{4.162}$$

where $\hat{\Lambda}$, δ, α, and $\hat{\alpha}_e$ are defined in (4.139), (4.106), and (4.111). Comparing (4.104) and (4.159) with (4.152), we conclude that the single-mode discretization fails to produce the correct (a) spatial variations of the drift term and the terms having the frequencies 2ω, 2Ω, $\Omega + \omega$, and $\Omega - \omega$; (b) linear shift of the frequency; (c) effective strength of the resonance; and (d) nonlinear frequency shift.

4.7. Case of Superharmonic Resonance of Order Three

In this case, we introduce the detuning parameter σ defined as

$$3\Omega = \omega + \varepsilon^2 \sigma \tag{4.163}$$

Attacking the original problem, Nayfeh and Bouguerra (1990) obtained the second-order expansion (4.152) where $A = \frac{1}{2} a \exp(i\beta)$,

$$a' = -\mu a + \frac{\Gamma B_4 \Lambda^3}{\omega(\alpha_1 + \Gamma)} \sin\gamma \tag{4.164}$$

$$a\beta' = \alpha_e a^3 + \frac{\Gamma}{\omega(\alpha_1 + \Gamma)} \left[-B_4 \Lambda^3 \cos\gamma + B_3 \Lambda^2 a \right] \tag{4.165}$$

$$\gamma = \sigma T_2 - \beta \tag{4.166}$$

$$B_4 = \alpha_3 - 2\alpha_2^2 \chi(2\Omega) \tag{4.167}$$

Starting with the assumed form (4.158) and using the time-averaged Lagrangian, we obtain the same expansion obtained by Nayfeh and Bouguerra (1990).

Attacking the single-mode discretized form (4.107), Nayfeh (1985) obtained the second-order expansion (4.159) where

$$a' = -\mu a + \left(\alpha - \frac{18\delta^2}{5\omega^2}\right)\frac{\hat{\Lambda}^3}{\omega}\sin\gamma \tag{4.168}$$

$$a\beta' = \left(\frac{3\alpha}{\omega} - \frac{6\delta^2}{5\omega^3}\right)\hat{\Lambda}^2 a + \hat{\alpha}_e a^3 - \left(\alpha - \frac{18\delta^2}{5\omega^2}\right)\frac{\hat{\Lambda}^3}{\omega}\cos\gamma \tag{4.169}$$

$$\gamma = \sigma T_2 - \beta \tag{4.170}$$

and $\hat{\Lambda}, \alpha, \delta$, and $\hat{\alpha}_e$ are defined in (4.139), (4.106), and (4.111). As in the case of subharmonic resonance of order one-third, the single-mode discretization fails to produce the correct (a) spatial variations of the drift term and the terms having the frequencies 2ω, 2Ω, $\Omega + \omega$, and $\Omega - \omega$; (b) effective nonlinearity ; (c) linear shift of the frequency; and (d) strength of the resonance.

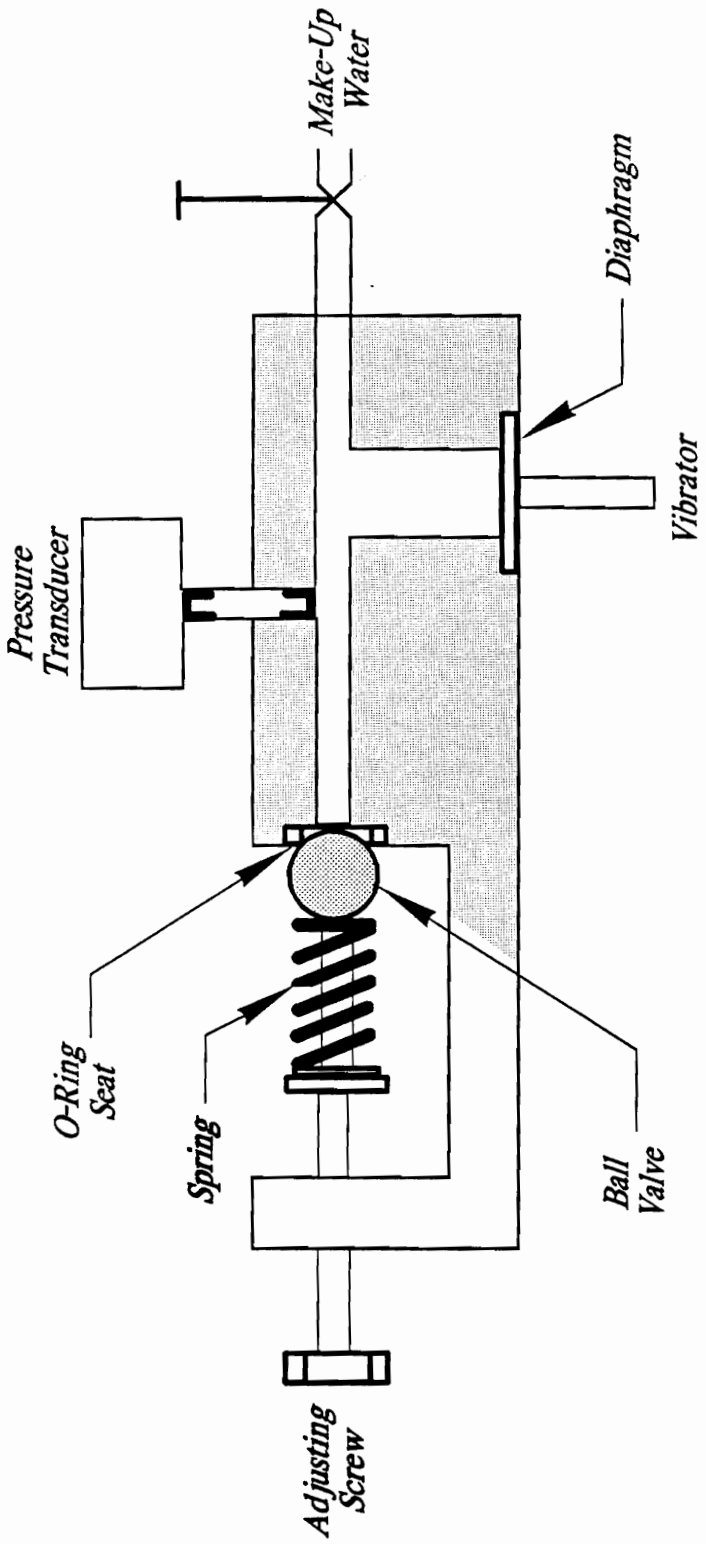

Figure 4.1. Experimental relief valve.

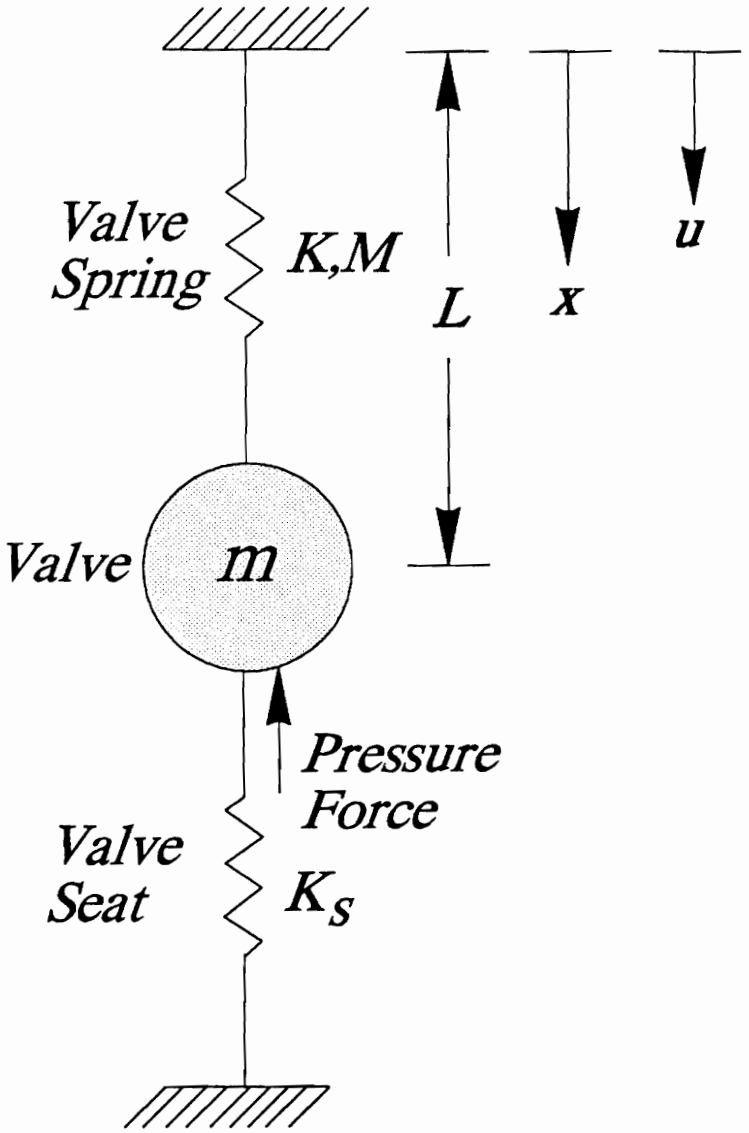

Figure 4.2. Schematic model of a relief valve.

5. NONLINEAR RESPONSE OF LAMINATED PLATES

In this chapter, following the solution procedure described in Chapter 4, we shall formulate the problem for the nonlinear vibrations of thick laminated plates and plate strips in cylindrical bending. Two first-order ordinary-differential equations are derived for the evolution of the amplitude and phase of the response for the following resonances: primary resonance, subharmonic resonance of order one-half, and superharmonic resonance of order two. The effects of the quadratic nonlinearities induced in the laminates by the bending-stretching coupling stiffnesses as well as the effects of the usual cubic nonlinearities caused by the stretching of the mid-plane of the laminates are taken into account, Although the procedure is quite general, antisymmetric cross-ply laminated plates and plate strips having simply-supported edge conditions are considered.

5.1. The Lagrangian in Terms of Displacements

In this section, we express the Lagrangian for a general laminated rectangular plate, which was previously derived in Section 2.5, in terms of the displacement variables u,v,w,ψ_x, and ψ_y. The expression for the kinetic energy was found to be (equation 2.13)

$$T=\frac{1}{2}\int_A \{I_1(\dot{u}^2+\dot{v}^2+\dot{w}^2)+\bar{I}_3(\dot{\psi}_x^2+\dot{\psi}_y^2)+2\bar{I}_2(\dot{u}\dot{\psi}_x+\dot{v}\dot{\psi}_y) -\frac{8}{3h^2}I_4(\dot{u}\dot{w}_{,x}+\dot{v}\dot{w}_{,y}) \\ -\frac{8}{3h^2}\bar{I}_5(\dot{\psi}_x\dot{w}_{,x}+\dot{\psi}_y\dot{w}_{,y})+\frac{16}{9h^4}I_7\,(\dot{w}_{,x}^2+\dot{w}_{,y}^2)\}dxdy \tag{5.1}$$

By virtue of equations (2.17) and (2.18) in conjunction with (2.5), the expression for the potential energy in (2.15) can be expressed in terms of the five displacement variables as

$$
\begin{aligned}
V = \frac{1}{2}\int_A \Big\{ \Big[& A_{11}(u_{,x} + \tfrac{1}{2}w_{,x}^2) + A_{12}(v_{,y} + \tfrac{1}{2}w_{,y}^2) + A_{16}(u_{,y} + v_{,x} + w_{,x}w_{,y}) \\
& - B_{11}\psi_{x,x} + B_{12}\psi_{y,y} + B_{16}(\psi_{x,y} + \psi_{y,x}) - \frac{4E_{11}}{3h^2}(\psi_{x,x} + w_{,xx}) \\
& - \frac{4E_{12}}{3h^2}(\psi_{y,y} + w_{,yy}) - \frac{4}{3h^2}E_{16}(\psi_{x,y} + \psi_{y,x} + 2w_{,xy}) \Big](u_{,x} + \tfrac{1}{2}w_{,x}^2) \\
& + \Big[A_{12}(u_{,x} + \tfrac{1}{2}w_{,x}^2) + A_{22}(v_{,y} + \tfrac{1}{2}w_{,y}^2) + A_{26}(u_{,y} + v_{,x} + w_{,x}w_{,y}) \\
& + B_{12}\psi_{x,x} + B_{22}\psi_{y,y} + B_{26}(\psi_{x,y} + \psi_{y,x}) - \frac{4}{3h^2}E_{12}(\psi_{x,x} + w_{,xx}) \\
& - \frac{4}{3h^2}E_{22}(\psi_{y,y} + w_{,yy}) - \frac{4}{3h^2}E_{26}(\psi_{x,y} + \psi_{y,x} + 2w_{,xy}) \Big](v_{,y} + \tfrac{1}{2}w_{,y}^2) \\
& + \Big[A_{16}(u_{,x} + \tfrac{1}{2}w_{,x}^2) + A_{26}(v_{,y} + \tfrac{1}{2}w_{,y}^2) + A_{66}(u_{,y} + v_{,x} + w_{,x}w_{,y}) \\
& + B_{16}\psi_{x,x} + B_{26}\psi_{y,y} + B_{66}(\psi_{x,y} + \psi_{y,x}) - \frac{4}{3h^2}E_{16}(\psi_{x,x} + w_{,xx}) \\
& - \frac{4}{3h^2}E_{26}(\psi_{y,y} + w_{,yy}) - \frac{4}{3h^2}E_{66}(\psi_{x,y} + \psi_{y,x} + 2w_{,xy}) \Big](u_{,y} + v_{,x} + w_{,x}w_{,y}) \\
& + \Big[B_{11}(u_{,x} + \tfrac{1}{2}w_{,x}^2) + B_{12}(v_{,y} + \tfrac{1}{2}w_{,y}^2) + B_{16}(u_{,y} + v_{,x} + w_{,x}w_{,y}) \\
& + D_{11}\psi_{x,x} + D_{12}\psi_{y,y} + D_{16}(\psi_{x,y} + \psi_{y,x}) - \frac{4}{3h^2}F_{11}(\psi_{x,x} + w_{,xx}) \\
& - \frac{4}{3h^2}F_{12}(\psi_{y,y} + w_{,yy}) - \frac{4}{3h^2}F_{16}(\psi_{x,y} + \psi_{y,x} + 2w_{,xy}) \Big]\psi_{x,x} \\
& + \Big[B_{12}(u_{,x} + \tfrac{1}{2}w_{,x}^2) + B_{22}(v_{,y} + \tfrac{1}{2}w_{,y}^2) + B_{26}(u_{,y} + v_{,x} + w_{,x}w_{,y}) \\
& + D_{12}\psi_{x,x} + D_{22}\psi_{y,y} + D_{26}(\psi_{x,y} + \psi_{y,x}) - \frac{4}{3h^2}F_{12}(\psi_{x,x} + w_{,xx}) \\
& - \frac{4}{3h^2}F_{22}(\psi_{y,y} + w_{,yy}) - \frac{4}{3h^2}F_{26}(\psi_{x,y} + \psi_{y,x} + 2w_{,xy}) \Big]\psi_{y,y} \\
& + \Big[B_{16}(u_{,x} + \tfrac{1}{2}w_{,x}^2) + B_{26}(v_{,y} + \tfrac{1}{2}w_{,y}^2) + B_{66}(u_{,y} + v_{,x} + w_{,x}w_{,y}) \\
& + D_{16}\psi_{x,x} + D_{26}\psi_{y,y} + D_{66}(\psi_{x,y} + \psi_{y,x}) - \frac{4}{3h^2}F_{16}(\psi_{x,x} + w_{,xx}) \\
& - \frac{4}{3h^2}F_{26}(\psi_{y,y} + w_{,yy}) - \frac{4}{3h^2}F_{66}(\psi_{x,y} + \psi_{y,x} + 2w_{,xy}) \Big](\psi_{x,y} + \psi_{y,x})
\end{aligned}
$$

$$
\begin{aligned}
&-\frac{4}{3h^2}\Big[E_{11}(u_{,x}+\frac{1}{2}w_{,x}^2)+E_{12}(v_{,y}+\frac{1}{2}w_{,y}^2)+E_{16}(u_{,y}+v_{,x}+w_{,x}w_{,y})\\
&+F_{11}\psi_{x,x}+F_{12}\psi_{y,y}+F_{16}(\psi_{x,y}+\psi_{y,x})-\frac{4}{3h^2}H_{11}(\psi_{x,x}+w_{,xx})\\
&-\frac{4}{3h^2}H_{12}(\psi_{y,y}+w_{,yy})-\frac{4}{3h^2}H_{16}(\psi_{x,y}+\psi_{y,x}+2w_{,xy})\Big](\psi_{x,x}+w_{,xx})\\
&-\frac{4}{3h^2}\Big[E_{12}(u_{,x}+\frac{1}{2}w_{,x}^2)+E_{22}(v_{,y}+w_{,yy})+E_{26}(u_{,y}+v_{,x}+w_{,x}w_{,y})\\
&+F_{12}\psi_{x,x}+F_{22}\psi_{y,y}+F_{26}(\psi_{x,y}+\psi_{y,x})-\frac{4}{3h^2}H_{12}(\psi_{x,x}+w_{,xx})\\
&-\frac{4}{3h^2}H_{22}(\psi_{y,y}+w_{,yy})-\frac{4}{3h^2}H_{26}(\psi_{x,y}+\psi_{y,x}+2w_{,xy})\Big](\psi_{y,y}+w_{,yy})\\
&-\frac{4}{3h^2}\Big[E_{16}(u_{,x}+\frac{1}{2}w_{,x}^2)+E_{26}(v_{,y}+\frac{1}{2}w_{,y}^2)+E_{66}(u_{,y}+v_{,x}+w_{,x}w_{,y})\\
&+F_{16}\psi_{x,x}+F_{26}\psi_{y,y}+F_{66}(\psi_{x,y}+\psi_{y,x})-\frac{4}{3h^2}H_{16}(\psi_{x,x}+w_{,xx})\\
&-\frac{4}{3h^2}H_{26}(\psi_{y,y}+w_{,yy})-\frac{4}{3h^2}H_{66}(\psi_{x,y}+\psi_{y,x}+2w_{,xy})\Big](\psi_{x,y}+\psi_{y,x}+2w_{,xy})\\
&+\Big[A_{44}(\psi_y+w_{,y})+A_{45}(\psi_x+w_{,x})-\frac{4}{h^2}D_{44}(\psi_y+w_{,y})\\
&-\frac{4}{h^2}D_{45}(\psi_x+w_{,x})\Big](\psi_y+w_{,y})\\
&-\frac{4}{h^2}\Big[D_{44}(\psi_y+w_{,y})+D_{45}(\psi_x+w_{,x})-\frac{4}{h^2}F_{44}(\psi_y+w_{,y})\\
&-\frac{4}{h^2}F_{45}(\psi_x+w_{,x})\Big](\psi_y+w_{,y})\\
&+\Big[A_{45}(\psi_y+w_{,y})+A_{55}(\psi_x+w_{,x})-\frac{4}{h^2}D_{45}(\psi_y+w_{,y})\Big]\\
&-\frac{4}{h^2}D_{55}(\psi_x+w_{,x})\Big](\psi_x+w_{,x})\\
&-\frac{4}{h^2}\Big[D_{45}(\psi_y+w_{,y})+D_{55}(\psi_x+w_{,x})-\frac{4}{h^2}F_{45}(\psi_y+w_{,y})\\
&-\frac{4}{h^2}F_{55}(\psi_x+w_{,x})\Big](\psi_x+w_{,x})-Qw\Big\}dxdy
\end{aligned}
\tag{5.2}
$$

The Lagrangian is the difference between the kinetic and potential energies in equations (5.1) and (5.2), respectively,

$$L = T - V \tag{5.3}$$

5.2. Rectangular Plates: Case of Primary Resonance

5.2.1. One-term Galerkin solution

The linear free-vibration solutions were obtained in Chapter 3 for antisymmetric cross-ply rectangular plates having simply-supported edge conditions. In this section, we use a one-term Galerkin procedure in conjunction with the time-averaged-Lagrangian technique and study the nonlinear response of these plates. The analysis in this section is intended to provide the usual analysis attempted by several researchers in the field of structural mechanics. We shall show later on in this chapter that such an analysis not only is incomplete, but also misses the effects of the quadratic nonlinearities induced in the laminates due to the bending-stretching couplings.

The linear solutions can be expressed as

$$u = \sum_{m,n=1}^{\infty} A(t)\, \chi_{1mn}\, \cos \alpha_m x\, \sin \beta_n y\, e^{i\omega_{mn}t} + cc \tag{5.4}$$

$$v = \sum_{m,n=1}^{\infty} A(t)\, \chi_{2mn} \sin \alpha_m x \cos \beta_n y\, e^{i\omega_{mn}t} + cc \tag{5.5}$$

$$w = \sum_{m,n=1}^{\infty} A(t)\, \chi_{3mn} \sin \alpha_m x \sin \beta_n y\, e^{i\omega_{mn}t} + cc \tag{5.6}$$

$$\psi_x = \sum_{m,n=1}^{\infty} A(t)\, \chi_{4mn} \cos \alpha_m x \sin \beta_n y\, e^{i\omega_{mn}t} + cc \tag{5.7}$$

$$\psi_y = \sum_{m,n=1}^{\infty} A(t)\, \chi_{5mn} \sin \alpha_m x \cos \beta_n y\, e^{i\omega_{mn}t} + cc \tag{5.8}$$

where the α_m and β_n are defined in (3.30) and the ω_{mn} and the $\chi_{imn}(i = 1,2,...,5)$ are given in Table 3.1 for each pair of m and n. The function $A(t)$ describes the complex amplitude of the response and is determined by using the time-averaged-Lagrangian technique. Moreover, the loading Q is assumed to be expandable in terms of the double Fourier series

$$Q = \sum_{m,n}^{\infty} F \sin \alpha_m x \sin \beta_n y \cos \Omega t \tag{5.9}$$

where F and Ω are the amplitude and frequency of the excitation, respectively.

We consider the case in which Ω is near ω_{mn}, and ω_{mn} is not commensurable or nearly commensurable with any of the rest of the natural undamped frequencies of the plate. Because, in the presence of damping, all modes that are not directly excited by the external excitation or indirectly excited by an internal resonance decay

with time, the plate response consists of the mn mode only. Thus, we drop the summation signs in equations (5.4)-(5.9) and introduce a detuning parameter σ defined according to

$$\Omega = \omega_{mn} + \sigma \tag{5.10}$$

where σ is small ($\sigma << 1$).

Next, we use the time-averaged-Lagrangian technique to obtain the nonlinear evolution equations that describe the amplitude and phase of the response. According to this technique, we substitute equations (5.4)-(5.9) into the expression for the Lagrangian in (5.3), average the Lagrangian over the period $2\pi/\omega_{mn}$, integrate the result over the domain of the plate, and obtain

$$<L> = \omega_{mn}\delta_{0mn}\left[i(A\bar{A}' - \bar{A}A') + 4\alpha_e A^2\bar{A}^2 + \frac{1}{2} f(Ae^{-i\sigma t} + \bar{A}e^{i\sigma t}) \right] \tag{5.11}$$

where the prime indicates the derivative with respect to time and

$$\begin{aligned} \delta_{0mn} = & -\frac{1}{4} ab\Big[I_1(\chi_{1mn}^2 + \chi_{2mn}^2 + \chi_{3mn}^2) + \bar{I}_3(\chi_{4mn}^2 + \chi_{5mn}^2) \\ & - \frac{8}{3h^2} \bar{I}_5\chi_{3mn}(\alpha_m\chi_{4mn} + \beta_n\chi_{5mn}) \\ & + \frac{16}{9h^4} I_7\, \chi_{3mn}^2(\alpha_m^2 + \beta_n^2)\Big] \end{aligned} \tag{5.12}$$

$$\delta_{1mn} = \frac{3}{1024} ab\chi_{3mn}^4\left[9A_{11}(\alpha_m^4 + \beta_n^4) + 2(A_{12} + 2A_{66})\alpha_m^2\beta_n^2 \right] \tag{5.13}$$

$$\alpha_e = \frac{\delta_{1mn}}{\omega_{mn}\delta_{0mn}}, \quad f = \frac{ab\chi_{3mn}F}{4\omega_{mn}\delta_{0mn}} \tag{5.14}$$

In equations (5.12)-(5.14), the summation notation over the indices m and n is not adopted. Inspecting the expression for δ_{1mn} in (5.13) shows that all the

bending-stretching coupling terms are absent. This result indicates that such terms have no effect on the nonlinear response of antisymmetric cross-ply plates. We shall see later on in this chapter that this is not the case if we assume the correct form of the approximate solution in conjunction with the time-averaged Lagrangian. Substituting the polar form $A = \frac{1}{2} a(t) \exp[i\beta(t)]$ into (5.11), we obtain

$$< L > = \frac{1}{2} \omega_{mn} \delta_{0mn} a^2 (\sigma - \gamma') + \frac{1}{4} \delta_{1mn} a^4 + \frac{1}{2} af \cos \gamma \tag{5.15}$$

where $\gamma = \sigma t - \beta$. Writing the Euler-Lagrange equations corresponding to the Lagrangian (5.15), we obtain the following amplitude and phase equations:

$$a' = \frac{1}{2} \sin \gamma \tag{5.16}$$

$$a\gamma' = a\sigma + \alpha_e a^3 + \frac{1}{2} f \cos \gamma \tag{5.17}$$

where

$$\alpha_e = \frac{\delta_{1mn}}{\omega_{mn} \delta_{0mn}} \tag{5.18}$$

5.2.2. Second-order approximate solution

To determine a second-order uniform expansion by using the time-averaged-Lagrangian technique, we postulate that

$$u = \varepsilon \phi_{10}(x,y) A e^{i\omega T_0} + \varepsilon^2 \{ \phi_{11}(x,y) A \bar{A} + \phi_{12}(x,y) A^2 e^{2i\omega T_0} \} + cc \tag{5.19a}$$

$$v = \varepsilon\phi_{20}(x,y)Ae^{i\omega T_0} + \varepsilon^2\{\phi_{21}(x,y)A\bar{A} + \phi_{22}(x,y)A^2e^{2i\omega T_0}\} + cc \qquad (5.19b)$$

$$w = \varepsilon\phi_{30}(x,y)Ae^{i\omega T_0} + \varepsilon^2\{\phi_{31}(x,y)A\bar{A} + \phi_{32}(x,y)A^2e^{2i\omega T_0}\} + cc \qquad (5.19c)$$

$$\phi_x = \varepsilon\phi_{40}(x,y)Ae^{i\omega T_0} + \varepsilon^2\{\phi_{41}(x,y)A\bar{A} + \phi_{42}(x,y)A^2e^{2i\omega T_0}\} + cc \qquad (5.19d)$$

$$\phi_y = \varepsilon\phi_{50}(x,y)Ae^{i\omega T_0} + \varepsilon^2\{\phi_{51}(x,y)A\bar{A} + \phi_{52}(x,y)A^2e^{2i\omega T_0}\} + cc \qquad (5.19e)$$

The $\phi_{i0}(i = 1,2,...,5)$ in equations (5.19) are the linear undamped free-vibrations modes and are given by

$$\phi_{10} = \chi_1 \cos \alpha x \sin \beta y \qquad (5.20a)$$

$$\phi_{20} = \chi_2 \sin \alpha x \cos \beta y \qquad (5.20b)$$

$$\phi_{30} = \chi_3 \sin \alpha x \sin \beta y \qquad (5.20c)$$

$$\phi_{40} = \chi_4 \cos \alpha x \sin \beta y \qquad (5.20d)$$

$$\phi_{50} = \chi_5 \sin \alpha x \cos \beta y \qquad (5.20e)$$

The spatial functions ϕ_{i1} and $\phi_{i2}(i = 1,2,...,5)$ are to be determined from the analysis. The terms associated with these functions are responsible for the drift and second harmonic components in the response of the plate. They are due to the cubic nonlinear terms in the Lagrangian which are the source of the quadratic nonlinear terms in the governing partial-differential equations of motion and boundary conditions.

Substituting (5.19), (5.20) and $Q = \varepsilon^3 F\phi_{30}\cos\Omega t$ into (5.3), keeping terms up to $0(\varepsilon^4)$, and averaging the resulting Lagrangian over the period $2\pi/\omega$, we obtain

$$
\begin{aligned}
&<L> = \varepsilon^4 \omega \delta_0 \left[i(A\bar{A}' - \bar{A}A') + 4\alpha_e A^2 \bar{A}^2 + \frac{1}{2} f(Ae^{-i\sigma T_2} + \bar{A}e^{i\sigma T_2}) \right] \\
&\text{or} \\
&<L> = \varepsilon^4 \omega \delta_0 \left[\frac{1}{2} a^2(\sigma - \gamma') + \frac{1}{4} \alpha_e a^4 + \frac{1}{2} f \cos \gamma \right]
\end{aligned}
\tag{5.21}
$$

$$
\alpha_e = \delta_1 / \omega \delta_0 \text{ and } f = F/\omega\delta_0
$$

where the prime indicates the derivative with respect to T_2, $\Omega - \omega = \varepsilon^2\sigma$, $\gamma = \sigma T_2 - \beta$, and the coefficients δ_0 and δ_1 are given by

$$
\begin{aligned}
\delta_0 = -\int_0^a \int_0^b \{ & c_1^2 I_7 \phi_{30,y}^2 + c_1^2 I_7 \phi_{30,x}^2 - 2c_1 \bar{I}_5 \phi_{30,y} \phi_{50} - 2c_1 \bar{I}_5 \phi_{30,x} \phi_{40} \\
& + \bar{I}_3 \phi_{50}^2 + \bar{I}_3 \phi_{40}^2 + I_1 \phi_{30}^2 + I_1 \phi_{20}^2 + I_1 \phi_{10}^2 \} dx dy
\end{aligned}
\tag{5.22}
$$

$$
\begin{aligned}
4\delta_1 = \int_0^a \int_0^b \Big\{ & - A_{11}\Big[\frac{3}{2}\phi_{30,x}^4 + \frac{3}{2}\phi_{30,y}^4 + 2\phi_{30,x}^2 (\phi_{11,x} + \phi_{12,x}) + 2\phi_{30,y}^2(\phi_{21,y} + \phi_{22,y}) \\
& + 4\phi_{10,x}\phi_{30,x}(\phi_{31,x} + \phi_{32,x}) + 4\phi_{20,y}\phi_{30,y}(\phi_{31,y} + \phi_{32,y}) + \phi_{11,x}^2 + 2\phi_{12,x}^2 + \phi_{21,y}^2 + 2\phi_{22,}^2 y\Big] \\
& - A_{12}\Big[3\phi_{30,x}^2\phi_{30,y}^2 + 4\phi_{10,x}\phi_{30,y}(\phi_{31,y} + \phi_{32,y}) + 4\phi_{30,x}\phi_{20,y}(\phi_{31,x} + \phi_{32,x}) \\
& + 2\phi_{30,y}^2(\phi_{11,x} + \phi_{12,x}) + 2\phi_{30,x}^2(\phi_{21,y} + \phi_{22,y}) + 2\phi_{11,x}\phi_{21,y} + 4\phi_{12,x}\phi_{22,y}\Big] \\
& - A_{66}\Big[4\phi_{30,y}(\phi_{10,y} + \phi_{20,x})(\phi_{31,x} + \phi_{32,x}) + 4\phi_{30,x}(\phi_{10,y} + \phi_{20,x})(\phi_{31,y} + \phi_{32,y}) \\
& + 4\phi_{30,x}\phi_{30,y}(\phi_{11,y} + \phi_{12,y} + \phi_{21,x} + \phi_{22,x}) + 6\phi_{30,x}^2\phi_{30,y}^2\phi_{11,y}^2 \\
& + 2\phi_{11,y}\phi_{21,x} + \phi_{21,x}^2 + 2\phi_{12,y}^2 + 4\phi_{12,y}\phi_{22,x} + 2\phi_{22,x}^2\Big] \\
& - A_{44}\Big[\phi_{31,x}^2 + \phi_{31,y}^2 + 2\phi_{32,x}^2 + 2\phi_{32,y}^2 + \phi_{41}^2 + 2\phi_{42}^2 + \phi_{51}^2 \\
& + 2\phi_{52}^2 + 2\phi_{31,x}\phi_{41} + 4\phi_{32,x}\phi_{42} + 2\phi_{31,y}\phi_{51} + 4\phi_{32,y}\phi_{52}\Big] \\
& - B_{11}\Big[- 2\phi_{30,y}^2(\phi_{51,y} + \phi_{52,y}) - 4\phi_{30,y}\phi_{50,y}(\phi_{31,y} + \phi_{32,y}) + 2\phi_{30,x}^2(\phi_{41,x} + \phi_{42,x}) \\
& + 4\phi_{30,x}\phi_{40,x}(\phi_{31,x} + \phi_{32,x}) + 2\phi_{11,x}\phi_{41,x} + 4\phi_{12,x}\phi_{42,x} + 2\phi_{21,y}\phi_{51,y} + 4\phi_{22,y}\phi_{52,y}\Big] \\
& - 2c_1E_{11}\Big[- \phi_{30,x}^2(\phi_{31,xx} + \phi_{32,xx} + \phi_{41,x} + \phi_{42,x}) + \phi_{30,y}^2(\phi_{31,yy} + \phi_{32,yy} + \phi_{51,y} + \phi_{52,y}) \\
& - 2\phi_{30,x}(\phi_{30,xx} + \phi_{40,xx})(\phi_{31,x} + \phi_{32,x}) + 2\phi_{30,y}(\phi_{30,yy} + \phi_{50,yy})(\phi_{31,y} + \phi_{32,y}) \\
& - \phi_{11,x}(\phi_{31,xx} + \phi_{41,x}) - 2\phi_{12,x}(\phi_{32,xx} + \phi_{42,x}) + \phi_{21,y}(\phi_{31,yy} + \phi_{51,y}) + 2\phi_{22,y}(\phi_{32,yy} + \phi_{52,y})\Big] \\
& - D_{11}\Big[\phi_{41,x}^2 + 2\phi_{42,x}^2 + \phi_{51,y}^2 + 2\phi_{52,y}^2\Big] - 2D_{12}\Big[\phi_{41,x}\phi_{51,y} + 2\phi_{42,x}\phi_{52,y}\Big] \\
& - D_{66}\Big[(\phi_{41,y} + \phi_{51,x})^2 + 2(\phi_{42,y} + \phi_{52,x})^2\Big] \\
& - 2c_2D_{44}\Big[(\phi_{31,x} + \phi_{41})^2 + (\phi_{31,y} + \phi_{51})^2 + 2(\phi_{32,y} + \phi_{52})^2 + 2(\phi_{32,x} + \phi_{42})^2\Big] \\
& - 2c_1F_{11}\Big[\phi_{41,x}^2 + 2\phi_{42,x}^2 + \phi_{51,y}^2 + 2\phi_{52,y}^2 + \phi_{31,xx}\phi_{41,x} \\
& + 2\phi_{32,xx}\phi_{42,x} + \phi_{31,yy}\phi_{51,y} + 2\phi_{32,yy}\phi_{52,y}\Big] \\
& + 2c_1F_{12}\Big[2\phi_{52,y}(\phi_{32,xx} + 2\phi_{42,x}) + \phi_{51,y}(\phi_{31,xx} + 2\phi_{41,x}) + \phi_{31,yy}\phi_{41,x} + 2\phi_{32,yy}\phi_{42,x}\Big] \\
& + 2c_1F_{66}\Big[2(\phi_{42,y} + \phi_{52,x})^2 + (\phi_{41,y} + \phi_{51,x})^2 + 2\phi_{31,xy}(\phi_{41,y} + \phi_{51,x}) + 4\phi_{32,xy}(\phi_{42,y} + \phi_{52,x})\Big] \\
& - c_2^2F_{44}\Big[(\phi_{31,x} + \phi_{41})^2 + (\phi_{31,y} + \phi_{51})^2 + 2(\phi_{32,x} + \phi_{42})^2 + 2(\phi_{32,y} + \phi_{52})^2\Big] \\
& - c_1H_{11}\Big[(\phi_{31,xx} + \phi_{41,x})^2 + (\phi_{31,yy} + \phi_{51,y})^2 + 2(\phi_{32,xx} + \phi_{42,x})^2 + 2(\phi_{32,yy} + \phi_{52,y})^2\Big] \\
& - 2c_1^2H_{12}\Big[2\phi_{42,x}\phi_{52,y} + 2\phi_{32,xx}\phi_{52,y}\phi_{41,x}\phi_{51,y} + \phi_{31,xx}\phi_{51,y} + 2\phi_{32,yy}\phi_{42,x} \\
& + \phi_{31,yy}\phi_{41,x} + 2\phi_{32,xx}\phi_{32,yy} + \phi_{31,xx}\phi_{31,yy}\Big] \\
& - c_1^2H_{66}\Big[2(\phi_{42,y} + \phi_{52,x})^2 + (\phi_{41,y} + \phi_{51,x})^2 + 4\phi_{31,xy}(\phi_{31,xy} + \phi_{41,y} + \phi_{51,x}) \\
& + 8\phi_{32,xy}(\phi_{32,xy} + \phi_{42,y} + \phi_{52,x})\Big]\Big\} dxdy
\end{aligned}
$$

(5.23)

Here, $c_1 = 4/3h^2$ and $c_2 = 4/h^2$. To solve for the ϕ_{i1} and $\phi_{i2}(i = 1,2,...,5)$, one can either use a finite-element method directly on the Lagrangian or find and solve the differential equations and boundary conditions governing them. In this work, we use the latter approach. To this end, we use calculus of variations and focus our attention on the coefficient δ_1. Moreover, we rename this coefficient as the functional $I = \delta_1$. The first variation of I is thus given by

$$
\begin{aligned}
4\delta I = \int_0^b \int_0^a \Big\{ & -2\big[A_{11}(\phi_{30,x}^2 + \phi_{11,x}) + A_{12}(\phi_{30,y}^2 + \phi_{21,y}) + B_{11}\phi_{41,x} - c_1 E_{11}(\phi_{31,xx} + \phi_{41,x})\big]\delta\phi_{11,x} \\
& - 2A_{66}\big[2\phi_{30,x}\phi_{30,y} + \phi_{21,x} + \phi_{11,y}\big]\delta\phi_{11,y} \\
& + 8I_1\omega^2\phi_{12}\delta\phi_{12} + 8I_1\omega^2\phi_{22}\delta\phi_{22} + 8I_1\omega^2\phi_{32}\delta\phi_{32} \\
& - 2\big[A_{11}(\phi_{30,x}^2 + 2\phi_{12,x}) + A_{12}(\phi_{30,y}^2 + 2\phi_{22,y}) + 2B_{11}\phi_{42,x} - 2c_1 E_{11}(\phi_{32,xx} + \phi_{42,x})\big]\delta\phi_{12,x} \\
& - 4A_{66}\big[\phi_{30,x}\phi_{30,y} + \phi_{12,y} + \phi_{22,x}\big]\delta\phi_{12,y} \\
& - 2A_{66}\big[2\phi_{30,x}\phi_{30,y} + \phi_{11,y} + \phi_{21,x}\big]\delta\phi_{21,x} \\
& - 2\big[A_{11}(\phi_{30,y}^2 + \phi_{21,y}) + A_{12}(\phi_{30,x}^2 + \phi_{11,x}) - B_{11}\phi_{51,y} + c_1 E_{11}(\phi_{31,yy} + \phi_{51,y})\big]\delta\phi_{21,y} \\
& - 4A_{66}\big[\phi_{30,x}\phi_{30,y} + \phi_{12,y} + \phi_{22}\big]\delta\phi_{22,x} \\
& - 2\big[A_{11}(\phi_{30,y}^2 + 2\phi_{22,y}) + A_{12}(\phi_{30,x}^2 + 2\phi_{12,x}) - 2B_{11}\phi_{52,y} + 2c_1 E_{11}(\phi_{32,yy} + \phi_{52,y})\big]\delta\phi_{22,y} \\
& - 2\big[2A_{11}\phi_{10,x}\phi_{30,x} + 2A_{12}\phi_{20,y}\phi_{30,x} + 2A_{66}\phi_{30,y}(\phi_{10,y} + \phi_{20,x}) + 2B_{11}\phi_{30,x}\phi_{40,x} \\
& - 2c_1 E_{11}\phi_{30,x}(\phi_{30,xx} + \phi_{40,x}) + (A_{44} - 2c_2 D_{44} + c_2^2 F_{44})(\phi_{31,x} + \phi_{41})\big]\delta\phi_{31,x} \\
& - 2\big[2A_{11}\phi_{20,y}\phi_{30,y} + 2A_{12}\phi_{10,x}\phi_{30,y} + 2A_{66}\phi_{30,x}(\phi_{10,y} + \phi_{20,x}) - 2B_{11}\phi_{30,y}\phi_{50,y} \\
& + 2c_1 E_{11}\phi_{30,y}(\phi_{30,yy} + \phi_{50,y}) + (A_{44} - 2c_2 D_{44} + c_2^2 F_{44})(\phi_{31,y} + \phi_{51})\big]\delta\phi_{31,y} \\
& - 4\big[-2c_1\omega^2 I_7\phi_{32,x} + 2c_1\omega^2\bar{I}_5\phi_{42} + A_{11}\phi_{10,x}\phi_{30,x} + A_{12}\phi_{20,y}\phi_{30,x} + A_{66}\phi_{30,y}(\phi_{10,y} + \phi_{20,x}) \\
& + A_{44}(\phi_{32,x} + \phi_{42}) + B_{11}\phi_{30,x}\phi_{40,x} - c_1 E_{11}\phi_{30,x}(\phi_{30,xx} + \phi_{40,x}) - 2c_2 D_{44}(\phi_{32,x} + \phi_{42})\big]\delta\phi_{32,x} \\
& - 4\big[-2c_1^2\omega^2 I_7\phi_{32,y} + 2c_1\omega^2\bar{I}_5\phi_{52} + A_{11}\phi_{20,y}\phi_{30,y} + A_{12}\phi_{10,x}\phi_{30,y} + A_{66}\phi_{30,x}(\phi_{10,y} + \phi_{20,x}) \\
& - B_{11}\phi_{30,y}\phi_{50,y} + c_1 E_{11}\phi_{30,y}(\phi_{30,yy} + \phi_{50,y}) + (A_{44} - 2c_2 D_{44} + c_2^2 F_{44})(\phi_{32,y} + \phi_{52})\big]\delta\phi_{32,y} \\
& - 2\big[(A_{44} - 2c_2 D_{44} + c_2^2 F_{44})(\phi_{31,x} + \phi_{41})\big]\delta\phi_{41} \\
& - 2\big[(B_{11} - c_1 E_{11})(\phi_{30,x}^2 + \phi_{11,x}) + D_{11}\phi_{41,x} + D_{12}\phi_{51,y} + (c_1^2 H_{11} - c_1 F_{11})(\phi_{31,xx} + \phi_{41,x}) \\
& + c_1^2 H_{12}(\phi_{31,yy} + \phi_{51,y}) - c_1 F_{12}(\phi_{31,yy} + 2\phi_{51,y})\big]\delta\phi_{41,x}\Big\} dx dy
\end{aligned}
\tag{5.24}
$$

Integrating (5.24) by parts so that δI contains only the $\delta\phi_{i1}$ and $\delta\phi_{i2}$, requiring that $\delta I = 0$, and setting the coefficient of each of the $\delta\phi_{i1}$ and $\delta\phi_{i2}$ equal to zero, one can obtain a set of ten partial-differential equations and their associated boundary conditions. These equations can be solved by a numerical method (e.g., the finite-element method or a finite-difference method) and the results are then used in

calculating the coefficient δ_1 in (5.23). The solution has the same form as equations (5.16)-(5.18). We choose not to proceed any further in formulating and solving the plate equations, instead we shall reduce the analysis in the next sections to the case of plate strips in cylindrical bending.

5.3. Plate Strips

5.3.1. Case of primary resonance

In this case, the excitation frequency Ω is near ω, where ω is one of the linear undamped natural frequencies of the plate strip (see Table 3.2). To carry out the analysis, we introduce a small dimensionless parameter ε as a bookkeeping device which can be set equal to unity in the final analysis. To quantitatively relate the nearness of the natural frequency ω to the excitation frequency Ω, we introduce a detuning parameter σ defined according to

$$\Omega = \omega + \varepsilon^2 \sigma \tag{5.25}$$

The linear solution, obtained earlier in Chapter 3, is a linear combination of all modes. However, in the presence of modal damping, all modes that are not directly excited by the external excitation or indirectly excited by an internal resonance decay with time. Because Ω is assumed to be near ω, only the mode corresponding to ω is directly excited. Moreover, we consider the case in which this mode is not involved

in an internal resonance with any other mode. Thus, we express the response of the plate strip to second order in ε as

$$u = \varepsilon\phi_{10}(x)Ae^{i\omega T_0} + \varepsilon^2\{\phi_{11}(x)A\bar{A} + \phi_{12}(x)A^2e^{2i\omega T_0}\} + cc \tag{5.26a}$$

$$w = \varepsilon\phi_{30}(x)Ae^{i\omega T_0} + \varepsilon^2\{\phi_{31}(x)A\bar{A} + \phi_{32}(x)A^2e^{2i\omega T_0}\} + cc \tag{5.26b}$$

$$\psi_x = \varepsilon\phi_{40}(x)Ae^{i\omega T_0} + \varepsilon^2\{\phi_{41}(x)A\bar{A} + \phi_{42}(x)A^2e^{2i\omega T_0}\} + cc \tag{5.26c}$$

Here, the $\phi_{i0}(i = 1,3,4)$ are the linear undamped free-vibrations modes and are given by

$$\phi_{10} = \chi_1 \cos \alpha x \tag{5.27a}$$

$$\phi_{30} = \chi_3 \sin \alpha x \tag{5.27b}$$

$$\phi_{40} = \chi_4 \cos \alpha x \tag{5.27c}$$

Using the time-averaged-Lagrangian technique, we obtain equation (5.21). The expressions for δ_0 and δ_1 are as follows:

$$\delta_0 = \int_0^a \{I_1(\phi_{10}^2 + \phi_{30}^2) + \bar{I}_3\phi_{40}^2 + c_1^2 I_7\phi_{30}'^2 - 2c_1\bar{I}_5\phi_{30}'\phi_{40}\}dx \tag{5.28}$$

$$
\begin{aligned}
4\delta_1 = \int_0^a \Big\{ & - A_{11}\Big[\frac{3}{2}\phi_{30}'^4 + 4\phi_{10}'\phi_{30}'(\phi_{31}' + \phi_{32}') + 2\phi_{30}'^2(\phi_{11}' + \phi_{12}') + \phi_{11}'^2 + 2\phi_{12}'^2 \Big] \\
& - 2B_{11}\Big[\phi_{30}'^2(\phi_{41}' + \phi_{42}') + \phi_{11}'\phi_{41}' + \phi_{12}'\phi_{42}' \Big] \\
& - D_{11}(\phi_{41}'^2 + \phi_{42}'^2) + 2c_1E_{11}\Big[\phi_{30}'^2(\phi_{31}'' + \phi_{32}'' + \phi_{41}' + \phi_{42}') \\
& + 2\phi_{30}'\phi_{30}''(\phi_{31}' + \phi_{32}') + \phi_{11}'(\phi_{31}'' + \phi_{41}') + 2\phi_{12}'(\phi_{32}'' + \phi_{42}') \Big] \\
& - 4(B_{11} - c_1E_{11})\phi_{30}'\phi_{40}'(\phi_{31}' + \phi_{32}') + 2c_1F_{11}\Big[\phi_{41}'(\phi_{31}'' + \phi_{41}') \\
& + 2\phi_{42}'(\phi_{32}'' + \phi_{42}') \Big] - c_1^2H_{11}\Big[(\phi_{31}'' + \phi_{41}')^2 + 2(\phi_{32}'' + \phi_{42}')^2 \Big] \\
& - (A_{44} - 2c_2D_{44} + c_2^2F_{44})\Big[(\phi_{31}' + \phi_{41})^2 + 2(\phi_{32}' + \phi_{42})^2 \Big] \Big\} dx
\end{aligned}
\tag{5.29}
$$

Thus, the functional $I = \delta_1$ can be written as

$$
I = I(\phi_{11}', \phi_{12}', \phi_{31}', \phi_{31}'', \phi_{32}', \phi_{32}'', \phi_{41}, \phi_{41}', \phi_{42}, \phi_{42}') \tag{5.30}
$$

The first variation is

$$
\begin{aligned}
4\delta I = \int_0^a \Big\{ & \Big[- 2A_{11}(\phi_{30}'^2 + \phi_{11}') - 2(B_{11} - c_1E_{11})\phi_{41}' + 2c_1E_{11}\phi_{31}'' \Big]\delta\phi_{11}' \\
& + 8\omega^2 I_1\phi_{12}\delta\phi_{12} + 8I_1\omega^2\phi_{32}\delta\phi_{32} \\
& + \Big[- 2A_{11}(\phi_{30}'^2 + 2\phi_{12}') - 4(B_{11} - c_1E_{11})\phi_{42}' + 4c_1E_{11}\phi_{32}'' \Big]\delta\phi_{12}' \\
& + \Big[- 4A_{11}\phi_{10}'\phi_{30}' + 4c_1E_{11}\phi_{30}'\phi_{30}'' - 2(A_{44} - 2c_2D_{44} + c_2^2F_{44})(\phi_{31}' + \phi_{41}) \\
& - 4(B_{11} - c_1E_{11})\phi_{30}'\phi_{40}' \Big]\delta\phi_{31}' \\
& + \Big[- 4(A_{44} - 2c_2D_{44} + c_2^2F_{44})(\phi_{32}' + \phi_{42}) + 8c_1\omega^2(c_1I_7\phi_{32}' - \bar{I}_5\phi_{42}) \\
& - 4(B_{11} - c_{11}E_{11})\phi_{30}'\phi_{40}' - 4A_{11}\phi_{10}'\phi_{30}' + 4c_1E_{11}\,\phi_{30}'\phi_{30}'' \Big]\delta\phi_{32}' \\
& - \Big[2(A_{44} - 2c_2D_{44} + c_2^2F_{44})(\phi_{31}' + \phi_{41}) \Big]\delta\phi_{41} \\
& - \Big[- 2(B_{11} - c_1E_{11})(\phi_{30}'^2 + \phi_{11}') + 2c_1(F_{11} - c_1H_{11})\phi_{31}'' - 2(D_{11} - 2c_1F_{11} + c_1^2H_{11})\phi_{41}' \Big]\delta\phi_{41}' \\
& + \Big[- 4(A_{44} - 2c_2D_{44} + c_2^2F_{44})(\phi_{32}' + \phi_{42}) + 8\omega^2(\bar{I}_3\phi_{42} - c_1\bar{I}_5\phi_{32}') \Big]\delta\phi_{42} \\
& + \Big[- 2(B_{11} - c_1E_{11})(\phi_{30}'^2 + 2\phi_{12}') - 4(D_{11} - 2c_1F_{11} + c_1^2H_{11})\phi_{42}' \\
& + 4c_1\,(F_{11} - c_1H_{11})\,\phi_{32}'' \Big]\delta\phi_{42}' \Big\} dx
\end{aligned}
\tag{5.31}
$$

Integrating (5.31) by parts so that δI contains only the $\delta\phi_{i1}$ and the $\delta\phi_{i2}$, requiring that $\delta I = 0$, and invoking the fundamental lemma of calculus of variations by assuming that the $\delta\phi_{i1}$ and the $\delta\phi_{i2}$ are independently arbitrary nonzero constants, we arrive at the following Euler-Lagrange equations and their associated boundary conditions:

$\delta\phi_{i1}$:

$$-e_1\phi_{11}'' + e_4\phi_{31}''' - e_5\phi_{41}'' = 2e_1\phi_{30}'\phi_{30}'' \tag{5.32a}$$

$$\begin{aligned} e_8\phi_{31}'''' + e_4\phi_{11}''' - e_{10}\phi_{41}''' - e_{12}(\phi_{31}'' + \phi_{41}') = 2e_1(\phi_{10}'\phi_{30}'' + \phi_{10}''\phi_{30}') \\ + 2e_5(\phi_{40}'\phi_{30}'' + \phi_{40}''\phi_{30}') \end{aligned} \tag{5.32b}$$

$$-e_{19}\phi_{31}''' - e_{21}(\phi_{31}' + \phi_{41}) + e_{22}\phi_{11}'' + e_{25}\phi_{41}'' = -2e_{22}\phi_{30}'\phi_{30}'' \tag{5.32c}$$

$$A_{11}\phi_{11}' + B_{11}\phi_{41}' - c_1E_{11}(\phi_{31}'' + \phi_{41}') = -A_{11}\phi_{30}'^2 \text{ at } x = 0,a \tag{5.32d}$$

$$B_{11}\phi_{11}' + D_{11}\phi_{41}' - c_1F_{11}(\phi_{41}' + \phi_{31}'') = -B_{11}\phi_{30}'^2 \text{ at } x = 0,a \tag{5.32e}$$

$$E_{11}\phi_{11}' - c_1H_{11}(\phi_{31}'' + \phi_{41}') + F_{11}\phi_{41}' = -E_{11}\phi_{30}'^2 \text{ at } x = 0,a \tag{5.32f}$$

$\delta\phi_{i2}$:

$$-4\omega^2\phi_{12} - e_1\phi_{12}'' + e_4\phi_{32}'''' - e_5\phi_{42}'' = e_1\phi_{30}'\phi_{30}'' \tag{5.33a}$$

$$\begin{aligned} -4\omega^2(\phi_{32} - e_6\phi_{32}'' + e_7\phi_{42}') + e_8\phi_{32}'''' + e_4\phi_{12}''' - e_{10}\phi_{42}''' - e_{12}\phi_{32}'' \\ = e_1(\phi_{10}'\phi_{30}'' + \phi_{10}''\phi_{30}') + e_5(\phi_{30}'\phi_{40}'' + \phi_{30}''\phi_{40}') \end{aligned} \tag{5.33b}$$

$$\begin{aligned} -4\omega^2(\phi_{42} - e_{18}\phi_{32}') + e_{19}\phi_{32}''' - e_{21}(\phi_{42} + \phi_{32}') + e_{22}\phi_{12}'' + e_{25}\phi_{42}'' \\ = -e_{22}\phi_{30}'\phi_{30}'' \end{aligned} \tag{5.33c}$$

$$A_{11}\phi'_{12} + B_{11}\phi'_{42} - c_1E_{11}(\phi''_{32} + \phi'_{42}) = -\frac{1}{2}A_{11}\phi'^2_{30} \tag{5.33d}$$

$$B_{11}\phi'_{12} + D_{11}\phi'_{42} - c_1E_{11}(\phi''_{32} + \phi'_{42}) = -\frac{1}{2}B_{11}\phi'^2_{30} \tag{5.33e}$$

$$E_{11}\phi'_{12} - c_1H_{11}(\phi''_{32} + \phi'_{42}) + F_{11}\phi'_{42} = -\frac{1}{2}E_{11}\phi'^2_{30} \tag{5.33f}$$

The constants $e_i (i = 1,2,...,5)$ are given in Appendix C. Equations (5.32) and (5.33) are solved numerically by using the IMSL boundary-value-problem finite-difference subroutine DBVPFD. The numerical values of the ϕ_{i1} and the ϕ_{i2} are then substituted into the expression for δ_1 in (5.29). The integrals in (5.29) are evaluated numerically to obtain δ_1.

Next, writing the Euler-Lagrange equations corresponding to the time-averaged Lagrangian in (5.15), we obtain the following amplitude and phase equations:

$$a' = \mu a + \frac{1}{2}f \sin\gamma \tag{5.34}$$

$$a\gamma' = \sigma a + \alpha_e a^3 + \frac{1}{2}f\cos\gamma \tag{5.35}$$

where a damping term has been added to equation (5.34) and α_e is given by

$$\alpha_e = \frac{\delta_1}{\omega\delta_0} \tag{5.36}$$

Therefore, to the second approximation,

$$u = a\phi_{10}(x)\cos(\Omega t - \gamma) + \frac{1}{2}a^2[\phi_{11}(x) + \phi_{12}(x)\cos(2\Omega t - 2\gamma)] + ... \tag{5.37a}$$

$$w = a\phi_{30}(x)\cos(\Omega t - \gamma) + \frac{1}{2}a^2[\phi_{31}(x) + \phi_{32}(x)\cos(2\Omega t - 2\gamma)] + \ldots \quad (5.37b)$$

$$\psi_x = a\phi_{40}(x)\cos(\Omega t - \gamma) + \frac{1}{2}a^2[\phi_{41}(x) + \phi_{42}(x)\cos(2\Omega t - 2\gamma)] + \ldots \quad (5.37c)$$

where a and γ are defined by (5.34) and (5.35).

It follows from (5.37) that periodic solutions of the plate strip correspond to constant values of a and γ; that is, the fixed or equilibrium or stationary or singular points of (5.34) and (5.35). Letting $a' = \gamma' = 0$ in (5.34) and (5.35) yields the following equations governing the fixed points:

$$\mu a = -\frac{1}{2}f\sin\gamma \quad (5.38)$$

$$a\sigma + \alpha_e a^3 = -\frac{1}{2}f\cos\gamma \quad (5.39)$$

Eliminating γ from equations (5.38) and (5.39) yields the frequency-response equation

$$\sigma = -\alpha_e a^2 \pm \left[\frac{f^2}{4a^2} - \mu^2\right]^{1/2} \quad (5.40)$$

Figure 5.1 shows variation of the nondimensional undamped fundamental frequency $\hat{\omega}$ with the length to thickness ratio a/h and the number of layers N. It shows that for a certain value of a/h, $\hat{\omega}$ increases as the number of layers is increased, until $N = 10$, after which $\hat{\omega}$ remains approximately the same. Moreover, for values of $a/h \geq 10$, $\hat{\omega}$ approaches an asymptotic value for a given number of layers. The results are also tabulated in Table 3.2 for different values of a/h and N.

Figure 5.2 shows variation of the value of the effective nonlinearity α_e with the length to thickness ratio a/h and the number of layers N. It shows that α_e has its

maximum when $N = 2$ and it decreases as the number of layers is increased for a specific value of a/h. It also shows the asymptotic behavior of α_e for $a/h \geq 10$. Moreover, the value of α_e does not increase as the number of layers increases beyond $N = 10$ when a/h is kept constant. The numerical values of α_e are also shown in Table 5.1 for various values of a/h and N. A representative frequency-response curve is shown in Figure 5.3, which shows variation of the response amplitude a with the detuning parameter σ. Similarly, representative force-response curves are shown in Figure 5.4, which shows variation of the response amplitude with the excitation amplitude.

To determine the stability of the fixed points, we perturb them according to

$$a = a_0 + a_1(T_2) \tag{5.41}$$

$$\gamma = \gamma_0 + \gamma_1(T_2) \tag{5.42}$$

where a_0 and γ_0 correspond to a given fixed point. Substituting (5.41) and (5.42) into (5.34) and (5.35) and linearizing the result, we obtain

$$\begin{Bmatrix} a'_1 \\ \gamma'_1 \end{Bmatrix} = [A] \begin{Bmatrix} a_1 \\ \gamma_1 \end{Bmatrix} \tag{5.43}$$

where

$$[A] = \begin{bmatrix} \mu & \frac{f}{2}\cos\gamma_0 \\ 2\alpha_e a_0 - \frac{f}{2a_0^2}\cos\gamma_0 & \frac{-f}{2a_0}\sin\gamma_0 \end{bmatrix} \tag{5.44}$$

is the Jacobi of the system of equations in (5.34) and (5.35). For the solution in the local neighborhood of a given fixed point to be asymptotically stable, the two

eigenvalues of the matrix [A] must have negative real parts. Consequently, a local stability analysis has been carried out for the steady-state solutions displayed in both Figures 5.3 and 5.4; the solid lines represent stable solutions whereas the dashed lines represent unstable solutions. It is obvious that the multi-valuedness of the solutions in Figures 5.3 and 5.4 causes what is called the jump phenomenon (Nayfeh and Mook, 1979). In order to explain the physical significance of this phenomenon on the response of the structure, we consider the following example. Suppose that an experiment is conducted in which the amplitude of the excitation is held constant, the frequency of excitation is varied slowly by changing σ up and down through the linear natural frequency, and the amplitude of the harmonic response of the structure is recorded. Figure 5.3 shows that the response depends on the direction of the sweep. To illustrate this dependence, suppose that the experiment is started at a frequency σ corresponding to point 1 on the curve in Figure 5.3. If σ is slowly reduced, the response amplitude a slowly increases through point 2 until point 3 is reached. If σ is decreased further, an upward jump from point 3 to point 4 takes place. In fact, the jump phenomenon at point 3 is caused by a fold (saddle-node) bifurcation at which a collision between the stable and unstable fixed points occurs. A further decrease in σ results in a decrease in the response amplitude. On the other hand, if the experiment is started at point 5 and σ is slowly increased, the amplitude of the response a increases slowly through point 4 until point 6 is reached. As σ is increased further, a downward jump from point 6 to point 2 takes place. The frequency corresponding to point 6 again signifies another fold (saddle-node) bifurcation similar to that at point 3. The portion of the response curve joining the upper (5-4-6) and lower (1-2-3) branches of the solution (i.e., connecting points 3 and 6) is unstable and hence cannot be realized experimentally. For frequencies

corresponding to the interval between points 3 and 6, the initial conditions determine the response.

If the same experiment is repeated with the excitation frequency Ω being held constant while the amplitude of excitation is being varied slowly, a similar jump phenomenon, for certain values of σ, can be observed. For instance, consider the curve corresponding to $\sigma = 2$ in Figure 5.4 and suppose that the experiment is started at point 1. As f is increased, a slowly increases through point 2 to point 3. As f is increased further, a fold (saddle-node) bifurcation takes place causing an upward jump in the response amplitude a from point 3 to point 4, after which a increases slowly with f. If the process is reversed by starting at point 5 and slowly decreasing f, a decreases slowly until point 6, where another fold (saddle-node) bifurcation takes place, and the response amplitude jumps down to point 2.

5.3.2. Case of subharmonic resonance of order one-half

In this case, the excitation frequency Ω is approximately twice a linear natural frequency of the plate strip. The detuning parameter σ is accordingly defined by

$$\Omega = 2\omega + \varepsilon^2\sigma \tag{5.45}$$

Again, any mode of vibration that is neither directly excited nor indirectly excited through an internal resonance will decay with time. To determine a second-order uniform solution describing the response of the plate strip, we postulate that

$$u = \varepsilon A\phi_{10}e^{i\omega T_0} + \varepsilon^2\left[\Lambda_1(x)e^{i\Omega T_0} + \phi_{11}(x)A\bar{A} + \phi_{12}(x)A^2e^{2i\omega T_0}\right] + cc \tag{5.46a}$$

$$w = \varepsilon A\phi_{30}e^{i\omega T_0} + \varepsilon^2\left[\Lambda_3(x)e^{i\Omega T_0} + \phi_{31}(x)A\bar{A} + \phi_{32}(x)A^2e^{2i\omega T_0}\right] + cc \tag{5.46b}$$

$$\psi_x = \varepsilon A\phi_{40}e^{i\omega T_0} + \varepsilon^2\left[\Lambda_4(x)e^{i\Omega T_0} + \phi_{41}(x)A\bar{A} + \phi_{42}(x)A^2e^{2i\omega T_0}\right] + cc \qquad (5.46c)$$

where the $\phi_{i0}(i = 1,3,4)$ are defined by (5.27), the $\Lambda_i(x)(i = 1,3,4)$ are the particular solutions to the linear problem obtained by using the state-space concept, as in Chapter 3, and the ϕ_{i1} and $\phi_{i2}(i = 1,3,4)$ turn out to be the same as in the preceding section.

Substituting (5.46) into the Lagrangian (5.3), putting $Q = \varepsilon^2 F\cos\Omega t$, and averaging the Lagrangian over the period $2\pi/\omega$, we obtain

$$<L> = \varepsilon^4\omega\delta_0\left[i(A\bar{A}' - \bar{A}A') + 4\alpha_e A^2\bar{A}^2 + \Lambda\left(A^2e^{-i\sigma T_2} + \bar{A}^2e^{i\sigma T_2}\right)\right] \qquad (5.47)$$

where the prime indicates the derivative with respect to T_2 and

$$\begin{aligned}\Lambda = \frac{1}{\omega\delta_0}\int_0^a \Big\{ & -(D_{11} + c_1^2H_{11} - 2c_1F_{11})\phi'_{42}\Lambda'_3 - c_1(c_1H_{11} - F_{11})\phi''_{32}\Lambda'_3 \\ & + \frac{1}{2}(c_1E_{11} - B_{11})\phi'^2_{30}\Lambda'_3 + (c_1E_{11} - B_{11})\phi'_{12}\Lambda'_3 - c_1(c_1H_{11} - F_{11})\phi'_{42}\Lambda''_2 \\ & - c_1^2H_{11}\phi''_{32}\Lambda''_2 + \frac{1}{2}c_1E_{11}\phi'^2_{30}\Lambda''_2 + c_1E_{11}\phi'_{12}\Lambda''_2 - \frac{3}{2}A_{11}\phi'_{32}\Lambda'^3_2 \\ & + 2c_2D_{44}\phi_{42}\Lambda'_2 + 2(c_2D_{44} + c_1^2I_7\omega\Omega)\phi'_{32}\Lambda'_2 \\ & - (2c_1\bar{I}_5\omega\Omega + 2c_2^2F_{44} + A_{44})\phi_{42}\Lambda'_2 + (c_1E_{11} - B_{11})\phi'_{30}\phi'_{40}\Lambda'_2 \\ & - (c_2^2F_{44} + A_{44})\phi'_{32}\Lambda'_2 + c_1E_{11}\phi'_{30}\phi''_{30}\Lambda'_2 - A_{11}\phi'_{10}\phi'_{30}\Lambda'_2 \\ & + (c_1E_{11} - B_{11})\phi'_{42}\Lambda'_1 + c_1E_{11}\phi''_{32}\Lambda'_1 - \frac{1}{2}A_{11}\phi'^2_{30}\Lambda'_1 - A_{11}\phi'_{12}\Lambda'_1 \\ & - (A_{44} - 2c_2D_{44} + c_2^2F_{44} - 2c_1\bar{I}_5\omega\Omega)\phi'_{32}\Lambda_3 \\ & - (A_{44} - 2c_2D_{44} + c_2^2F_{44} - 2\bar{I}_3\omega\Omega)\,\phi_{42}\Lambda_3\Big\}dx\end{aligned} \qquad (5.48)$$

Substituting the polar form $A = \frac{1}{2}a(T_2)\exp[i\beta(T_2)]$ into (5.47) yields

$$< L > = \varepsilon^4 \omega \delta_0 \left[\frac{1}{2} a^2 \beta' + \frac{1}{4} \alpha_e a^4 + \frac{1}{2} a^2 \Lambda \cos(\sigma T_2 - \beta) \right] \tag{5.49}$$

Consequently, the equations governing the modulation of the amplitude and phase of the response are

$$a' = -\mu a - \Lambda a \sin \gamma \tag{5.50}$$

$$a\beta' = \alpha_e a^3 + \Lambda a \cos \gamma \tag{5.51}$$

where

$$\gamma = \sigma T_2 - 2\beta \tag{5.52}$$

and a damping term has been added to (5.50). Again, the fixed points can be determined by letting $a' = \gamma' = 0$ in (5.50)-(5.52). There are two possibilities: either $a = 0$ or

$$a = \frac{1}{\sqrt{\alpha_e}} \left[\frac{1}{2} \sigma \pm \sqrt{\Lambda^2 - \mu^2} \right] \tag{5.53}$$

Figure 5.5 and Table 5.2 show variation of the strength of the resonance Λ obtained from equation (5.48) with a/h and N. The resonance strength decreases as the number of layers N increases from $N = 2$ to $N = 10$ for a certain value of a/h. Moreover, the value of Λ reaches an asymptotic value if N is increased beyond $N = 10$.

A representative frequency-response curve is shown in Figure 5.6. Depending on the value of the detuning parameter σ, one, two, or three solutions are possible. When $\sigma < \sigma_1$, only the trivial solution is possible, which is stable. When $\sigma_1 < \sigma < \sigma_2$,

there are two possible solutions: the trivial solution, which is unstable, and a nontrivial solution, which is stable. when $\sigma > \sigma_2$, there are three possible solutions: the trivial solution, which is stable, and two nontrivial solutions, the larger of which is stable. In the latter case, the response depends on the initial conditions. Figure 5.3 suggests that subharmonic resonances can be excited for large values of the detuning parameter σ. This is not the case in a real situation or an experiment. In fact, the present analysis is valid only when the excitation frequency is within a narrow interval near twice the natural frequency of the structure and therefore the perturbation solution breaks down for large values of σ. Furthermore, if the analysis is carried out to a higher order, it is expected to yield frequency-response curves in which the upper and lower branches merge and terminate at a finite value of σ.

Figure 5.7 shows a representative variation of the response amplitude with the excitation amplitude when equation (5.52) has two nontrivial solutions. When $f < f_1$, only the trivial solution is possible, which is stable. When $f_1 < f < f_2$, there are three possible solutions: the trivial solution, which is stable, and two nontrivial solutions, the larger of which is stable. When $f > f_2$, there are two possible solutions: the trivial solution, which is stable, and a nontrivial solution which is also stable. Thus subharmonic resonances of order one-half are not excited when $f < f_1$, may or may not be excited, depending on the initial conditions, when $f_1 < f < f_2$, and are always excited when $f > f_2$. As an illustration, if we imagine an experiment conducted with a fixed σ and slowly varying f from a point below f_1, the response continues to be trivial until f reaches f_2. A small increase in f beyond f_2 results in an upward jump from zero to point A. The value f_2 corresponds to a reverse pitchfork bifurcation. As f is increased further, the response amplitude continues to increase gradually toward point B. On the other hand, if the experiment is started at point B and f is slowly decreased, the amplitude of the response also decreases gradually until point C is reached. A

further decrease of f results in a downward jump of the response to zero and continues to be trivial as f approaches zero. The point C corresponds to a saddle-node bifurcation.

Figure 5.8 shows another representative variation of the response amplitude with the excitation amplitude when equation (5.53) has only one nontrivial solution. In this case, there is only one bifurcation value, which is a pitchfork bifurcation, and there are no jumps in the response.

5.3.3. Case of superharmonic resonance of order two

This type of resonance occurs when $\Omega \approx \frac{1}{2}\omega$. The detuning parameter σ is therefore defined according to

$$2\Omega = \omega + \varepsilon^2\sigma \tag{5.54}$$

To determine a second-order uniform solution describing the response of the plate strip, we postulate that

$$u = \varepsilon A\phi_{10}e^{i\omega T_0} + \varepsilon^{3/2}\Lambda_1(x)e^{i\Omega T_0} + \varepsilon^2\left[\phi_{11}(x)A\bar{A} + \phi_{12}(x)A^2e^{2i\omega T_0}\right] + cc \tag{5.55a}$$

$$w = \varepsilon A\phi_{30}e^{i\omega T_0} + \varepsilon^{3/2}\Lambda_3(x)e^{i\Omega T_0} + \left[\phi_{31}(x)A\bar{A} + \varepsilon^2\phi_{32}(x)A^2e^{2i\omega T_0}\right] + cc \tag{5.55b}$$

$$\psi_x = \varepsilon A\phi_{40}e^{i\omega T_0} + \varepsilon^{2/3}\Lambda_4(x)e^{i\Omega T_0} + \left[\phi_{41}(x)A\bar{A} + \varepsilon^2\phi_{42}(x)A^2e^{2i\omega T_0}\right] + cc \tag{5.55c}$$

where the $\phi_{i0}(i = 1,3,4)$ are defined by (5.27), the $\Lambda_i(x)(i = 1,3,4)$ are the particular solutions to the linear problem obtained by using the state-space concept, as in

Chapter 3, and the ϕ_{i1} and $\phi_{i2}(i = 1,3,4)$ turn out to be the same as in the preceding section.

Substituting (5.55) into the Lagrangian (5.3), putting $Q = \varepsilon^{3/2} F \cos \Omega t$, and averaging the Lagrangian over the period $2\pi/\omega$, we obtain

$$< L > = \varepsilon^4 \omega \delta_0 \left[i(A\bar{A}' - \bar{A}A') + 4\alpha_e A^2 \bar{A}^2 + \Lambda\left(Ae^{-i\sigma T_2} + \bar{A}e^{i\sigma T_2}\right)\right] \tag{5.56}$$

where

$$\begin{aligned} \Lambda = \frac{1}{\omega \delta_0} \int_0^1 \Big\{ & (c_1 E_{11} - B_{11}) \phi_{30}' \Lambda_2' \Lambda_3 + \frac{1}{2} (c_1 E_{11} - B_{11}) \phi_{40}' \Lambda_2'^2 - \frac{1}{2} A_{11} \phi_{10}' \Lambda_2'^2 \\ & - A_{11} \phi_{30}' \Lambda_1' \Lambda_2' + c_1 E_{11} \phi_{30}' \Lambda_2' \Lambda_2'' + \frac{1}{2} c_1 E_{11} \phi_{30}'' \Lambda_2'^2 \Big\} dx \end{aligned} \tag{5.57}$$

Then, the equations governing the modulation of the amplitude and phase are

$$a' = -\mu a - \Lambda \sin \gamma \tag{5.58}$$

$$a\beta' = \alpha_e a^3 + \Lambda \cos \gamma \tag{5.59}$$

where

$$\gamma = \sigma T_2 - \beta \tag{5.60}$$

and a damping term has been added to (5.58). It follows from equations (5.58)-(5.60) that the frequency-response equation is

$$\Lambda^2 = \mu^2 a^2 + (\alpha_e a^3 - \sigma a)^2 \tag{5.61}$$

Figure 5.9 and Table 5.3 show variation of the strength of the resonance Λ obtained from equation (5.57) with a/h and N. As in the case of subharmonic

resonance of order one-half, for a certain value of a/h, the resonance strength Λ decreases as the number of layers increases from $N = 2$ to $N = 10$. Again, Λ approaches an asymptotic value for $N \geq 10$ for any value of a/h.

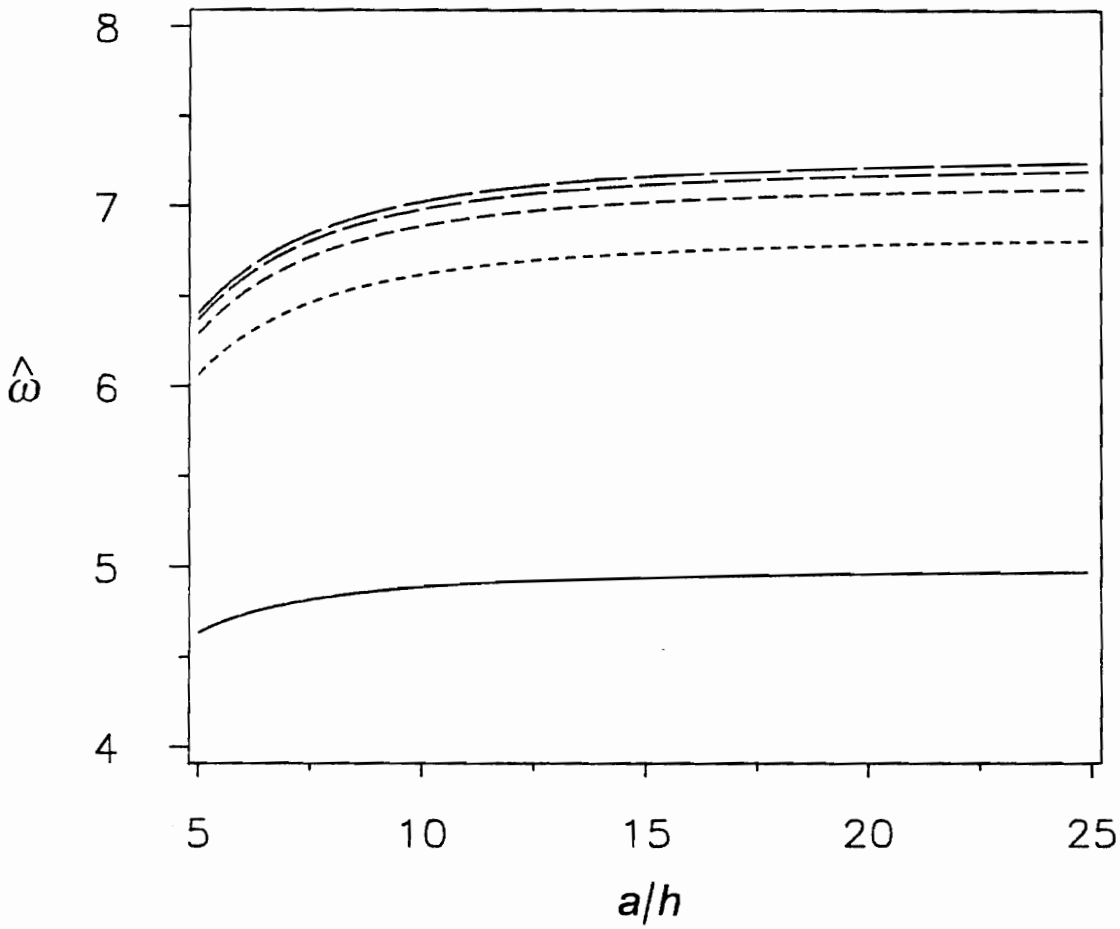

Figure 5.1. Variation of the nondimensional undamped linear fundamental natural frequency ($\hat{\omega} = \omega a^2\sqrt{\rho/h^2E_2}$) with the length to thickness ratio (a/h) and the number of layers (N): (____) 2 layers, (- - -) 4 layers, (---) 6 layers, (—-) 8 layers, and (——) 10 layers.

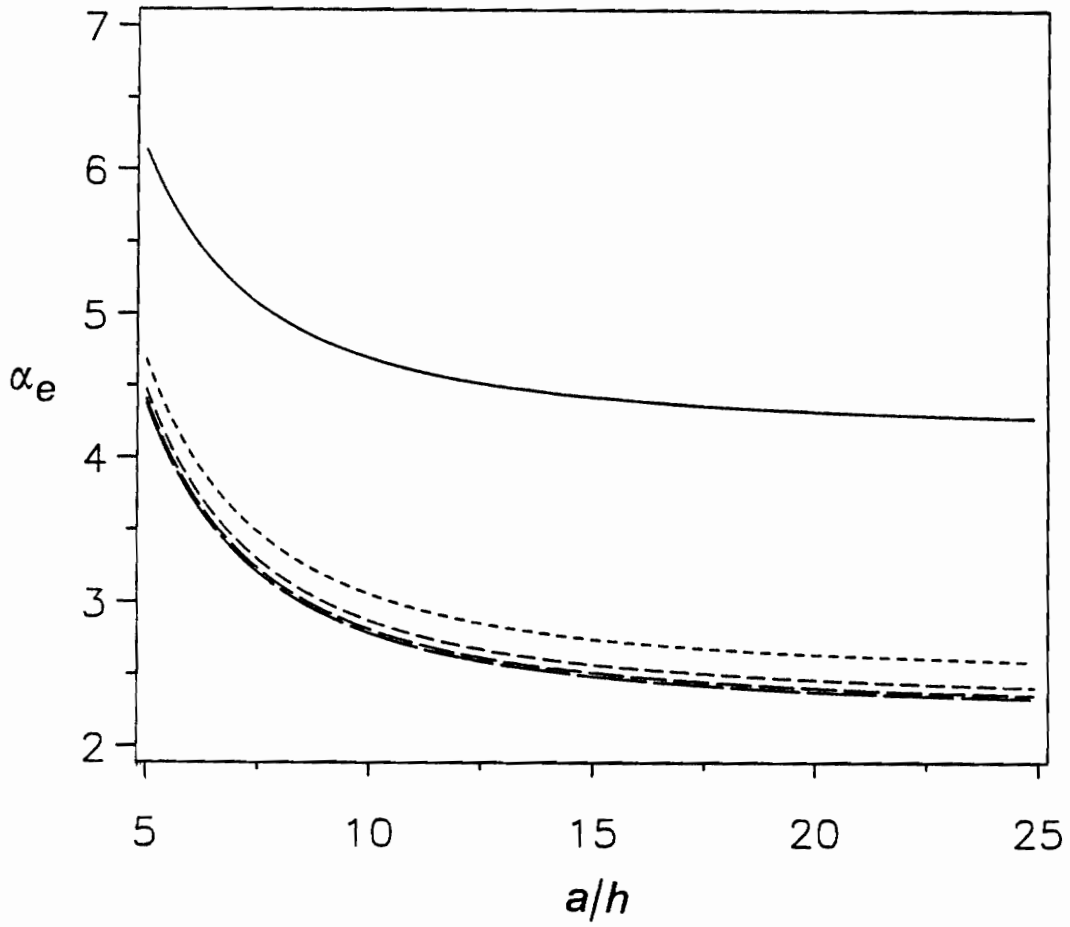

Figure 5.2. Variation of the effective nonlinearity α_e with the length to thickness ratio (a/h) and the number of layers (N): (____) 2 layers, (- - -) 4 layers, (–––) 6 layers, (—·—) 8 layers, and (——) 10 layers.

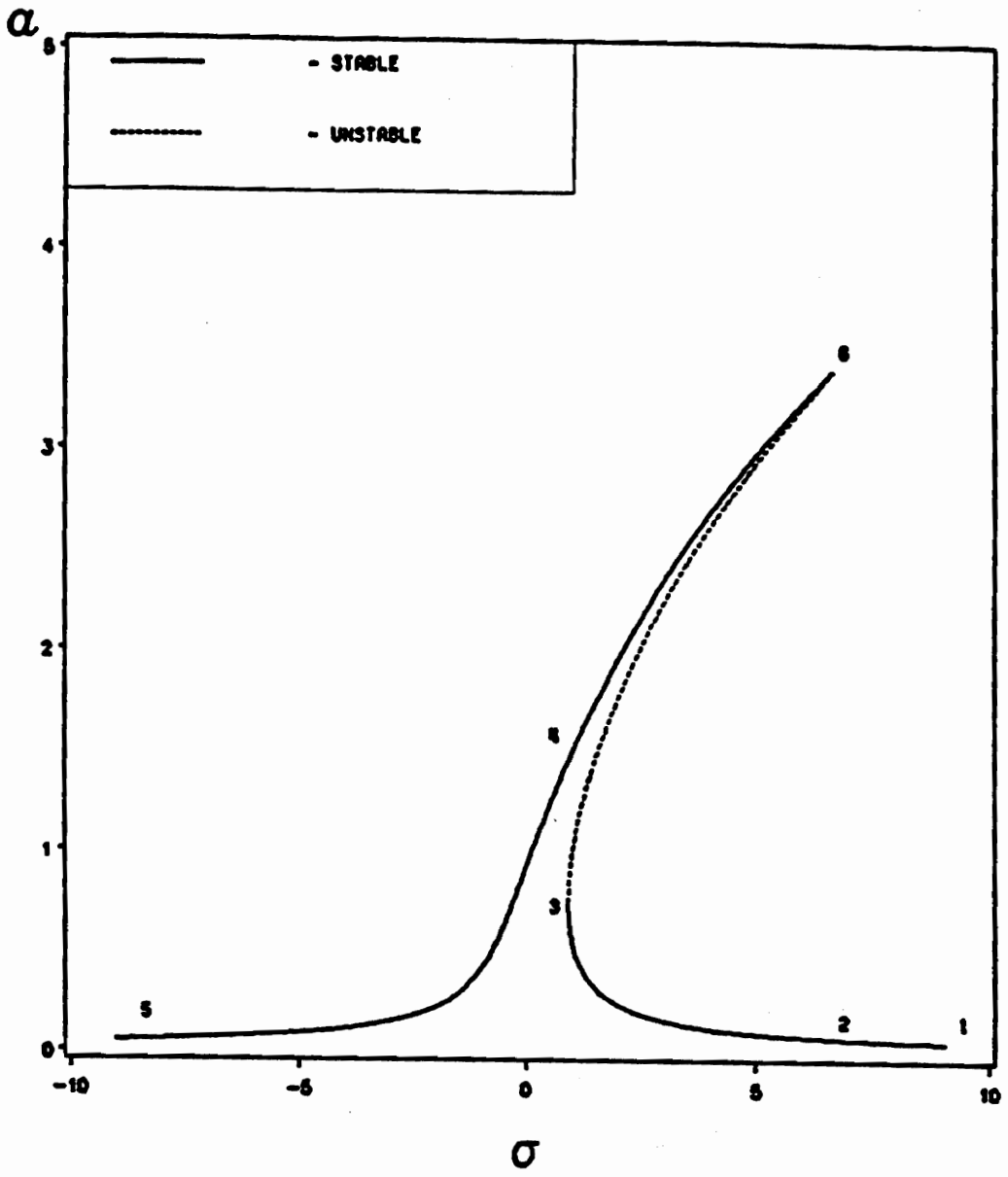

Figure 5.3. A representative frequency-response curve for the case of primary resonance (length to thickness ratio $a/h = 10$, number of layers $N = 2$, $f = 25$, $\mu = 0.15$).

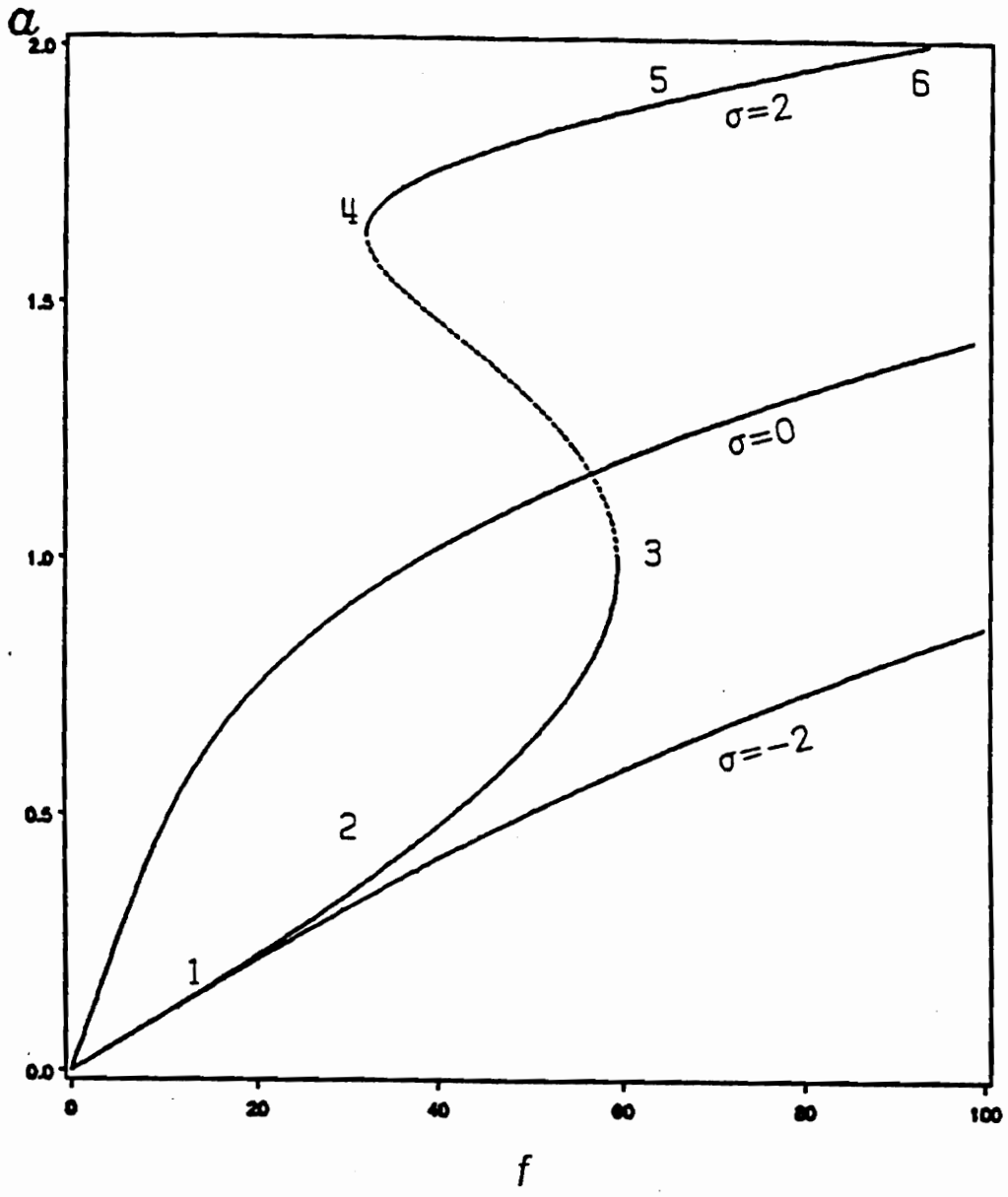

Figure 5.4. Representative variations of the response amplitude with the excitation amplitude for several detunings for the case of primary resonance (length to thickness ratio $a/h = 10$, number of layers $N = 2$, $\mu = 0.5$).

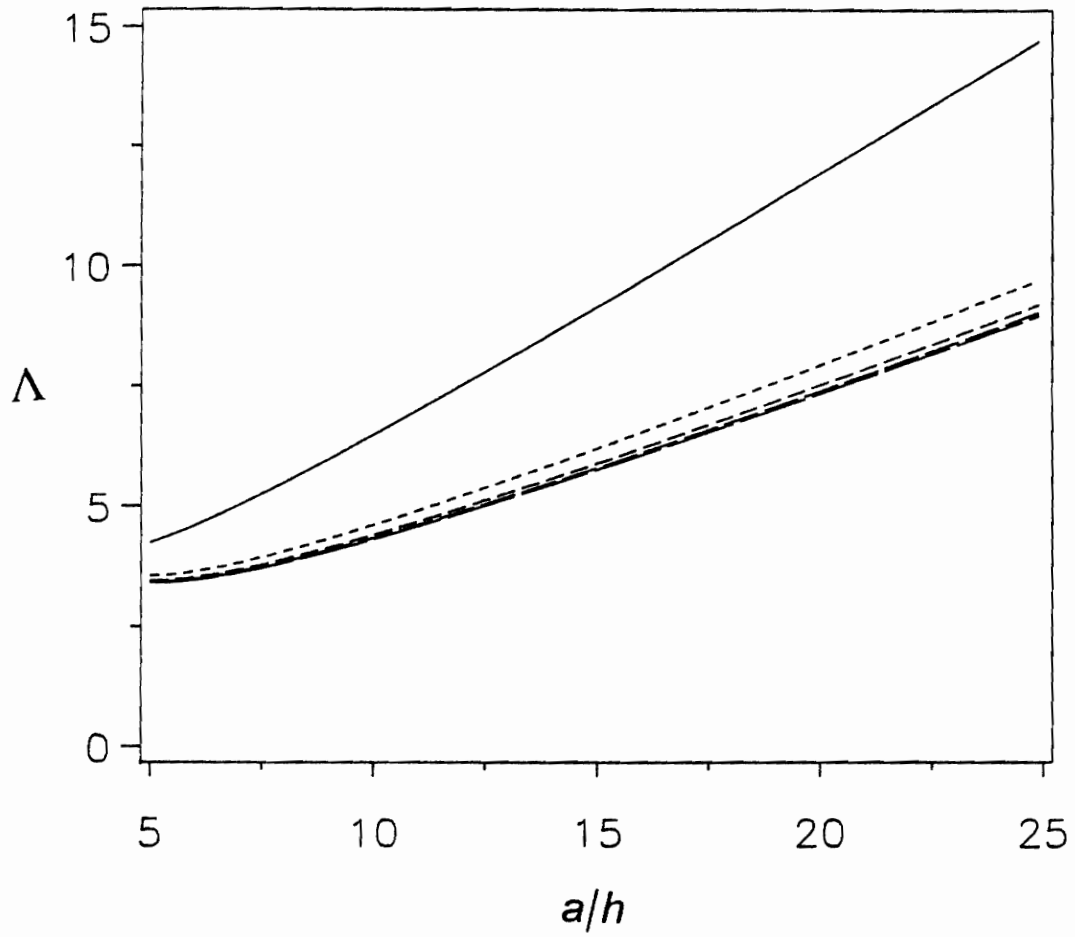

Figure 5.5. Subharmonic resonance of order one-half: variation of the strength of the resonance (Λ) with the length to thickness ratio (a/h) and the number of layers (N): (____) 2 layers, (- - -) 4 layers, (– – –) 6 layers, (— — —) 8 layers, and (— —) 10 layers.

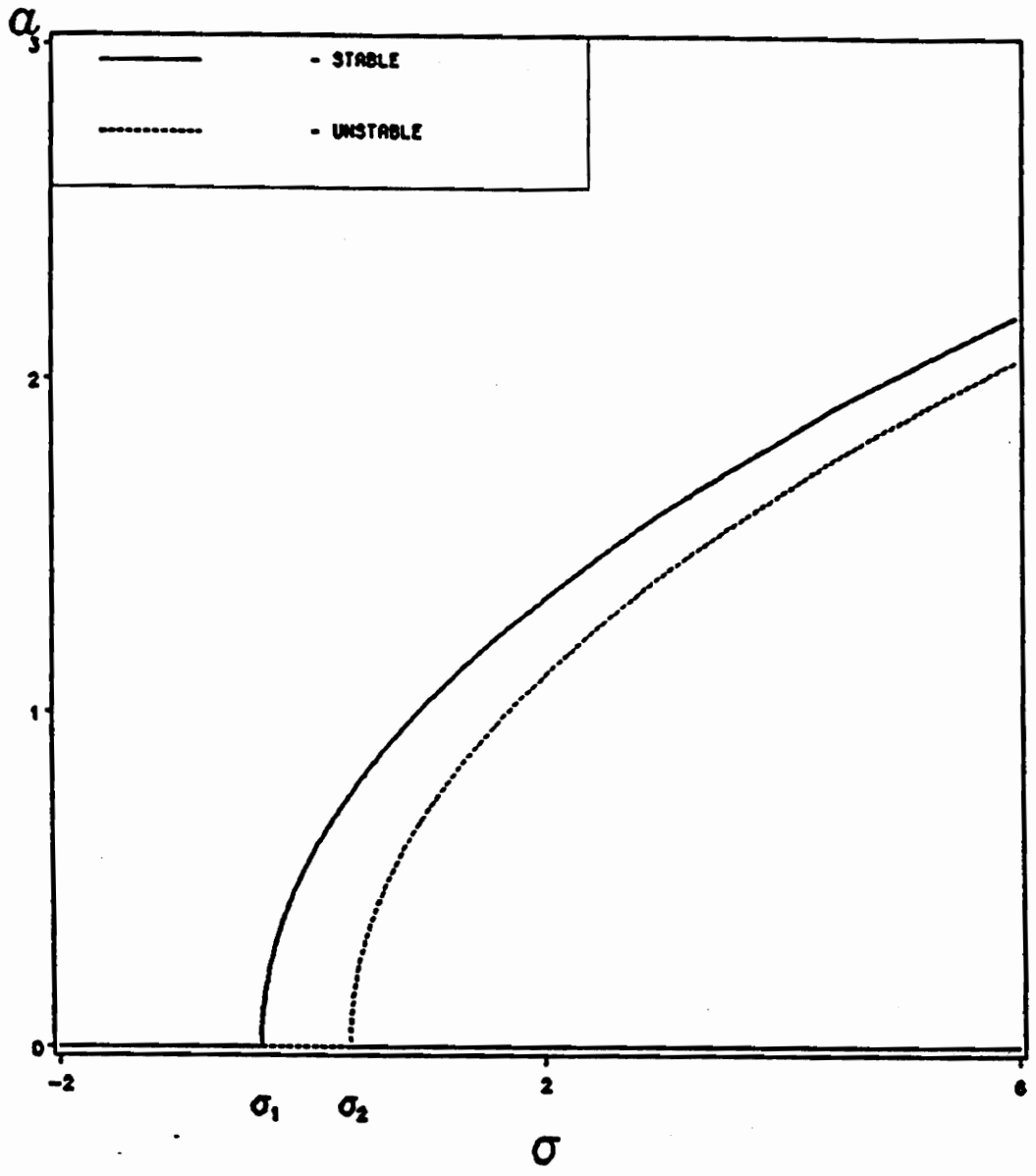

Figure 5.6. A representative frequency-response curve for the case of subharmonic resonance of order one-half (length to thickness ratio $a/h = 10$, number of layers $N = 2$, $f = 20$, $\mu = 0.005$).

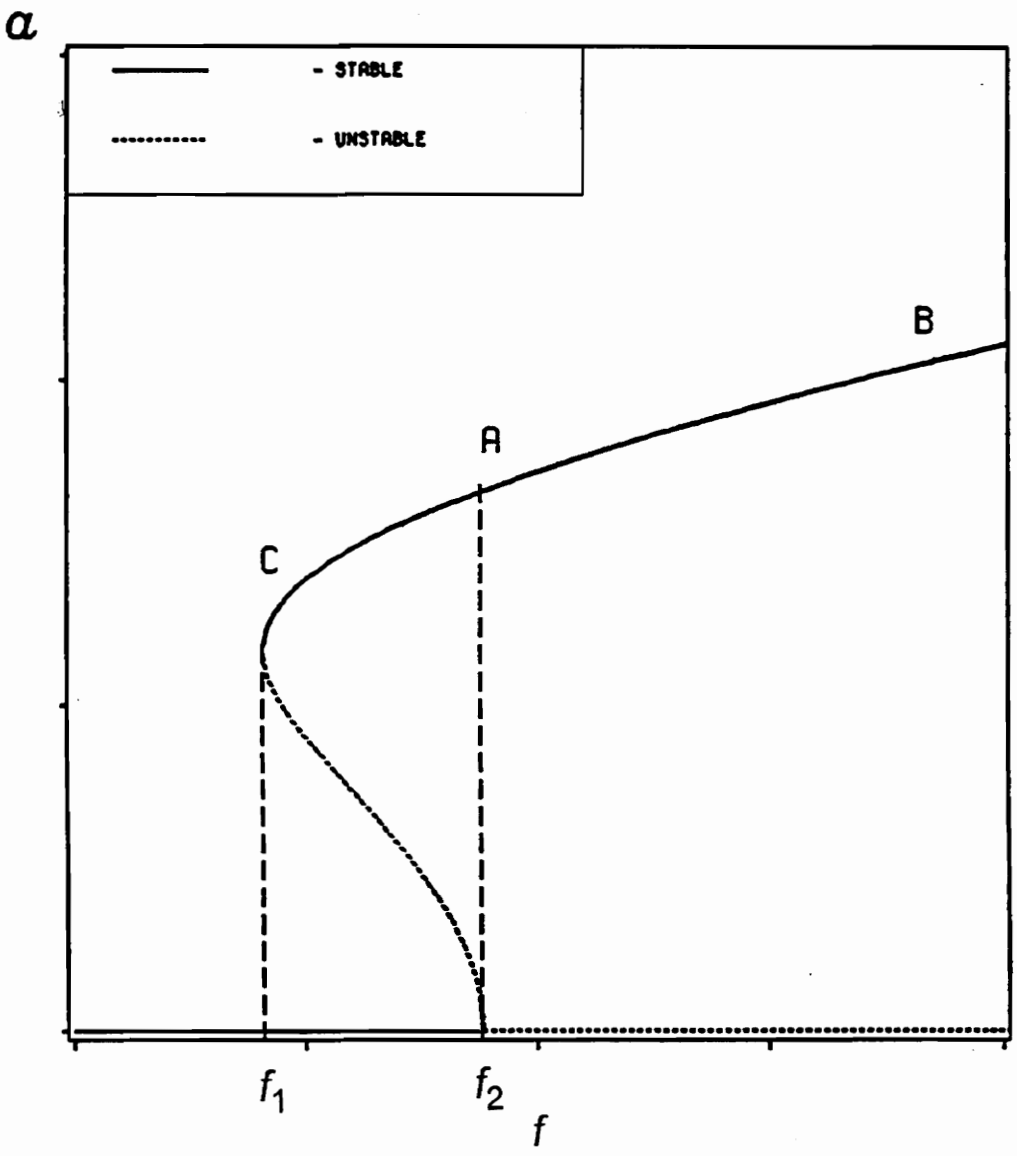

Figure 5.7. A representative variation of the response amplitude with the excitation amplitude for the case of subharmonic resonance of order one-half (length to thickness ratio $a/h = 10$, number of layers $N = 2$, $\sigma = 2$, $\mu = 0.5$).

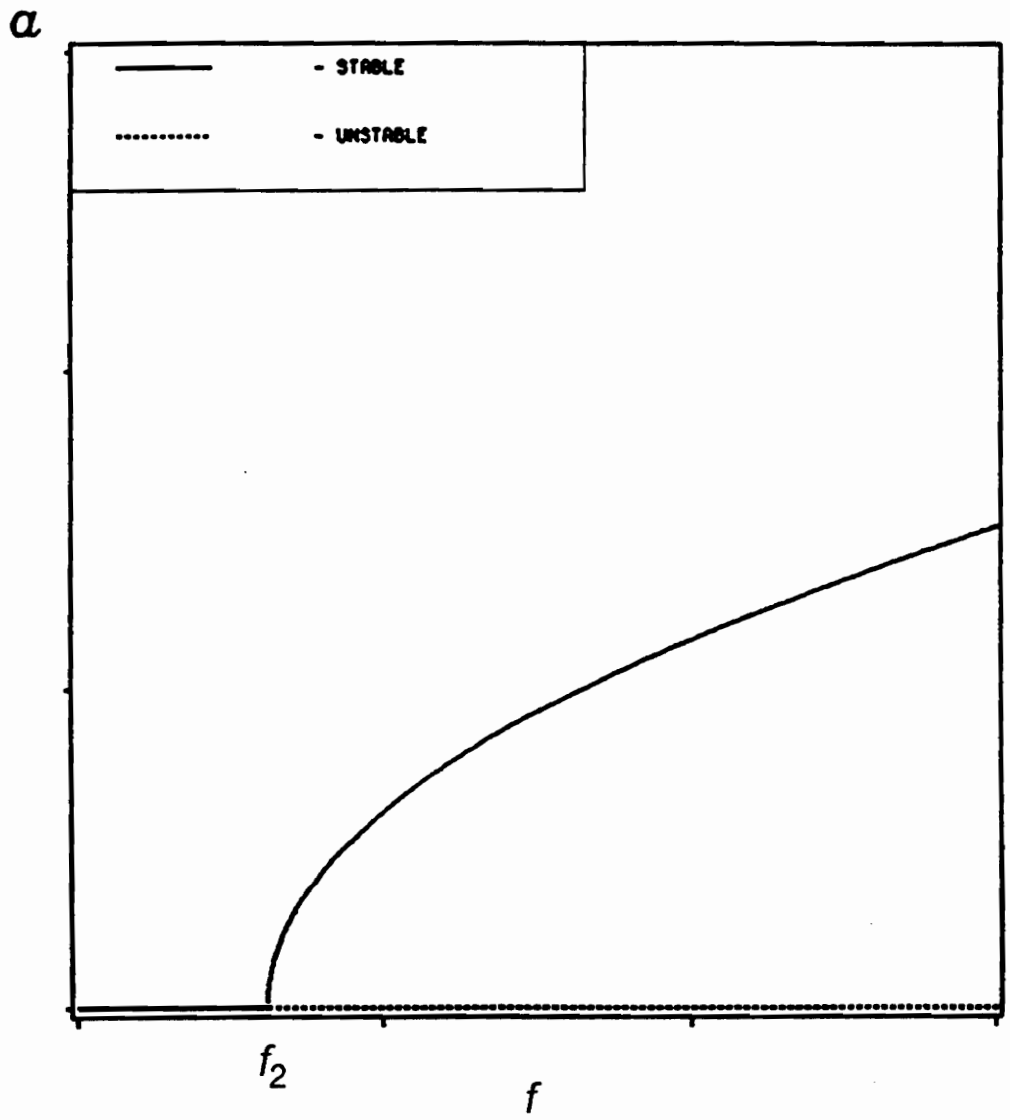

Figure 5.8. A representative variation of the response amplitude with the excitation amplitude for the case of subharmonic resonance of order one-half (length to thickness ratio $a/h = 10$, number of layers $N = 2$, $\sigma = -2$, $\mu = 0.5$).

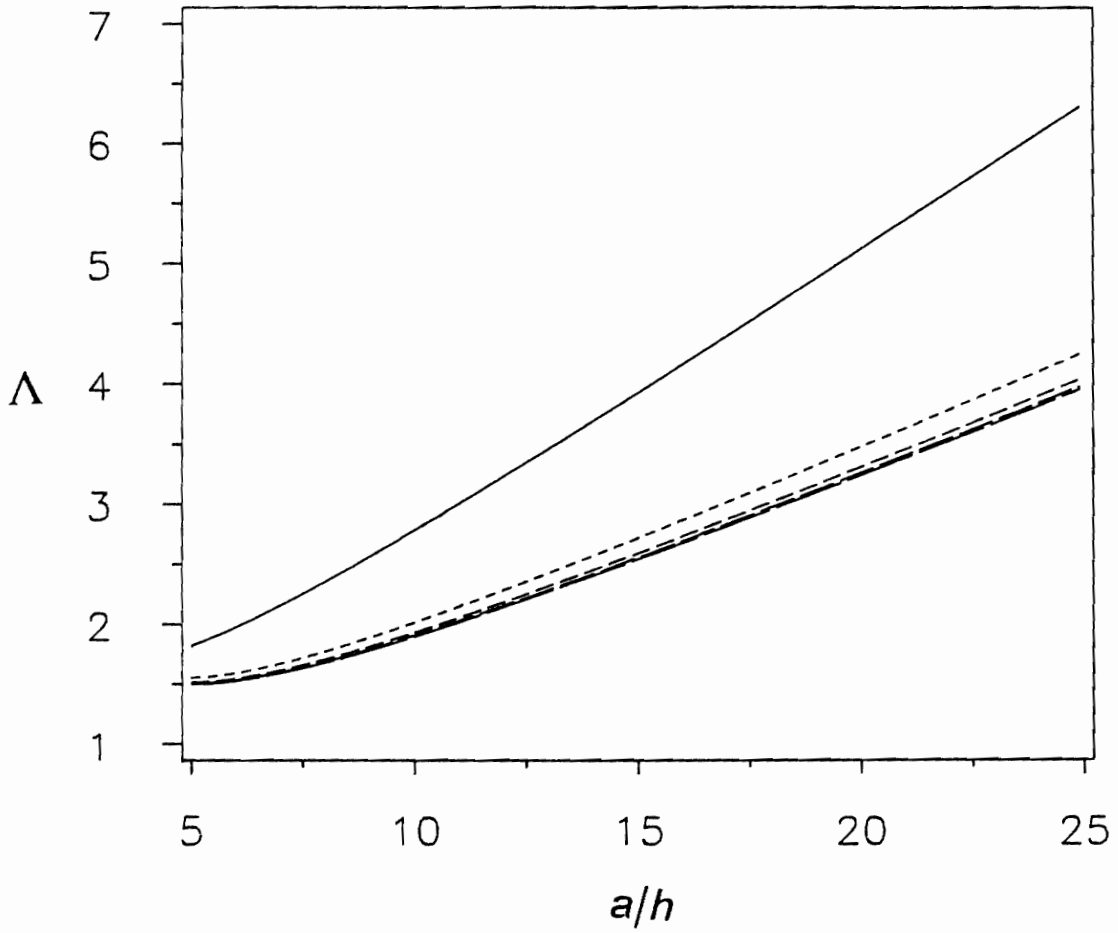

Figure 5.9. Superharmonic resonance of order two: the strength of the resonance (Λ) as a function of the length to thickness ratio (a/h) and the number of layers (N): (____) 2 layers, (- - -) 4 layers, (– – –) 6 layers, (– — –) 8 layers, and (— —) 10 layers.

Table 5.1. The effective nonlinearity α_e as a function of the length to thickness ratio (a/h) and the number of layers ($N = 2,4, 6, 8,$ and 10).

	Number of Layers				
a/h	2	4	6	8	10
5	6.134542	4.680862	4.475493	4.405833	4.373936
10	4.685128	3.046576	2.864788	2.805989	2.779536
15	4.411836	2.739222	2.561735	2.504880	2.479396
20	4.315803	2.631215	2.455224	2.399044	2.373895
25	4.271288	2.581143	2.405843	2.349973	2.324979

Table 5.2. Subharmonic resonance of order one-half: the strength of the resonance (Λ) as a function of the length to thickness ratio (a/h) and the number of layers ($N = 2,4,6,8,$ and 10).

	Number of Layers				
a/h	2	4	6	8	10
5	4.237573	3.531781	3.429651	3.397667	3.384759
10	6.476005	4.600228	4.393492	4.330619	4.304672
15	9.147711	6.204526	5.893408	5.799177	5.760087
20	11.931535	7.946588	7.531244	7.405610	7.353398
25	14.760616	9.744234	9.224741	9.067697	9.002373

Table 5.3. Superharmonic resonance of order two: the strength of the resonance (Λ) as a function of the length to thickness ratio (a/h) and the number of layers ($N = 2,4,6,8,$ and 10).

	Number of Layers				
a/h	2	4	6	8	10
5	1.819819	1.547227	1.508450	1.496959	1.492724
10	2.779698	2.014049	1.931135	1.906768	1.897183
15	3.926330	2.716293	2.590273	2.553231	2.538482
20	5.121153	3.478920	3.310101	3.260468	3.240623
25	6.335415	4.265896	4.054407	3.992223	3.967310

6. SURFACE WAVES IN CLOSED BASINS UNDER PRINCIPAL AND AUTOPARAMETRIC RESONANCES

6.1. Introduction

In this chapter, the method of multiple scales is used to analyze the nonlinear response of the surface of a liquid in a cylindrical container to a principal parametric resonant excitation in the presence of a two-to-one internal (autoparametric) resonance. Four autonomous first-order ordinary-differential equations are derived for the modulation of the amplitudes and phases of the two modes involved in the internal resonance when the higher mode is being excited by a principal parametric resonance. The modulation equations are used to determine the periodic oscillations and their stability. The force-response curves exhibit the jump and saturation phenomena as well as a Hopf bifurcation whereas the frequency-response curves exhibit the jump phenomenon and supercritical and subcritical Hopf bifurcations.

Limit-cycle solutions of the modulation equations are found between the Hopf frequencies; they correspond to aperiodic motions of the liquid surface. All limit cycles deform and lose stability by either pitchfork or cyclic-fold bifurcations as the excitation frequency or amplitude is varied. The pitchfork bifurcation breaks the symmetry of the limit cycles whereas the cyclic-fold bifurcation causes cyclic jumps, which may result in a transition to chaos. Period three motions are found in a very narrow range of the excitation frequency.

6.2. *Analysis*

We consider the nonlinear surface oscillations of a liquid that fills a rigid cylindrical container to a quiescent depth d* when the container is longitudinally excited (see Figure 6.1). The fluid is assumed to be inviscid and its motion to be irrotational so that its velocity can be derived from a potential function. The influence of surface tension on the surface motion is neglected. Distances are made dimensionless using a characteristic length ℓ of the cross section of the container and time is made dimensionless using the characteristic time $(\ell/g)^{1/2}$, where g is the gravitational acceleration.

6.2.1. Discretization of equations

Using either a Lagrangian formulation (Miles, 1984) or a formulation that attacks the governing partial-differential equation and boundary conditions (Nayfeh, 1987a), one can express the potential function ϕ and surface height η as

$$\phi(x,y,z,t) = \sum \phi_m(t)\psi_m(x,y)\text{sech}k_m d\cosh k_m(z+d). \tag{6.1}$$

$$\eta(x,y,t) = \sum \eta_m(t)\phi_m(x,y). \tag{6.2}$$

where $d = d^*/\ell$ and the ψ_m are the linear normal mode shapes. They are governed by

$$\nabla^2\psi_m + k_m^2\psi_m = 0 \tag{6.3}$$

subject to the condition

$$\nabla\psi_m \cdot \mathbf{n} = 0 \quad \text{on} \quad \delta S. \tag{6.4}$$

where, δS is the surface of the container cross section S and $\mathbf{n}$ is the outwardly directed normal to the surface. The ψ_m are orthonormalized so that

$$\iint \psi_m\psi_n dS = \delta_{mn}S, \tag{6.5}$$

where δ_{mn} is the Kronecker delta. For simple geometries, the ψ_m can be determined analytically. However, for complicated geometries, they are determined numerically. The equations governing the η_n are (Miles, 1984; Nayfeh, 1987a)

$$\ddot{\eta}_n + \omega_n^2\eta_n + \kappa_n\ddot{z}_0\eta_n + \sum\Gamma_{nms}\eta_m\ddot{\eta}_s + \sum\chi_{nms}\dot{\eta}_m\dot{\eta}_s = 0, \tag{6.6}$$

where

$$\omega_n^2 = \kappa_n = k_n \tanh k_n \tag{6.7}$$

$$\Gamma_{nms} = \frac{1}{2}\kappa_n C_{nms}\left[2 + \frac{k_m^2 - k_n^2 - k_s^2}{\kappa_n\kappa_s}\right] \tag{6.8}$$

$$\chi_{nms} = \frac{1}{2}\kappa_n C_{nms}\left[1 + \frac{k_m^2 + k_s^2 - k_n^2}{2\kappa_m\kappa_s} + \frac{k_m^2 - k_n^2 - k_s^2}{\kappa_n\kappa_s}\right] \tag{6.9}$$

and

$$C_{nms} = S^{-1}\int\int\psi_n\psi_m\psi_s dS \tag{6.10}$$

For the general case, the C_{nms} and hence the Γ_{nms} and χ_{nms} need to be determined numerically.

In this chapter, we determine an approximate solution to equations (6.6) for small but finite amplitudes when

$$z_0 = -F\cos\Omega t, \tag{6.11}$$

the second natural frequency ω_2 is approximately twice the first natural frequency ω_1, and $\Omega \approx 2\omega_2$. We note that Miles (1984), Nayfeh (1987a), and Gu and Sethna (1987) considered the case in which the first rather than the second mode is excited by a principal parametric resonance; that is, $\Omega \approx 2\omega_1$. As shown below, the dynamics of the system in the two cases is very much different.

6.2.2. Modulation equations

To express the nearness of the resonances, we introduce two detuning parameters σ_1 and σ_2 defined according to

$$\omega_2 = 2\omega_1 + \varepsilon\sigma_1 \quad \text{and} \quad \Omega = 2\omega_2 + \varepsilon\sigma_2 \tag{6.12}$$

where ε is a small dimensionless parameter that is the order of the amplitude of oscillations and it serves as a bookkeeping device. Using the method of multiple scales and following a procedure similar to that used in the paper by Nayfeh (1987a), we obtain a second-order expansion of equations (6.6) in the form

$$\eta_n = A_n(T_1)e^{i\omega_n T_0} + \bar{A}_n(T_1)e^{-i\omega_n T_0} + \ldots \tag{6.13}$$

for n = 1 and 2 and

$$\eta_n = 0 \text{ for } n \geq 3 \tag{6.14}$$

where $T_0 = t$, $T_1 = \varepsilon t$,

$$2i(A'_1 + \mu_1 A_1) - 4\Lambda_1 A_2 \bar{A}_1 e^{i\sigma_1 T_1} = 0 \tag{6.15}$$

$$2i(A'_2 + \mu_2 A_2) - 4\Lambda_2 A_1^2 e^{-i\sigma_1 T_1} + 2f\bar{A}_2 e^{i\sigma_2 T_1} = 0 \tag{6.16}$$

$$4\omega_1 \Lambda_1 = \Gamma_{121}\omega_1^2 + \Gamma_{112}\omega_2^2 - \omega_1\omega_2(\chi_{112} + \chi_{121}) \tag{6.17}$$

$$4\omega_2 \Lambda_2 = \omega_1^2(\Gamma_{211} + \chi_{211}) \tag{6.18}$$

and the prime indicates the derivative with respect to T_1. We note that if the cylindrical basin slightly deviates from a circular, one has to include two azimuthal modes and the radial mode in the analysis, thereby obtaining a sixth- rather than a fourth-order system of modulation equations. Substituting the polar form $A_n = \frac{1}{2} a_n \exp(i\beta_n)$ into equations (6.15) and (6.16) and separating real and imaginary parts, we obtain

$$a'_1 + \mu_1 a_1 - \Lambda_1 a_1 a_2 \sin\gamma_1 = 0 \tag{6.19}$$

$$a'_2 + \mu_2 a_2 + \Lambda_2 a_1^2 \sin\gamma_1 + f a_2 \sin\gamma_2 = 0 \tag{6.20}$$

$$a_1\beta'_1 + \Lambda_1 a_1 a_2 \cos\gamma_1 = 0 \tag{6.21}$$

$$a_2\beta_2' + \Lambda_2 a_1^2 \cos\gamma_1 - f a_2 \cos\gamma_2 = 0 \tag{6.22}$$

where

$$\gamma_1 = \beta_2 - 2\beta_1 + \sigma_1 T_1 \text{ and } \gamma_2 = \sigma_2 T_1 - 2\beta_2 \tag{6.23}$$

Alternatively, one can express the A_n in the Cartesian form

$$A_n = \frac{1}{2}(p_n - q_n)e^{i\nu_n T_1} \tag{6.24}$$

where the p_n and q_n are real and

$$\nu_1 = \frac{1}{2}\left(\frac{1}{2}\sigma_2 + \sigma_1\right) \text{ and } \nu_2 = \frac{1}{2}\sigma_2 \tag{6.25}$$

Substituting equations (6.24) and (6.25) into equations (6.15) and (6.16) and separating real and imaginary parts, we obtain the modulation equations

$$p'_1 = -\nu_1 q_1 - \mu_1 p_1 + \Lambda_1(p_2 q_1 - p_1 q_2) \tag{6.26}$$

$$q'_1 = \nu_1 p_1 - \mu_1 q_1 + \Lambda_1(p_1 p_2 + q_1 q_2) \tag{6.27}$$

$$p'_2 = -\nu_2 q_2 - \mu_2 p_2 - 2\Lambda_2 p_1 q_1 - f q_2 \tag{6.28}$$

$$q'_2 = \nu_2 p_2 - \mu_2 q_2 + \Lambda_2(p_1^2 - q_1^2) - f p_2 \tag{6.29}$$

We note that the modulation equations (6.19)-(6.23) and (6.26)-(6.29) differ from the modulation equations derived by Miles (1984) and Nayfeh (1987a) for the case of principal parametric resonance of the first mode in that the influence of the parametric excitation appears in the equations describing the second mode rather than the first mode. In the study of Miles (1984) and Nayfeh (1987a) the terms $fa_2 \sin\gamma_2$ and $-fa_2\cos\gamma_2$ in equations (6.20) and (6.22) are zero and equations (6.19) and (6.21) have the terms $ga_1 \sin\gamma_2$ and $-ga_1\cos\gamma_2$, where γ_2 in equation (6.23) is replaced with $\gamma_2 = \sigma_2 T_1 - 2\beta_1$. Moreover, the terms $-fq_2$ and $-fp_2$ are zero in equations (6.28) and (6.29) and equations (6.26) and (6.27) have instead the terms $-gq_1$ and $-gp_1$. Consequently, the frequency- and force-response curves and hence the dynamics described by these equations are very different. We note that although the modulation equations (6.26)-(6.29) are similar to those of Becker and Miles (1986) and Nayfeh (1987b), the present bifurcation analysis is far more comprehensive than theirs.

We note that, whereas the one-to-one autoparametric resonance leads to modulation equations with cubic nonlinearities, the two-to-one autoparametric resonance leads to modulation equations with quadratic nonlinearities. Hence, the frequency- and force-response curves have qualitatively as well as quantitatively different behavior in the two cases. Consequently, the two cases have different dynamics.

6.2.3. Fixed points

The fixed points of equations (6.19)-(6.23) and hence periodic solutions of equations (6.6) correspond to $a'_n = 0$ and $\gamma'_n = 0$. It follows from equations (6.23) and (6.25) that

$$\beta'_1 = \nu_1 \text{ and } \beta'_2 = \nu_2 \tag{6.30}$$

Hence, the fixed points of equations (6.19)-(6.23) are given by

$$\mu_1 a_1 - \Lambda_1 a_1 a_2 \sin \gamma_1 = 0 \tag{6.31}$$

$$\mu_2 a_2 + \Lambda_2 a_1^2 \sin \gamma_1 + f a_2 \sin \gamma_2 = 0 \tag{6.32}$$

$$\nu_1 a_1 + \Lambda_1 a_1 a_2 \cos \gamma_1 = 0 \tag{6.33}$$

$$\nu_2 a_2 + \Lambda_2 a_1^2 \cos \gamma_1 - f a_2 \cos \gamma_2 = 0 \tag{6.34}$$

There are two possibilities. Either

$$a_1 = a_2 = 0 \tag{6.35}$$

or

$$a_2 = |\Lambda_1|^{-1}\left[\mu_1^2 + \nu_1^2\right]^{1/2} \tag{6.36}$$

$$a_1^2 = -\chi_1 \pm \left[(fa_2/\Lambda_2)^2 - \chi_2^2\right]^{1/2} \tag{6.37}$$

where

$$\chi_1 = \frac{1}{\Lambda_1\Lambda_2}(\mu_1\mu_2 - \nu_1\nu_2) \text{ and } \chi_2 = \frac{1}{\Lambda_1\Lambda_2}(\mu_1\nu_2 + \mu_2\nu_1) \tag{6.38}$$

When $\chi_1 > 0$, equation (6.37) has no real roots when $f < \zeta_2$ and one real root when $f > \zeta_2$, where

$$\zeta_2 = (\mu_2^2 + \nu_2^2)^{1/2} \tag{6.39}$$

In this case, there are two possible fixed-point solutions: the trivial solution and a finite solution. When $\chi_1 < 0$, equation (6.37) has no real roots when $f < \zeta_1$, one real root when $f > \zeta_2$, and two real roots when $\zeta_1 < f < \zeta_2$, where

$$\zeta_1 = |\Lambda_1\Lambda_2\chi_2|(\mu_1^2 + \nu_1^2)^{-1/2} = |\mu_1\nu_2 + \mu_2\nu_1|(\mu_1^2 + \nu_1^2)^{-1/2} \tag{6.40}$$

In this case, there are three possible fixed-point solutions: the trivial solution and two finite solutions.

These fixed-point solutions are very much different from those obtained by Miles (1984) and Nayfeh (1987a) for the case of principal parametric resonance of the first mode. The present solutions demonstrate the presence of a saturation phenomenon. Equation (6.36) shows that the amplitude a_2 of the directly excited mode is independent of the amplitude of the excitation. It depends only on the damping

coefficient of the first mode and the detuning parameters σ_1 and σ_2. On the other hand, equation (6.37) shows that the amplitude a_1 of the indirectly excited first mode is strongly dependent on the excitation amplitude f.

6.2.4. Stability of fixed points

The stability of the fixed points and hence the stability of the periodic solutions depends on the real parts of the eigenvalues of the Jacobian matrix of equations (6.26)-(6.29), that is, the roots of

$$\begin{vmatrix} \lambda+\mu_1+\Lambda_1 q_2 & \nu_1-\Lambda_1 p_2 & -\Lambda_1 q_1 & \Lambda_1 p_1 \\ -\nu_1-\Lambda_1 p_2 & \lambda+\mu_1-\Lambda_1 q_2 & -\Lambda_1 p_1 & -\Lambda_1 q_1 \\ 2\Lambda_2 q_1 & 2\Lambda_2 p_1 & \lambda+\mu_2 & \nu_2+f \\ -2\Lambda_2 p_1 & 2\Lambda_2 q_1 & -\nu_2+f & \lambda+\mu_2 \end{vmatrix} = 0 \qquad (6.41)$$

A given fixed point is stable if and only if all the λ's lie in the left-half of the complex plane and unstable if at least one eigenvalue lies in the right-half of the complex plane.

To investigate the stability of the trivial solution, we put $p_n = q_n = 0$ in equation (6.41) and, after expanding the determinant, obtain

$$\left[(\lambda+\mu_2)^2+\nu_2^2-f^2\right]\left[(\lambda+\mu_1)^2+\nu_1^2\right]^2 = 0 \qquad (6.42)$$

or

$$\lambda = -\mu_2 + (f^2 - v_2^2)^{1/2}, -\mu_1 \pm iv_1 \tag{6.43}$$

Hence, the trivial solution is asymptotically stable if and only if

$$f < \zeta_2 = (\mu_2^2 + v_2^2)^{1/2} \tag{6.44}$$

which is condition (6.39) for the existence of one real root of equation (6.37). It follows from equations (6.43) that the trivial solution is a sink when $f < \zeta_2$ and a saddle when $f > \zeta_2$.

To analyze the stability of the nontrivial fixed points, we expand equation (6.41), make use of equations (6.31)-(6.34), and obtain

$$\begin{aligned}\lambda^4 &+ 2(\mu_1 + \mu_2)\lambda^3 + [\mu_2^2 + 4\mu_1\mu_2 + v_2^2 - f^2 + 4\Lambda_1\Lambda_2 a_1^2]\lambda^2 \\ &+ 2[\mu_1\mu_2^2 + 2\mu_1 v_2^2 - 2\mu_1 f^2 + 4\Lambda_1\Lambda_2(\mu_1 + \mu_2)a_1^2]\lambda \\ &+ 8\Lambda_1\Lambda_2 a_1^2[\Lambda_1\Lambda_2 a_1^2 + \mu_1\mu_2 - v_1 v_2] = 0\end{aligned} \tag{6.45}$$

The necessary and sufficient conditions that none of the roots of equation (6.45) have positive real parts are

$$r_1 r_2 - r_3 > 0,\ r_3(r_1 r_2 - r_3) - r_1^2 r_4 > 0,\ r_4 > 0 \tag{6.46}$$

where r_1, r_2, r_3, and r_4 are the coefficients of $\lambda^3, \lambda^2, \lambda$, and λ^0 in equation (6.45), respectively. The condition that $r_4 > 0$ in conjunction with equation (6.37) implies that the solution corresponding to the positive sign is stable whereas the solution corresponding to the negative sign is unstable. The violation of the second condition in (6.46) would imply the existence of a pair of complex-conjugate roots of equation (6.45) with a positive real part.

6.2.5. Stability of periodic orbits

The stability of the periodic solutions of the modulation equations (6.26)-(6.29) is determined using Floquet theory (Nayfeh and Mook, 1979). Thus, to determine the stability of a T-periodic limit cycle $\mathbf{p}^*(T_1) = \mathbf{p}^*(T_1 + T)$, where $p = [p_1, q_1, p_2, q_2]^T$ we superimpose on it a small displacement $\theta(T_1)$ and obtain the perturbed equation

$$\mathbf{p}^{*\prime} + \theta' = \mathbf{F}[\mathbf{p}^*(T_1) + \theta(T_1)] \tag{6.47}$$

Expanding equation (6.47) in a Taylor series for small $\theta(T_1)$ and linearizing the flow about the periodic orbit, we obtain the linear variational equation

$$\theta' = A(T_1)\theta \tag{6.48}$$

where $A(T_1) = [\nabla \mathbf{F}(\mathbf{p}^*(T_1))]$ is a square 4x4 variational matrix with T-periodic elements. We let $\Theta(T_1)$ be the fundamental-matrix solution satisfying

$$\Theta' = A(T_1)\Theta, \quad \Theta(0) = \mathrm{I} \tag{6.49}$$

Then, the Floquet multipliers are the eigenvalues of the monodromy matrix $\Theta(T)$. As a control parameter such as $\hat{\sigma}_2$ is varied, the positions of the multipliers relative to the unit circle in the complex plane determine the stability of the orbit. Because equations (6.26)-(6.29) are autonomous, one of the multipliers is always $+1$ corresponding to $\theta(T_1)$ along the trajectory $p^*(T_1)$ while the others describe what happens perpendicular to it. If all of the other multipliers lie inside the unit circle, then the orbit is asymptotically stable. If one of the multipliers leaves the unit circle, then the orbit is unstable. The type of the resulting bifurcation depends on the way a multiplier leaves the unit circle. There are three generic ways in which this

happens. First, a multiplier leaves the unit circle through +1, resulting in either a cyclic-fold (tangent) or pitchfork (symmetry-breaking) bifurcation. Second, a multiplier leaves the unit circle through -1, resulting in a flip or period-doubling bifurcation. Third, two complex conjugate multipliers leave the unit circle, resulting in a Hopf bifurcation. In our study, we observe cyclic-fold and pitchfork bifurcations associated with one of the three multipliers crossing the unit circle at +1 while the other two remaining inside the unit circle. The cyclic-fold bifurcations result in either the disappearance of the attractor or cyclic jumps. The latter causes the flow to jump to another limit-cycle attractor or to a chaotic attractor. Symmetry-breaking bifurcations take place when a multiplier touches +1 from within the inside of the unit circle, crosses it, and stays very close to the outside boundary.

Equations (6.26)-(6.29) can be reduced to a generic system of equations by applying the following transformation of variables: $p_1 = \hat{p}_1/\sqrt{\Lambda_1\Lambda_2}$, $q_1 = \hat{q}_1/\sqrt{\Lambda_1\Lambda_1}$, $p_2 = \hat{p}_2/\Lambda_1$, and $q_2 = \hat{q}_2/\Lambda_1$. The resulting modulation equations are

$$\hat{p}'_1 = -\nu_1\hat{q}_1 - \mu_1\hat{p}_1 + \hat{p}_2\hat{q}_1 - \hat{p}_1\hat{q}_2 \tag{6.50}$$

$$\hat{q}'_1 = -\nu_1\hat{p}_1 - \mu_1\hat{q}_1 + \hat{p}_1\hat{p}_2 + \hat{q}_1\hat{q}_2 \tag{6.51}$$

$$\hat{p}'_2 = -\nu_2\hat{q}_2 - \mu_2\hat{p}_2 - 2\hat{p}_1\hat{q}_1 - f\hat{q}_2 \tag{6.52}$$

$$\hat{q}'_2 = \nu_2\hat{p}_2 - \mu_2\hat{q}_2 + 2\hat{p}_1^2 - \hat{q}_1^2 - f\hat{p}_2 \tag{6.53}$$

where the prime indicates the derivative with respect to the slow time scale.

6.3. Numerical Results

Computer simulations are performed on the dynamical system governed by the autonomous modulation equations (6.26)-(6.29) rather than on the original equations of the waves. Once again, fixed points of the modulation equations correspond to periodic oscillations of the free surface, whereas limit-cycle solutions of the modulation equations correspond to aperiodic motions of the free surface. In this chapter, we examine bifurcations of co-dimension one. Either the detuning parameter $\hat{\sigma}_2 = \sigma_2/f$ or the excitation amplitude f is chosen as the bifurcation parameter; all other parameters (i.e., $\hat{\sigma}_1/f$, $\hat{\mu}_1 = \mu_1/f$, and $\hat{\mu}_2 = \mu_2/f$) are held constant.

We note that symmetry exists in the modulation equations (6.26)-(6.29). They are invariant under the transformations $(p_1, q_1, p_2, q_2) \Leftrightarrow (q_1, -p_1, -p_2, -q_2)$ $\Leftrightarrow (-q_1, p_1, -p_2, -q_2) \Leftrightarrow (-p_1, -q_1, p_2, q_2)$. This implies that the projection of a solution of the modulation equations onto the $q_1 - p_1$ plane remains unaffected by rotations through 90°, −90°, and 180° around the origin. Similarly, a 180° rotation around the origin in the $q_2 - p_2$ plane produces the same projection onto this plane. Hence, the fixed points, trajectories, limit cycles, and attractors occur in quadruple if they are not transformed into themselves by the symmetry. For example, if there is an attractor (i.e., a long-time solution of the modulation equations), then, for the same bifurcation parameter $\hat{\sigma}_2$ or f, three other attractors can be obtained by just applying the above transformations unless the attractor itself is symmetric. We will not mention the symmetric "quadruple" attractors unless the four interact in an interesting manner.

The numerical results have been obtained, unless otherwise stated, for the case of a circular cylinder filled with a liquid to a quiescent depth $d^*/R = 0.1300$, where d*

is the dimensional liquid depth and R is the radius of the cylinder. The corresponding values of the parameters used in studying the dynamics of the modulation equations are $\Lambda_1 = -1.6602$, $\Lambda_2 = -7.1695$, $\omega_1 = 0.6576$, $\omega_2 = 1.3285$, and $\sigma_1 = 0.0133$ (Table 1 in the paper by Nayfeh, 1987a).

Figure 6.2 shows a typical force-response curve for $\chi_1 < 0$ when $\varepsilon = 0.05$. The response exhibits the saturation and jump phenomena as well as a Hopf bifurcation. When $0 \leq f < f_1$, where $f_1 = 0.024$ only the trivial solution is possible and it is stable. When $f_1 < f < f$, where $f_2 = 0.100$, there are three possible solutions: the trivial solution, which is stable, and two nontrivial solutions for $\hat{a}_1 = \sqrt{\Lambda_1 \Lambda_2}\, a_1$ corresponding to a constant nontrivial solution for $\hat{a}_2 = |\Lambda_1| a_2$ with the large solution for $\hat{a}_1$ being stable and the small solution for $\hat{a}_1$ being unstable. When $f_2 < f < f_3$, where $f_3 = 0.103$, there are two possible solutions: the trivial solution, which is unstable, and a nontrivial solution, which is stable. When $f > f_3$, there are two possible solutions: the trivial solution, which is unstable with an eigenvalue being positive, and a nontrivial solution, which is unstable with the real part of a complex conjugate pair of eigenvalues having a positive real part. Consequently, as the amplitude f of excitation increases slowly from zero, the response remains trivial until f reaches f_2. At the threshold value $f = f_2$, the trivial fixed point loses its stability and a jump to the nontrivial solution occurs. The response in this case is nonlinear, periodic, and consists of both modes. A further increase in f results in the saturation of the higher mode. It responds with a constant amplitude and spills over the extra input energy into the coupled lower mode, which responds nonlinearly with a large amplitude. We note that the saturation phenomenon does not appear when the lower rather than the second mode is excited by a principal parametric resonance. Moreover, it does not appear in one-to-one autoparametric resonance cases, such as those studied by

Miles (1984), Feng and Sethna (1989), Umeki and Kambe (1989), and Simonelli and Gollub (1989). The nontrivial fixed point undergoes a Hopf bifurcation at $f = f_3$, resulting in amplitude- and phase-modulated (quasi-periodic) oscillations of the liquid surface. On the other hand, as f decreases beyond f_3, the higher mode responds with a constant amplitude while the amplitude of the lower mode decreases. At $f = f_2$, the trivial fixed point becomes stable and an unstable fixed point of the lower mode is born. At $f = f_1$, the nontrivial stable and unstable fixed points of the lower mode collide in a fold bifurcation, resulting in a jump to the stable trivial fixed point. For values of f between f_1 and f_2, an unstable fixed point separates two stable fixed points of the lower mode. In this region, the solution tends to either one of the point attractors depending on the initial conditions.

Figure 6.3 shows a typical force-response curve for $\chi_1 > 0$ when $\varepsilon = 0.05$. In this case, no fold bifurcation takes place and the jump occurs only in the higher mode.

Figures 6.4(a-d) show the Hopf-bifurcation curves in the parameter space $\hat{\sigma}_1 - \hat{\sigma}_2$ for different values of the damping parameter $\hat{\mu}_n$. In the shaded regions the fixed points of the modulation equations are asymptotically stable and hence correspond to periodic motions of the liquid surface. These charts are completely different from that obtained for the case of principal parametric resonance of the first mode (Nayfeh, 1987a). A complex conjugate pair of eigenvalues of the Jacobi matrix crosses the imaginary axis into the right-half of the complex plane with nonzero speed at the transition curves. The loss of stability thus fits within the framework of the Hopf bifurcation theorem, according to which the modulation equations possess limit-cycle solutions near the bifurcation curves. The curves on the left are supercritical Hopf-bifurcation boundaries whereas those on the right are subcritical Hopf-bifurcation boundaries. Limit-cycle and chaotic attractors are found between the

two boundaries. The limit cycles near the supercritical Hopf-bifurcation boundaries have relatively small amplitudes when compared to those near the subcritical Hopf-bifurcation boundaries. Whereas limit cycles exist only to the right of the supercritical bifurcation boundary, they exist on both sides of the subcritical bifurcation boundary. In fact, limit-cycle and fixed-point attractors coexist in some region on the right of the subcritical boundary; the initial conditions determine which of these attractors is attained. Figures 6.4(a-d) show that increasing the damping moves the subcritical and supercritical boundaries closer to each other.

Figures 6.5(a-c) show three frequency-response curves for f = 1.0 and $\hat{\mu}_2 = 0.02$. The Hopf bifurcation points are indicated on the curves (see also Table 6.1). The left Hopf point is supercritical while the right one is subcritical. The response is symmetric for $\hat{\sigma}_1 = 0$; that is, the case of perfect tuning. When $\hat{\sigma}_1 = -0.266$, the curves are shifted to the right while when $\hat{\sigma}_1 = 0.266$ the curves are shifted to the left. The qualitative behavior of the solutions in the three cases is the same. In the following discussion, we consider the case $\hat{\sigma}_1 = 0.266$.

To describe the dynamics of the system, we need to determine the steady-state periodic waveforms (attractors) and unstable limit cycles. It is computationally inefficient to determine these solutions by conventional numerical-integration methods. To locate the limit cycles, we use an algorithm originally proposed by Aprille and Trick (1972) to eliminate transient responses, thereby latching onto a limit cycle and calculating its period. It uses a combination of a numerical integration scheme and a Newton-Raphson iteration procedure. This algorithm proved efficient in reducing the computation time but it is sensitive to the initial guesses and the step size of the integration when multiple solutions coexist. Using different step sizes, we found that the algorithm sometimes landed on different orbits for the same value

of $\hat{\sigma}_2$. Spectral analysis techniques are used to look for cyclical patterns or periodicities in signals. The algorithm developed by Cooley and Tukey (1965) and implemented by Singleton (1969) is used to compute the Fast Fourier Transform (FFT).

For values of $\hat{\sigma}_2$ less than the supercritical Hopf frequency (-1.9984) or greater than the subcritical Hopf frequency (1.9986), the modulation equations possess simple fixed point attractors, which represent stationary steady states. The fixed points are hyperbolic and therefore are structurally stable. They become nonhyperbolic and lose their stability at the Hopf bifurcation points. Based on the Hopf bifurcation theorem, near these bifurcation values the modulation equations possess limit-cycle solutions corresponding to a two-dimensional torus of the original system.

Next, we investigate global bifurcations of the periodic solutions of the modulation equations and the existence of chaotic attractors using the detuning $\hat{\sigma}_2$ of the excitation frequency as a control parameter. Figure 6.6 shows the bifurcation points and the solutions in the various detuning intervals in the neighborhood of the supercritical Hopf-bifurcation point. Below the supercritical value $\hat{\sigma}_2 = -1.9984$, the modulation equations possess only fixed-point solutions. As $\hat{\sigma}_2$ is increased beyond the supercritical Hopf-bifurcation frequency $\hat{\sigma}_2 = -1.9984$, attractors I and II and the unstable limit cycle III are born simultaneously. Attractor I is small compared with attractor II and the unstable limit cycle III, as shown in Figure 6.7. These solutions continue to coexist until $\hat{\sigma}_2$ is increased to -1.9978. At this value, attractor I loses its stability and undergoes a cyclic-fold bifurcation with one of its Floquet multipliers leaving the unit circle through $+1$. As a result, attractor I disappears while attractor II and limit cycle III deform smoothly and approach each other. The phase portraits

and time history shown in Figures 6.8(a-c) depict attractor II at $\hat{\sigma}_2 = -1.80$. The power spectrum of this attractor shown in Figure 6.8(d) is made up of a major peak at the fundamental frequency $1/T$ and smaller peaks at its harmonics. At $\hat{\sigma}_2 = -1.8197$, attractor IV (see Figure 6.9) is born and lives with attractor II and the unstable limit cycle until $\hat{\sigma}_2$ is increased to - 1.7858 where attractor II collides with the unstable limit cycle III and loses its stability through a cyclic-fold bifurcation, resulting in the two limit cycles annihilating each other. Attractor IV survives the collision, maintains its symmetry, and deforms smoothly as $\hat{\sigma}_2$ is increased to $\hat{\sigma}_2 = -1.6897$. As $\hat{\sigma}_2$ is increased further, the symmetry of attractor IV is broken and four asymmetric conjugate quadruple attractors are born. The phase portraits in Figure 6.10 show one such periodic orbit and its odd-symmetric clones. These quadruple attractors lose their stability at $\hat{\sigma}_2 = -1.6543$ through a cyclic-fold bifurcation, which results in the birth of a chaotic attractor . It evolves smoothly from $\hat{\sigma}_2 = -1.6543$ to $\hat{\sigma}_2 = -1.6297$, where it suddenly disappears, and gives way to attractor V (Figure 6.11), which survives as a unique attractor. It loses its stability through a cyclic-fold bifurcation at $\hat{\sigma}_2 = -1.5797$ and a chaotic attractor reappears again. As $\hat{\sigma}_2$ is increased further, the chaotic attractor evolves and its shape changes slowly but in a continuous way. It contracts in some directions and expands in others with the contraction outweighing the expansion. The Lyapunov exponents are computed and used to quantify the expansion and contraction occurring in the attractor. The algorithm proposed by Wolf et al. (1985) is used to calculate the Lyapunov exponents. They are found to be 0.566, 0.000, -0.057, and -0.624. The positive exponent indicates an exponential divergence of neighboring trajectories and thus confirms the chaotic nature of the attractor. The Lyapunov dimension d_L of the attractor is also calculated using the relation proposed by Frederickson et al. (1983). Accordingly the Lyapunov

dimension is $d_L = 3.8$. As we continue increasing the bifurcation parameter $\hat{\sigma}_2$, we observe that the chaotic attractor persists up to $\hat{\sigma}_2 = -1.2797$, which represents a boundary crisis. Suddenly, at this detuning value, the chaotic attractor disappears and the flow of the vector field (6.55)-(6.58) diverges with any initial conditions. The death of this chaotic attractor may be due to its collision with a saddle-type periodic orbit that encircles it. This collision destroys the boundedness of the chaotic attractor and thus provides an exit path for the trajectories to escape into the outer space.

The phase portrait displayed in Figure 6.12(a) demonstrates two important characteristics of the chaotic attractor: its irregular nature and the sensitive dependence on the initial conditions. The trajectories, therefore, converge towards some well-defined geometrical structure in the state space. The waveform in Figure 6.12(b) shows that the attractor is never periodic, nor almost periodic. In terms of the frequency content, the Fourier transform of the q_1 signal in Figure 6.12(c) has a broadband component. The Poincar&eac. section in Figure 6.12(d) shows that the chaotic attractor does not lie on a simple geometrical object. The attractor is geometrically invariant and thus repeats its structure on even finer spatial scales.

Figure 6.13 depicts the bifurcation points and the solutions near the subcritical Hopf-bifurcation point. Near the subcritical Hopf-bifurcation frequency ($\hat{\sigma}_2 = 1.9986$), attractor VII and an unstable limit cycle VIII exist and extend in two directions around the Hopf point. They penetrate into the region of the fixed-point attractor until they collide with each other at $\hat{\sigma}_2 = 2.0348$ where they disappear. Two- and three-dimensional projections of attractor VII are shown in Figures 6.14(a) and 6.14(b). In this region, the flow tends to either the fixed-point attractor or attractor VII depending on the initial conditions. Attractor VII continues to exist on the other side of the subcritical Hopf point ($\hat{\sigma}_2 = 1.9986$). At $\hat{\sigma}_2 = 1.9958$ another limit cycle (attractor

VI) is born and coexists with attractor VII. A two-dimensional projection of this attractor at $\hat{\sigma}_2 = 1.99$ is shown in Figure 6.15. At $\hat{\sigma}_2 = 1.9905$, attractor VII, shown in Figures 6.14(c) and 6.14(d), undergoes a cyclic-fold bifurcation and vanishes, leaving attractor VI occupying the whole phase space as the only periodic attractor until $\hat{\sigma}_2 = 1.9842$. Two interesting bifurcations take place at this frequency. First, attractor VI loses its symmetry and gives rise to a quadruple of conjugate asymmetric attractors. Two-dimensional projections of these attractors are shown in Figure 6.16. Second, an isolated period-three limit cycle attractor appears and shares the phase space with these four quadruple asymmetric attractors. The period-three attractor, whose phase portrait is shown in Figure 6.17, exists over a very narrow range of $\hat{\sigma}_2$. It deforms rapidly and undergoes a cyclic-fold bifurcation, collides with the quadruple attractors, and eventually disappears. Attractor VI survives the collision and deforms smoothly as $\hat{\sigma}_2$ is reduced. At $\hat{\sigma}_2 = 1.9821$, the asymmetric quadruples undergo reverse symmetry-breaking bifurcation and attractor VI regains its symmetry and continues to deform smoothly as $\hat{\sigma}_2$ is reduced furthermore. A cyclic-fold bifurcation takes place at $\hat{\sigma}_2 = 1.9818$, causing a jump to a chaotic attractor. It extends over a large parameter region where it evolves continuously and smoothly while maintaining its structural characteristics. The chaotic attractor suddenly disappears at $\hat{\sigma}_2 = 1.9105$. This excitation frequency signifies another boundary crisis and the same collision scenario that takes place at $\hat{\sigma}_2 = 1.2797$ happens here. It is responsible for the sudden death of the chaotic attractor and provides an exit path for the trajectories to escape into the outer space.

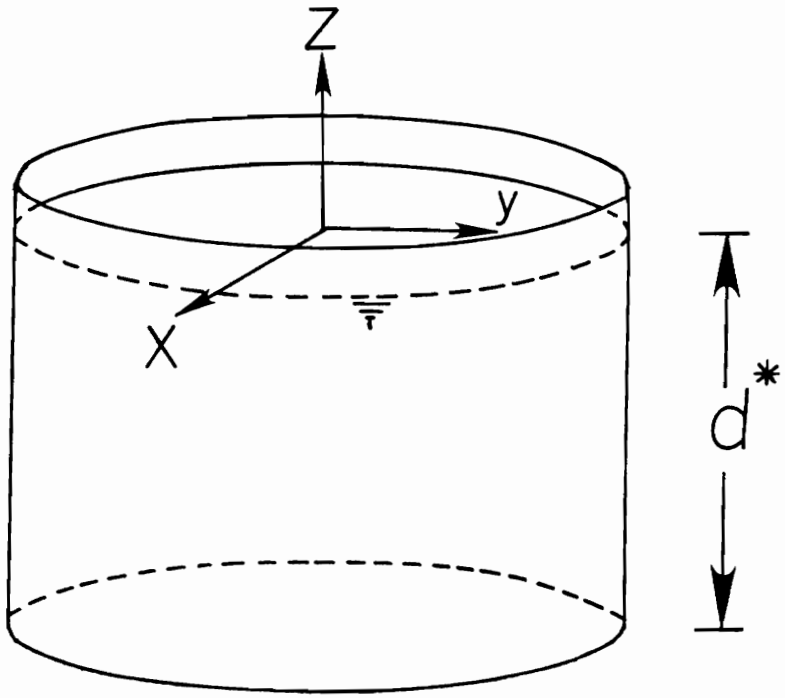

Figure 6.1. Geometry for a liquid in a cylindrical container.

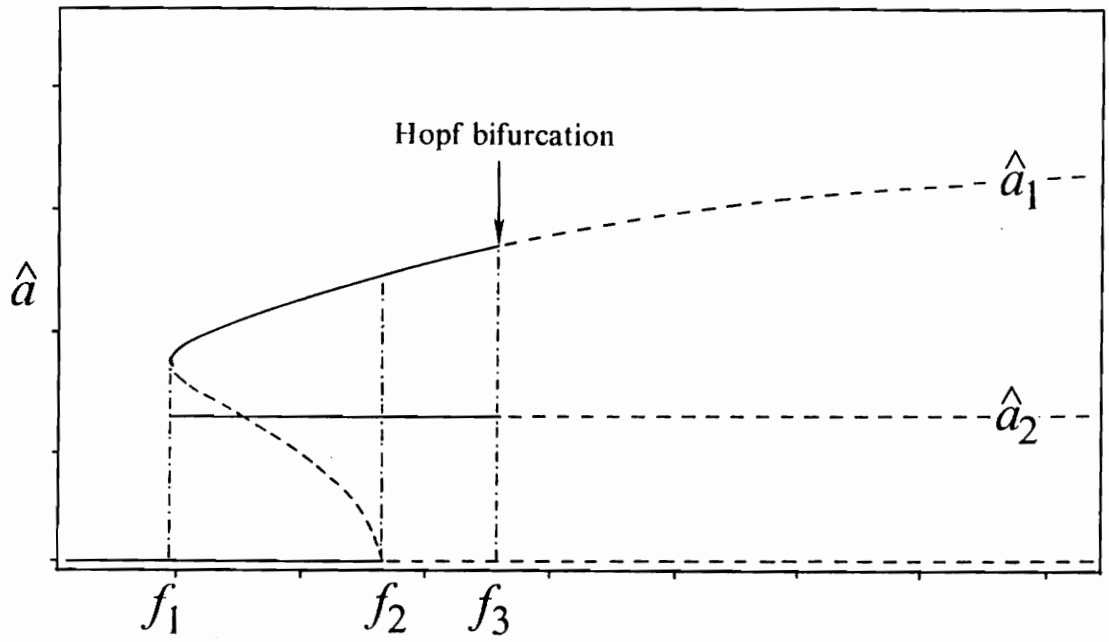

Figure 6.2. Typical force-response curves for the case $\chi_1 < 0$ when $\varepsilon = 0.05$; $\mu_{1,2} = 0.02$, $\sigma_1 = 0.266$ and $\sigma_2 = -0.2$: solid curves ____ , stable fixed-point solutions; --- unstable fixed-point solutions.

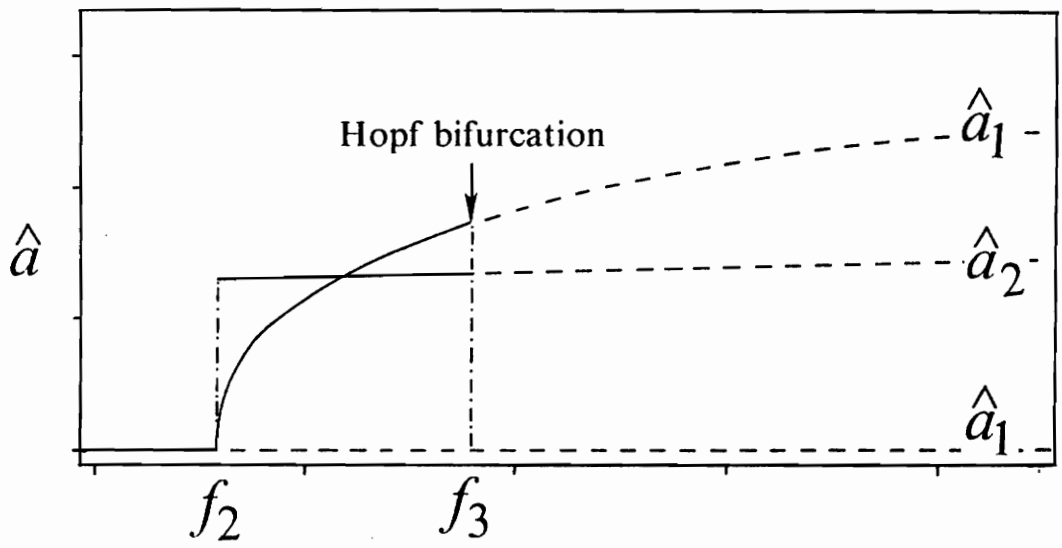

Figure 6.3. Typical force-response curves for the case $\chi_1 > 0$ when $\varepsilon = 0.05$; $\hat{\mu}_{1,2} = 0.02$, $\hat{\sigma}_1 = 0.266$ and $\sigma_2 = 0.2$: solid curves ____, stable fixed-point solutions; --- unstable fixed-point solutions.

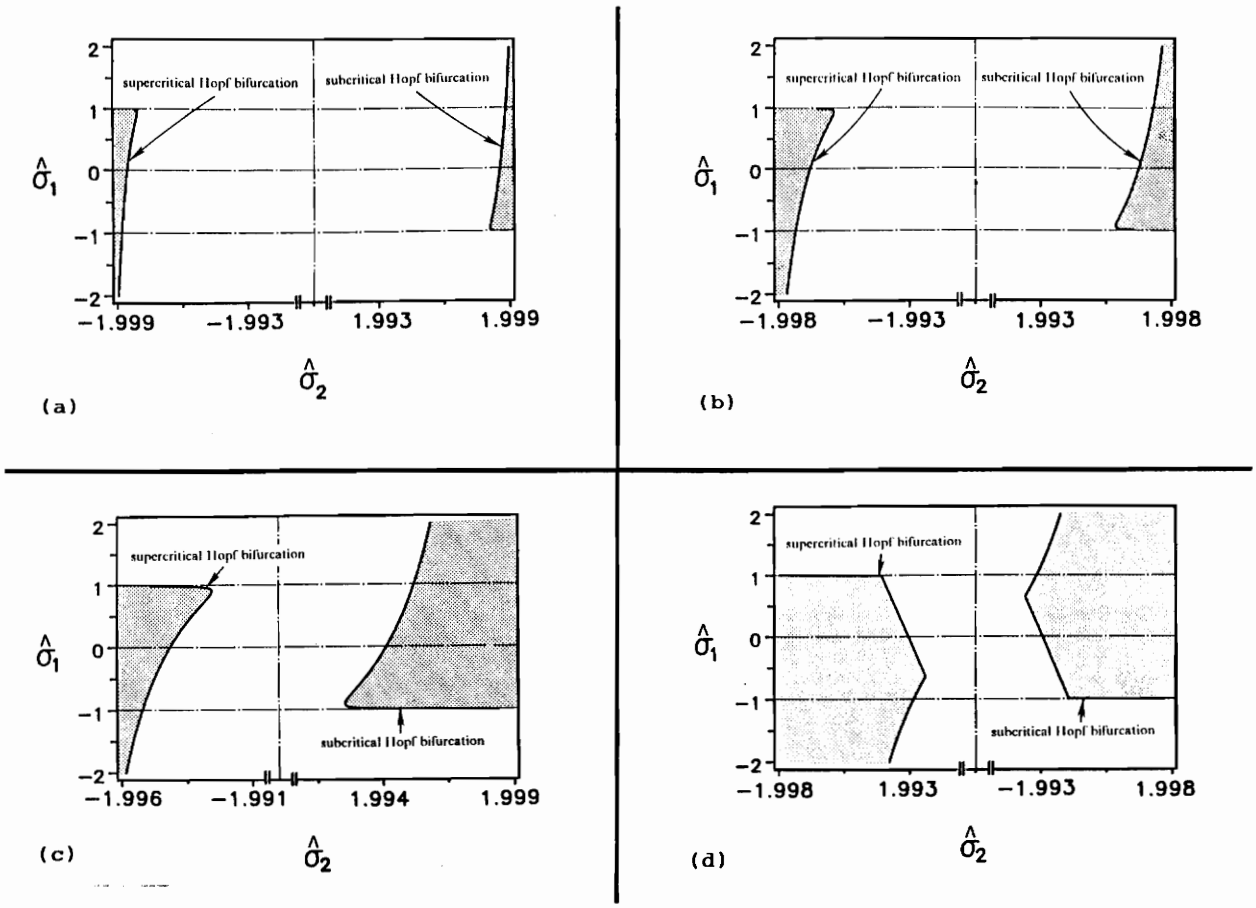

Figure 6.4. Hopf-bifurcation curves in the $\hat{\sigma}_1 - \hat{\sigma}_2$ parameter space; shaded area indicates stable region, left curve represents subcritical Hopf-bifurcation boundary and right curve represents supercritical Hopf-bifurcation boundary: (a) $\hat{\mu}_{1,2} = 0.02$, (b) $\hat{\mu}_{1,2} = 0.03$, (c) $\hat{\mu}_{1,2} = 0.04$, and (d) $\hat{\mu}_{1,2} = 0.05$.

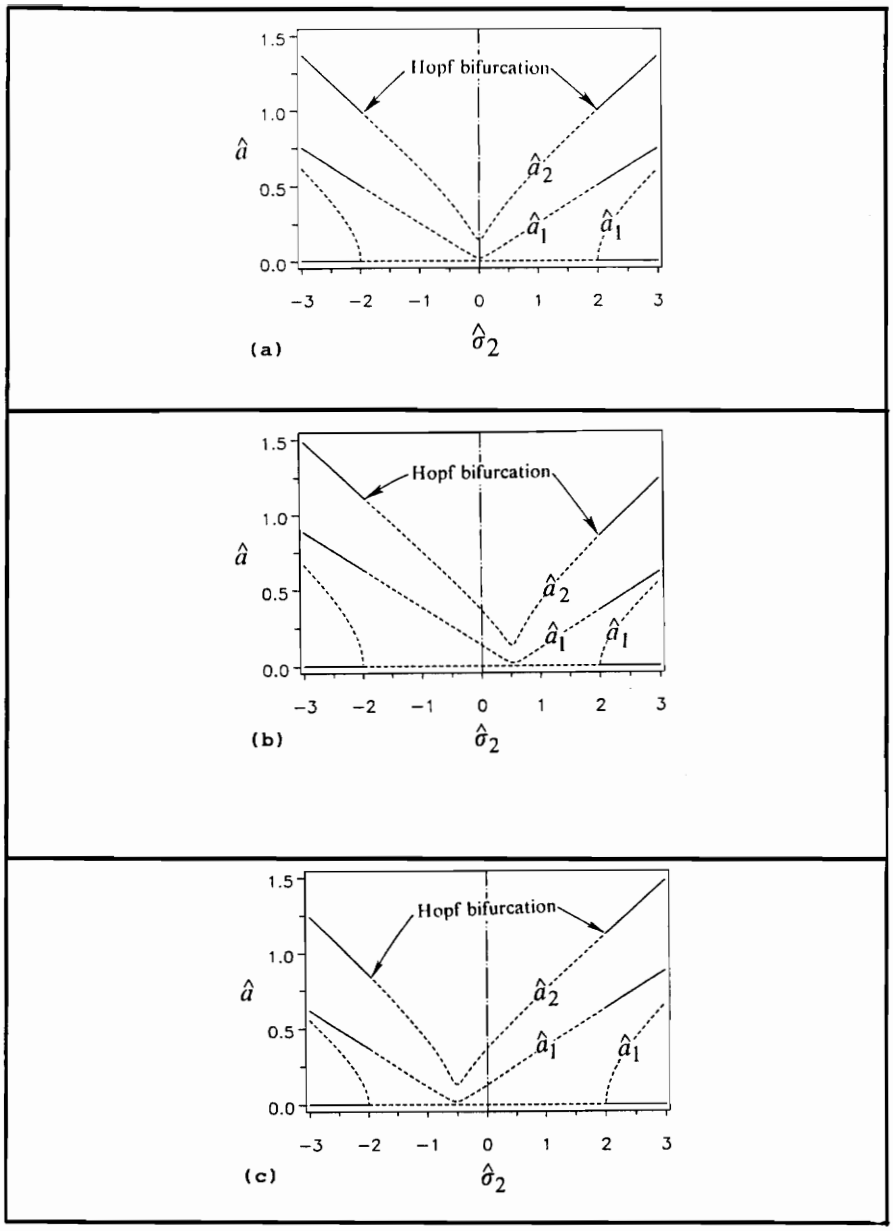

Figure 6.5. Typical frequency-response curves when $\hat{\mu}_{1,2} = 0.02$; solid curves ____, stable fixed-point solutions; --- unstable fixed-point solutions: (a) $\hat{\sigma}_1 = 0.0$, (b) $\hat{\sigma}_1 = -0.266$, and (c) $\hat{\sigma}_1 = 0.266$.

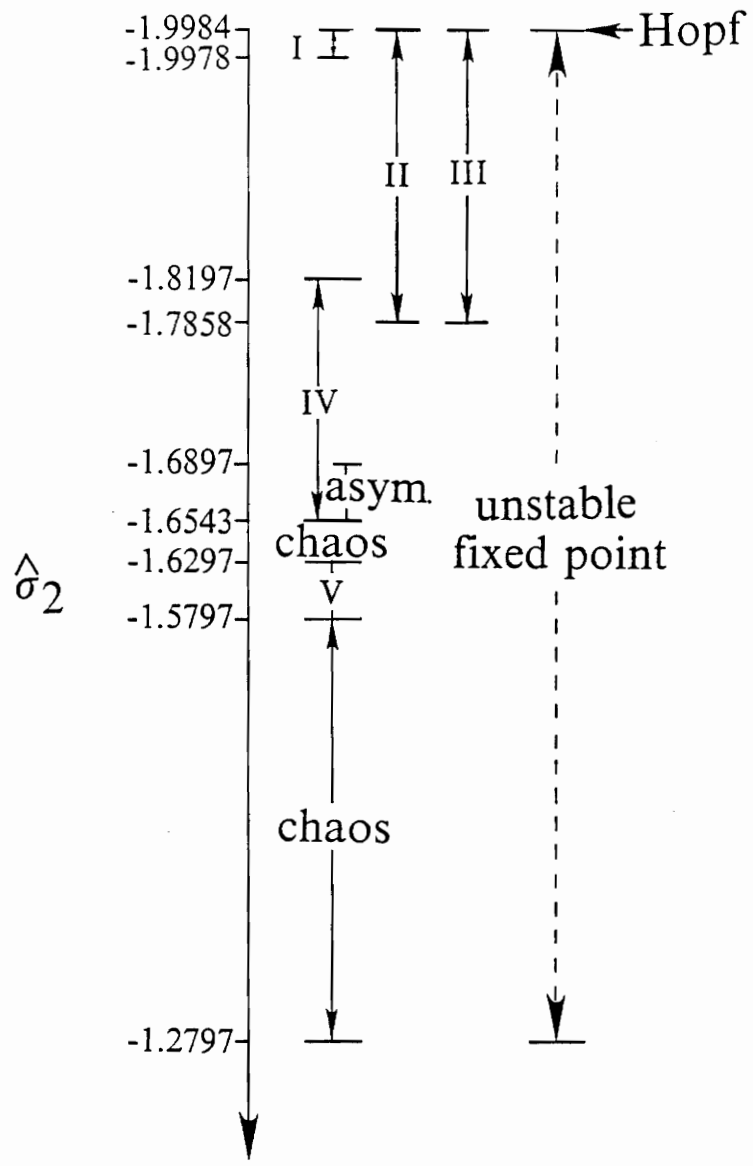

Figure 6.6. Bifurcation diagram of the modulation equations near the supercritical Hopf bifurcation excitation frequency: $\hat{\mu}_{1,2} = 0.02$ and $\hat{\sigma}_1 = 0.266$.

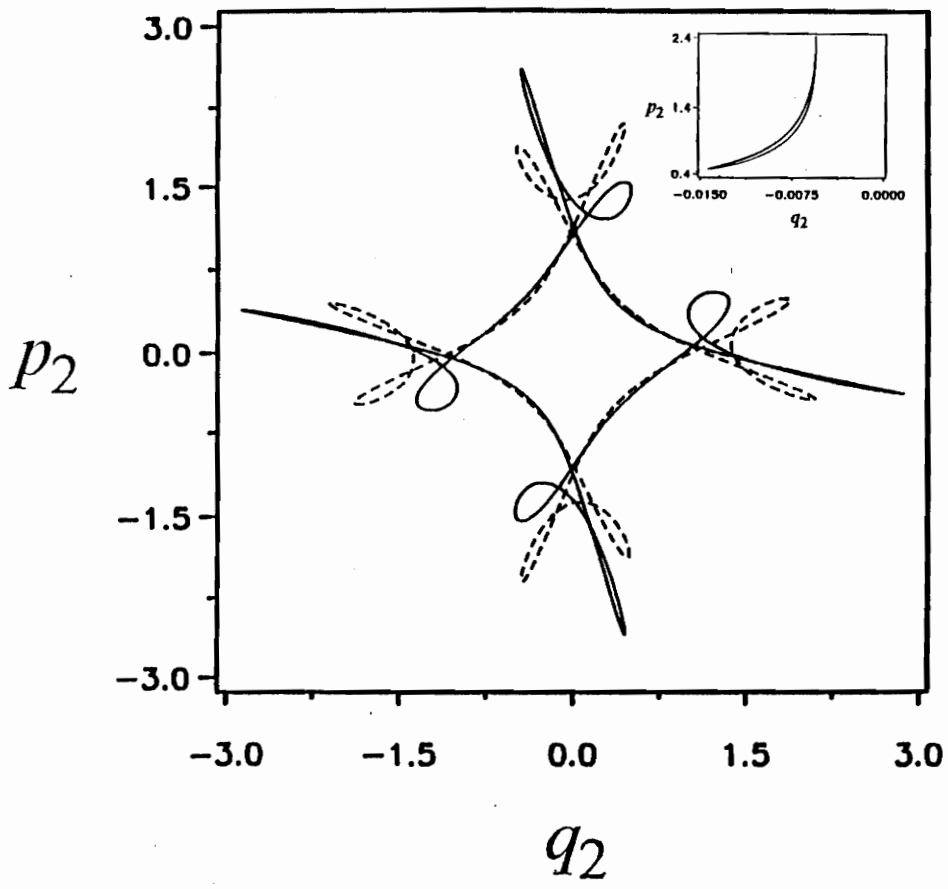

Figure 6.7. Projection of attractor I (insert), attractor II (large solid curve), and unstable limit cycle III (broken line) when $\hat{\sigma}_2 = -1.9980$.

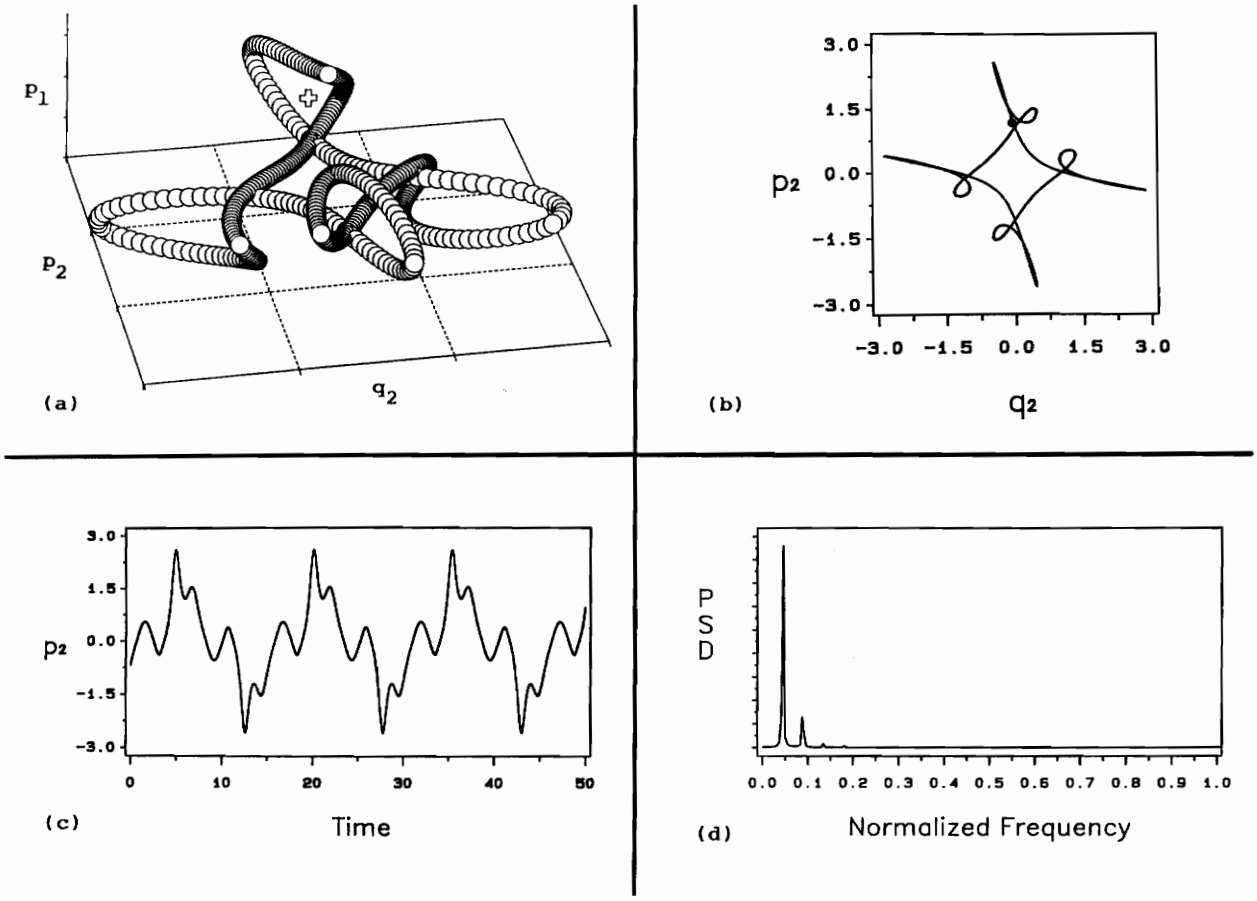

Figure 6.8. Attractor II when $\hat{\mu}_{1,2} = 0.02$, $\hat{\sigma}_1 = 0.266$, and $\hat{\sigma}_2 = -1.80$: (a) projection of the attractor on the 3-D space spanned by p_1, p_2, and q_2, "balloons" represent points on the attractor and the cross represents the unstable fixed point; (b) a projection of the phase space on the $p_2 - q_2$ plane, the dot "." represents the unstable fixed point; (c) long-time history of p_2; and (d) power spectral density (PSD) of the q_1 component.

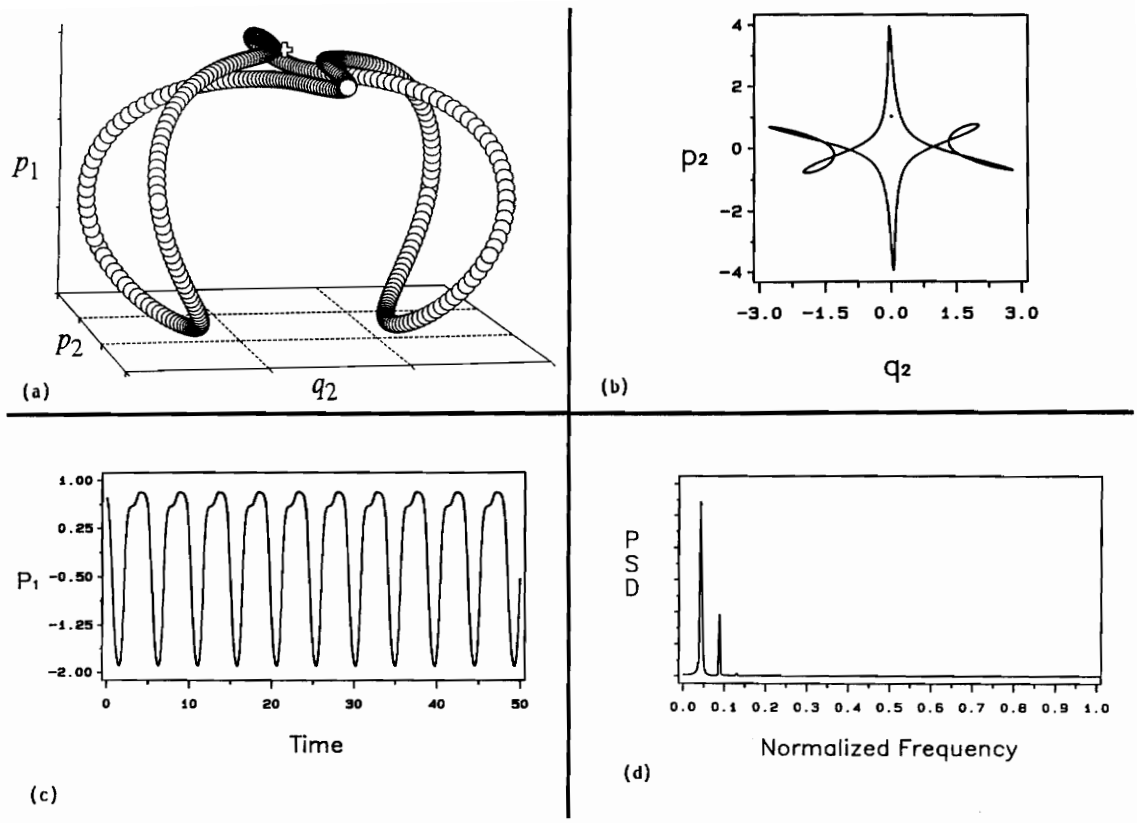

Figure 6.9. Attractor IV when $\hat{\mu}_{1,2} = 0.02$, $\hat{\sigma}_1 = 0.266$, and $\hat{\sigma}_2 = -1.80$: (a) projection of the attractor on the 3-D space spanned by p_1, p_2, and q_2, "balloons" represent points on the attractor and the cross represents the unstable fixed point; (b) a projection of the phase space on the $p_2 - q_2$ plane, the dot "." represents the unstable fixed point; (c) long-time history of p_1; and (d) power spectral density (PSD) of the q_1 component.

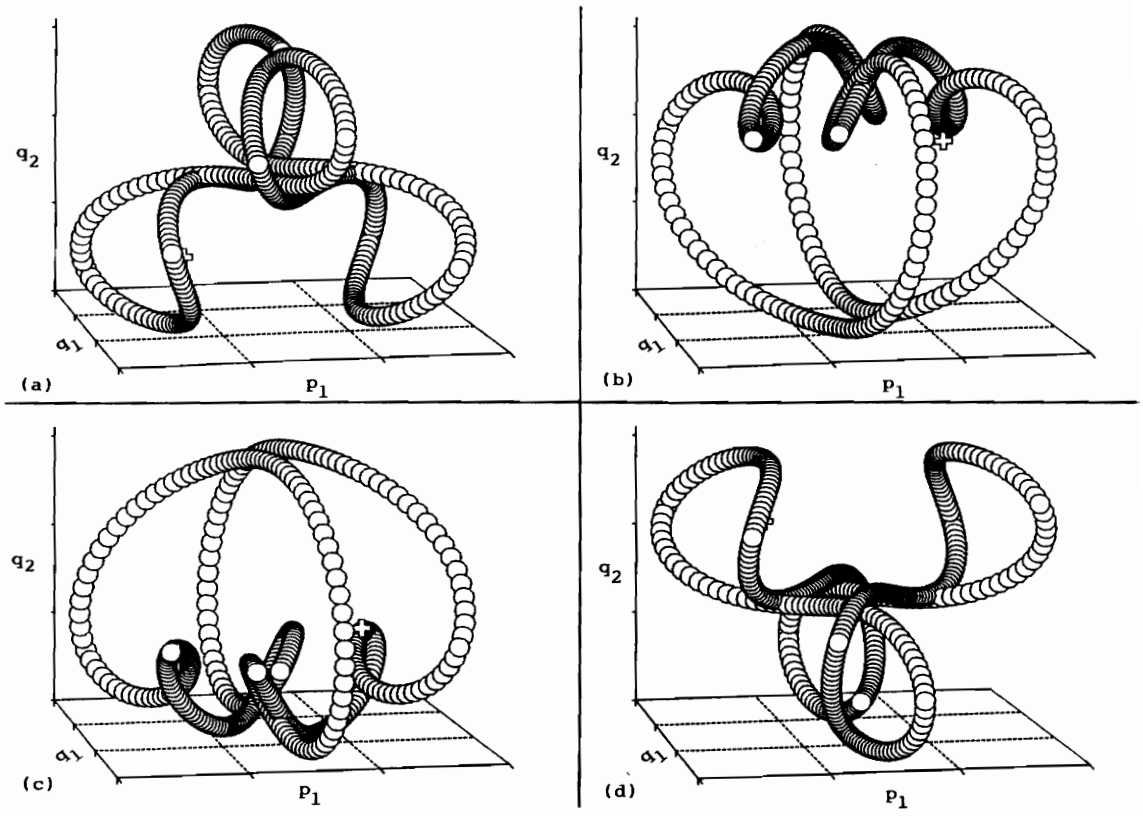

Figure 6.10. Limit-cycle attractors when $\hat{\mu}_{1,2} = 0.02$, $\hat{\sigma}_1 = 0.266$, and $\hat{\sigma}_2 = -1.68$: projections of the quadruple attractors on the 3-D space spanned by p_1, q_1, and q_2, "balloons" represent points on the attractors and the crosses represent the unstable fixed points.

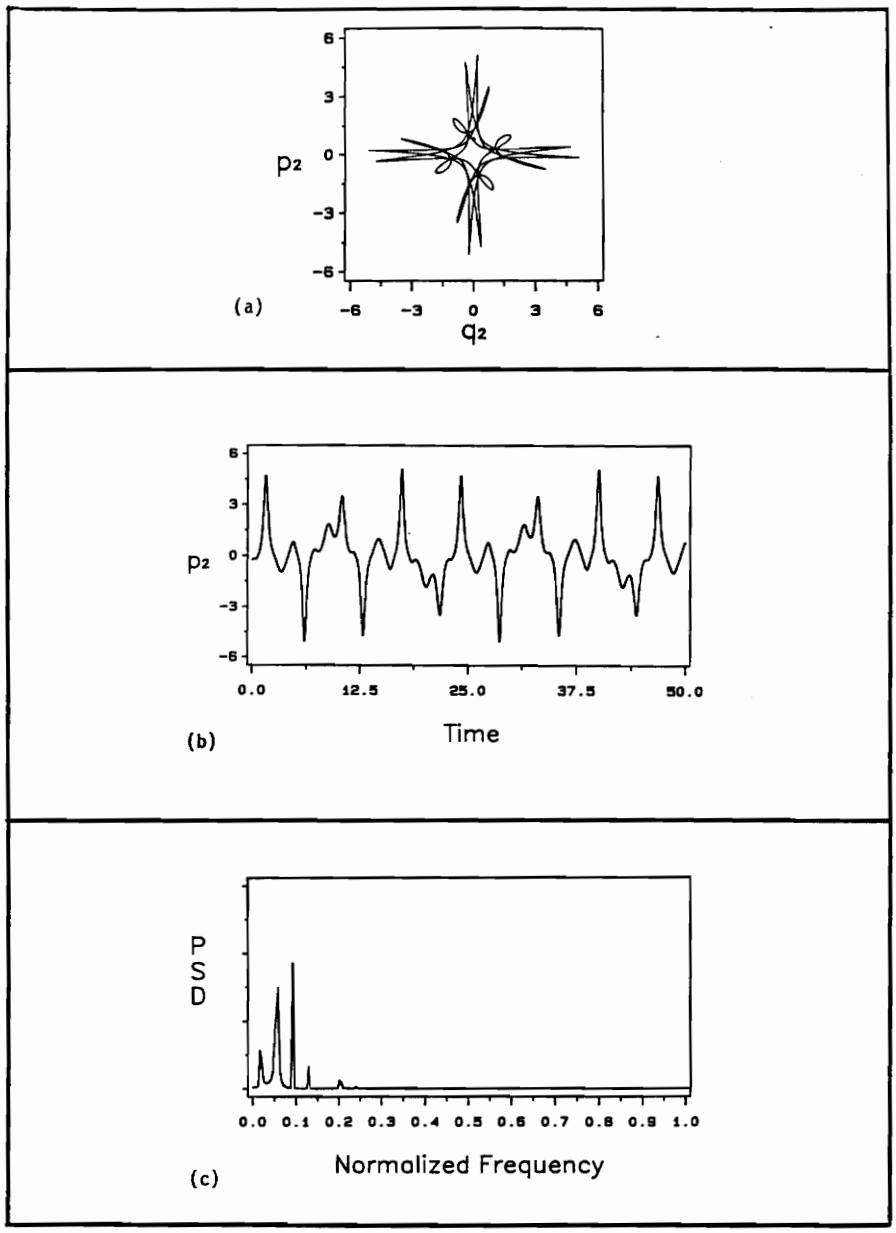

Figure 6.11. Attractor V when $\hat{\mu}_{1,2} = 0.02$, $\hat{\sigma}_1 = 0.266$, and $\hat{\sigma}_2 = -1.60$: (a) a projection of the phase space on the $p_2 - q_2$ plane, the dot "." represents the unstable fixed point; (b long-time history of p_2; and (c) power spectral density (PSD) of the q_1 component.

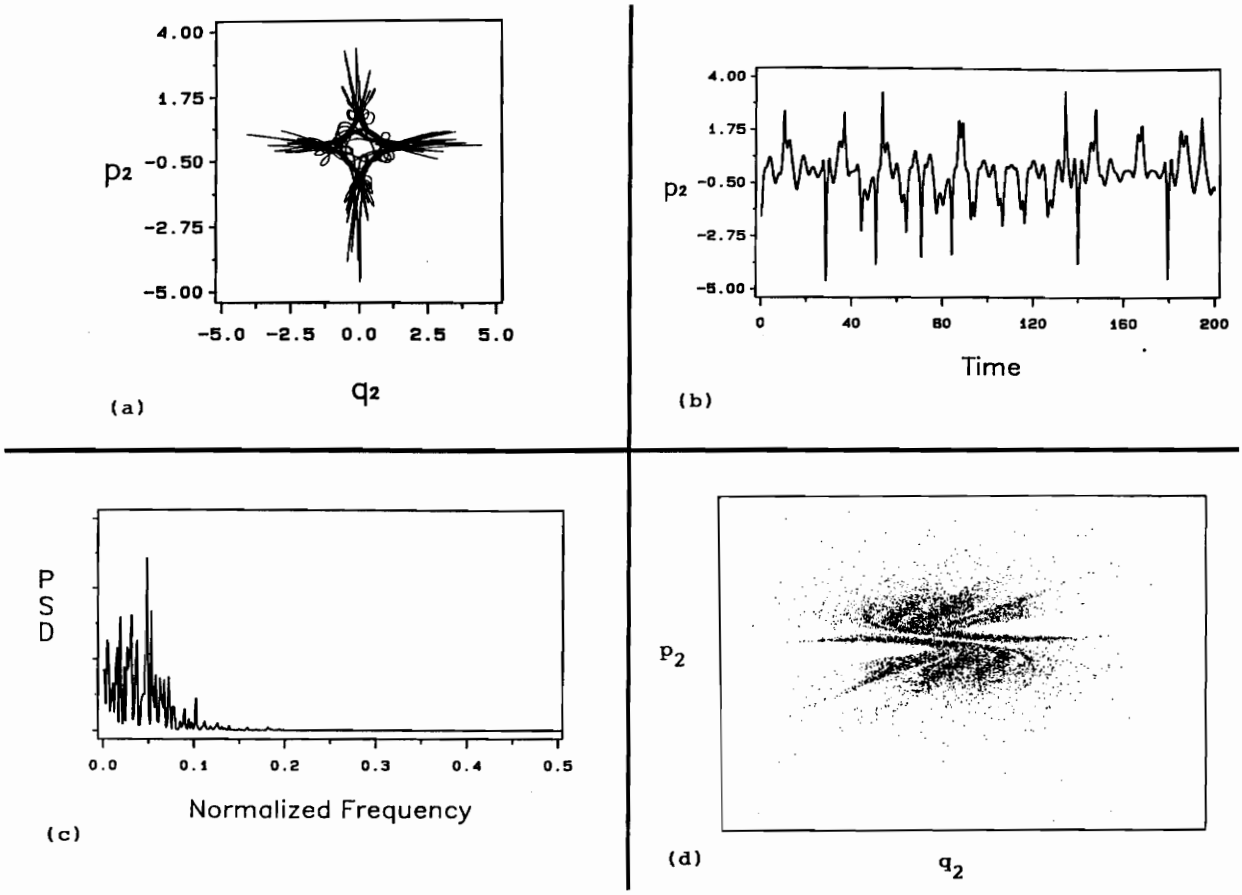

Figure 6.12. Chaotic attractor when $\hat{\mu}_{1,2} = 0.02$, $\hat{\sigma}_1 = 0.266$, and $\hat{\sigma}_2 = -1.50$: (a) two-dimensional projection of the attractor on the $p_2 - q_2$ plane, (b) long-time history of p_2, (c) power spectral density (PSD) of the q_1 component, and (d) two-dimensional projection of one-sided Poincare' section for $q_3 = 0$.

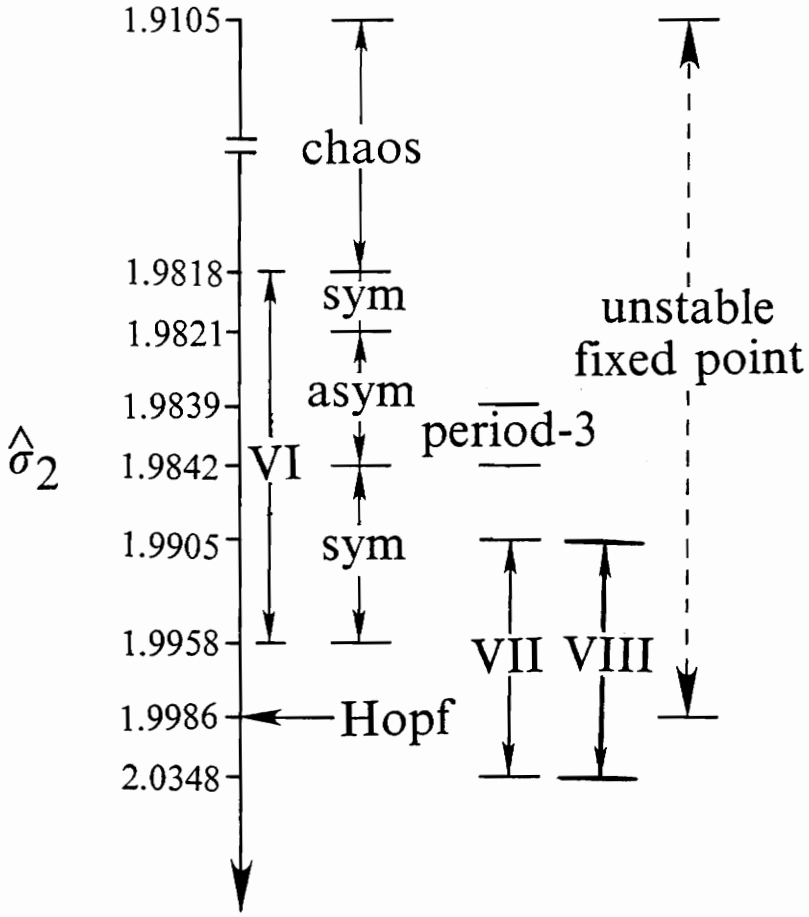

Figure 6.13. Bifurcation diagram of the modulation equations near the subcritical Hopf bifurcation excitation frequency: $\hat{\mu}_1 = 0.02$ and $\hat{\sigma}_1 = 0.266$.

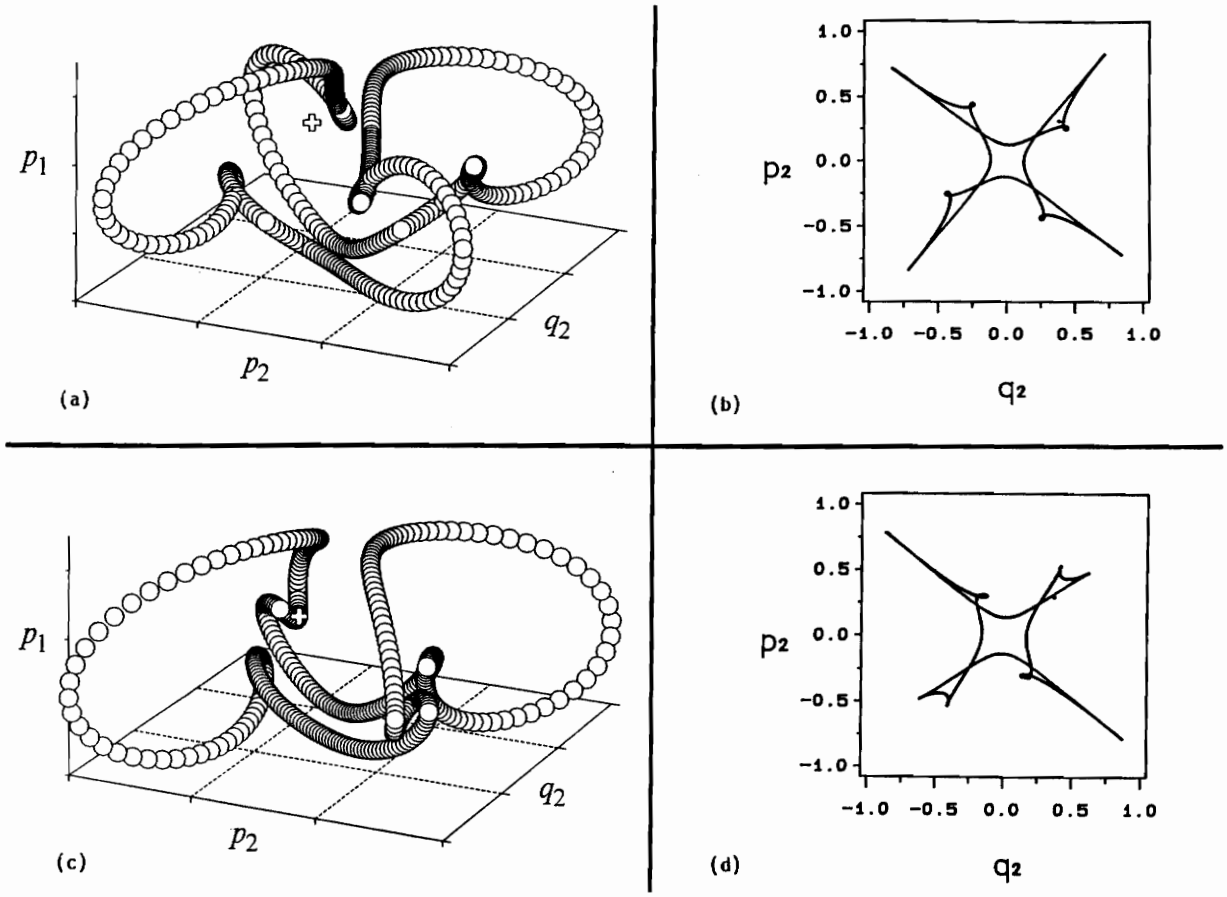

Figure 6.14. Two- and three-dimensional projections of attractor VII: (a) and (b) at $\hat{\sigma}_2 = 2.0348$ and (c) and (d) at $\hat{\sigma}_2 = 1.9905$. The balloons represent points on the attractors, the crosses in (a) and (c) represent the fixed points, and the dots in (b) and (d) represent the fixed points.

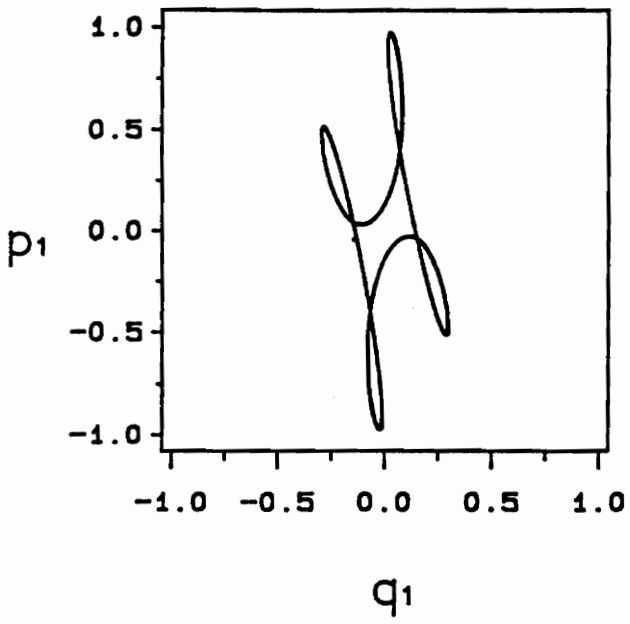

Figure 6.15. Two-dimensional projection of attractor VI at $\hat{\sigma}_2 = 1.99$.

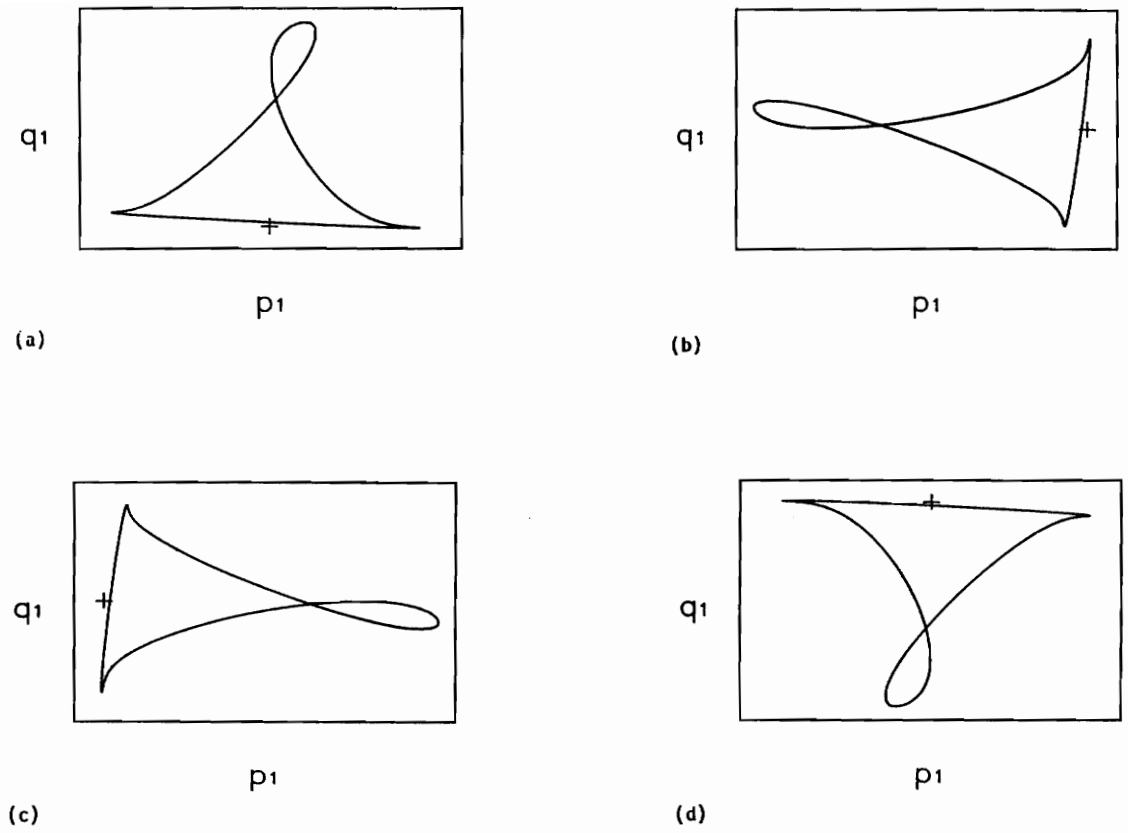

Figure 6.16. Two-dimensional projections of the asymmetric quadruple attractors VI at $\hat{\sigma}_2 = 1.9830$. The crosses represent the unstable fixed points.

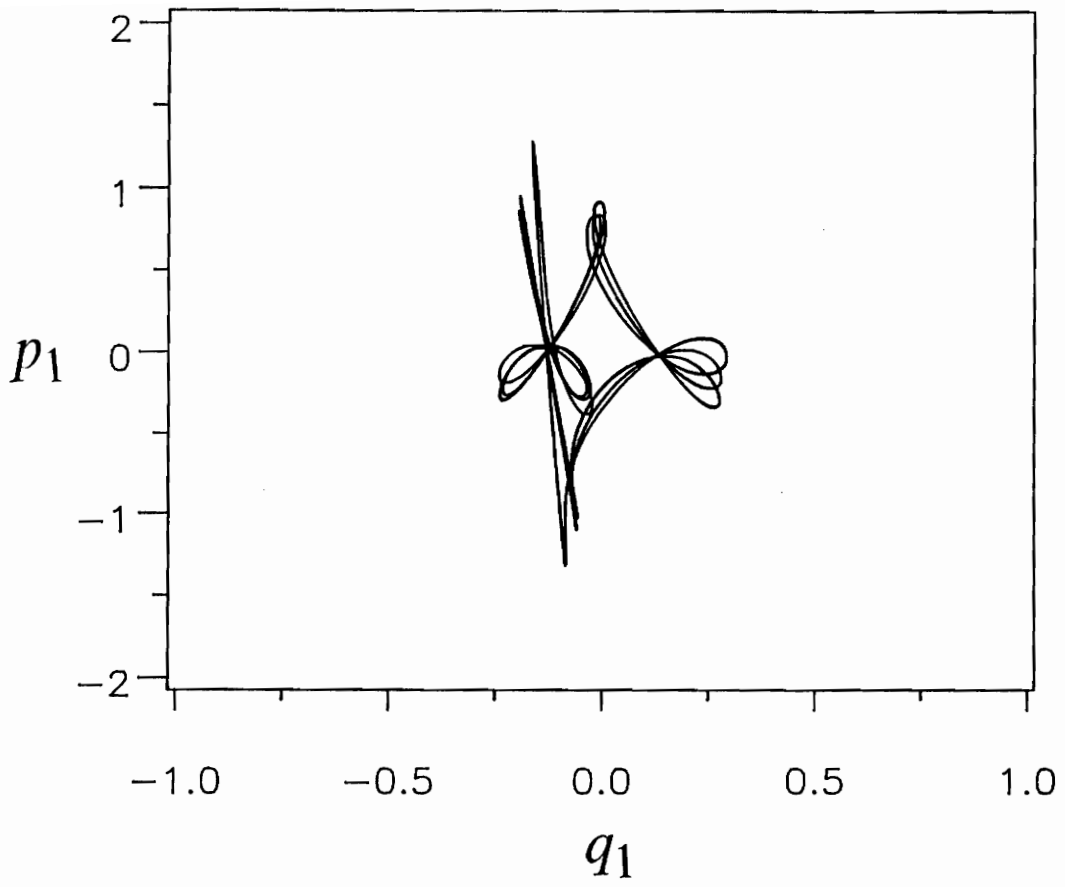

Figure 6.17. A two-dimensional projection of the period-three motion attractor when $\hat{\mu}_{1,2} = 0.02$, $\hat{\sigma}_1 = 0.266$, and $\hat{\sigma}_2 = 1.9834$.

Table 6.1. Hopf bifurcation points.

$\hat{\sigma}_1$	$\hat{\mu}_n$	Hopf $\hat{\sigma}_2$		$\hat{\mu}_n$	Hopf $\hat{\sigma}_2$	
		supercritical	subcritical		supercritical	subcritical
−.266	.02	−1.998625	1.998435	.04	−1.994485	1.993735
0	.02	−1.998535	1.998535	.04	−1.994135	1.994135
.266	.02	−1.998435	1.998625	.04	−1.993735	1.994485

7. SUMMARY, CONCLUSIONS, AND RECOMMENDATIONS

7.1. Summary and Conclusions

The computer algebra system MACSYMA is used to derive the nonlinear equations of motion of composite plate structures undergoing large deformations by using the higher-order shear-deformation theory of Reddy. It is based on the assumptions that there is a cubic variation of the in-plane displacements through the plate thickness and that the transverse shear strains vanish at the free surfaces of the plate. The plates under investigation are made of linearly elastic anisotropic layers, and the von Karman strains are used in the derivation of the equations of motion. The equations of motion and boundary conditions are derived by using Hamilton's principle.

Linear analysis is performed of the free-vibrations of laminated plates. The analysis is carried out by using MACSYMA. The case of antisymmetric cross-ply

laminates is considered. Uniform transverse harmonic loads are considered. The plate is simply-supported. Solutions are obtained for the case of plate strips in cylindrical bending. The free-vibration problem is solved by a Navier-type method, and the natural undamped frequencies and mode shapes are calculated. The state-space concept is used to solve exactly the linear dynamic equations for the case of cylindrical bending. The linear analysis is the first step in studying the nonlinear vibrations of the structures in Chapter 5.

An analytical technique for the analysis of the nonlinear response of a wide variety of physical systems that exhibit quadratic and cubic nonlinearities is described in Chapter 4. The technique is a perturbation method, such as the method of multiple scales or the method of averaging, that attacks the Lagrangian of the system rather than the equations of motion and boundary conditions. Writing down the Euler-Lagrange equations of the averaged Lagrangian yields ordinary-differential equations that govern the modulation or evolution of the amplitudes and phases of the response. The technique produces accurate second-order, uniformly valid, approximate solutions in the neighborhoods of different resonances that can arise in different physical systems.

As an application, the nonlinear response of a fluid relief valve is discussed in detail in Chapter 4. The equations of motion and boundary conditions are derived by using Hamilton's principle. First, the response is obtained by attacking the partial-differential equation and boundary conditions by using the method of multiple scales. Second, the solution is obtained by using the time-averaged-Lagrangian technique and is compared to the solution obtained first. The two solutions are found to be in full agreement. However, the second method requires less algebra and is therefore preferred over the first one. Moreover, the case in which the solution is approximated by a one-term Galerkin expansion is presented. The pitfalls and

shortcomings of this procedure are pointed out. Different external resonance conditions are treated in detail and the solution for each case is presented.

The time-averaged-Lagrangian technique is implemented in a MACSYMA code that produces second-order perturbation solutions of the nonlinear equations of composite-plate structures. The effects of the quadratic nonlinearities are incorporated into the solution. First-order differential equations are derived for the evolution of the amplitudes and phases for the following resonances: primary resonance, subharmonic resonance of order one-half, and superharmonic resonance of order two. The evolution equations are used to determine the frequency-response equations, which are used in turn to obtain representative frequency-response and force-response curves for each case. The local stability of these solutions is investigated. Stable and unstable solutions may coexist. Multi-valued solutions are possible, and in these cases the initial conditions determine which solution describes the response. Moreover, the multi-valuedness of the solutions is responsible for the jump phenomenon. The results show that subharmonic resonances of order one-half cannot be activated unless the excitation amplitude exceeds a threshold value.

A theoretical investigation of the response of the surface of a liquid in a cylindrical container to a longitudinal harmonic excitation is conducted for the case of a two-to-one internal resonance and a principal parametric excitation of the higher mode. The method of multiple scales is used to derive four first-order autonomous ordinary-differential equations for the modulation of the amplitudes and phases of the interacting modes. The constant solutions of the modulation equations and their stability are investigated. The jump and saturation phenomena are demonstrated in the force-response curves. The saturation phenomenon does not occur when the system has a one-to-one autoparametric resonance or when it has a two-to-one autoparametric resonance with the lower, rather than higher, mode being excited.

The transition in stability may be either through a cyclic fold or a Hopf bifurcation. The Hopf bifurcation can be of either the subcritical or supercritical type. Between the Hopf bifurcation values, the solutions of the modulation equations can be fixed-point, limit-cycle, and chaotic solutions. The bifurcated periodic solutions are constructed by a numerical algorithm and their stability is analyzed by using Floquet theory. Multiple limit cycles with different amplitudes and periods are detected and shown to coexist over some ranges of the bifurcation parameter $\hat{\sigma}_2$. Some limit cycles undergo pitchfork bifurcation while others undergo cyclic-fold bifurcation. The pitchfork bifurcation produces symmetry breaking, and the cyclic-fold bifurcation results in jumps. Some of these jumps are responsible for transition to chaos. The chaotic attractor is identified and its fractal dimension is calculated.

7.2. Recommendations for Future Study

The following topics concerning the dynamics and vibrations of composite structures are recommended for future study:

1. The classical and first-order shear-deformation theories should also be used in conjunction with the time-averaged-Lagrangian method and the results compared with those obtained here.

2. The time-averaged-Lagrangian technique, which was applied in this dissertation to rectangular plates and plate strips, need to be applied to other types of isotropic and composite structures, such as beams and shells.

3. It is not unusual in engineering practice for a composite structure to be subjected to more than one harmonic excitation. Thus, a study of multi-frequency excitations is indeed necessary.

4. When a structure is subjected to more than a single exciting force, an external resonance may occur even if the frequencies of the excitations are well below the lowest natural frequency of the structure. Therefore, the effects of combination external resonances should be studied.

5. The time-averaged-Lagrangian technique can be applied to discrete problems with more than a single degree of freedom. The first natural step is, of course, to apply it to a two-degree-of-freedom system.

6. The availability of highly reliable symbolic manipulator systems (e.g., MACSYMA) and the ability of interfacing their results with existing FORTRAN codes (e.g., IMSL) may be utilized in developing fully automated codes that can analyze and design high-performance composite structures.

7. Experimental investigations and verifications of the analytical results presented in this dissertation are highly recommended and remain a first priority.

References

1. Aprille, T. J. and Trick, T. N., 1972, "A Computer Algorithm to Determine the Steady-State Response of Nonlinear Oscillators," IEEE Transactions on Circuits Systems, CAS-4, pp. 354-366.

2. Ashton, J. E., 1969, "Approximate Solutions for Unsymmetrically Laminated Plates," Journal of Composite Materials, Vol. 3, pp. 189-191.

3. Ashton, J. E. and Whitney, J. M., 1970, **Theory of Laminated Plates,** Techomic, Wesport, CT.

4. Baharlou, B. and Leissa, A. W., 1987, "Vibration and Buckling of Generally Laminated Composite Plates with Arbitrary Edge Conditions," International Journal of Mechanical Sciences, Vol. 29, No. 8, pp. 545-555.

5. Basset, A. B., 1890, "On the Extension and Flexure of Cylindrical and Spherical Thin Elastic Shells," Phil. Trans. Royal Soc., London, Ser. A, Vol. 181, pp. 433-480.

6. Becker, J. and Miles, J. W., 1986, "Parametric Excitation of an Internally Resonant Double Pendulum, II," Journal of Applied Mathematics and Physics (ZAMP), Vol. 37, pp. 641-650.

7. Bennet, J. A., 1971, "Nonlinear Vibration of Simply Supported Angle-Ply Laminated Plates," AIAA Journal, Vol. 9, pp. 1977-2003.

8. Bhimaraddi, A., 1987a, "Static and Transient Response of Rectangular Plates," Thin-Walled Structures, Vol. 5, pp. 125-143.

9. Bhimaraddi, A., 1987b, "Static and Transient Response of Cylindrical Shells," Thin-Walled Structures, Vol. 5, pp. 157-179.

10. Bhimaraddi, A. and Stephens, L. K., 1984, "A Higher-Order Theory for Free Vibrations of Orthotropic, Homogeneous, and Laminated Rectangular Plates," Journal of Applied Mechanics, Vol. 51, p. 195-198.

11. Bert, C. W., 1973, "Nonlinear Vibration of Rectangular Plates Arbitrarily Laminated of Anisotropic Materials," Journal of Applied Mechanics, Vol. 40, pp. 452-458.

12. Bert, C. W., 1985, "Research on Dynamic Behavior of Composite and Sandwitch Plates," Shock and Vibration Digest, Vol. 17, pp. 3-15.

13. Bert, C. W. and Maybery, B. L., 1969, "Free Vibrations of Unsymmetrically Laminated Anisotropic Plates with Clamped Edges," Journal of Composite Materials, Vol. 3, pp. 282-293.

14. Biot, M. A., 1939, "Non-Linear Theory of Elasticity and the Linearized Case for a Body Under Initial Stress," London, Dublin, and Edinburgh Philosoph. Mag. J. Science, Series 7, Vol. 27, No. 183, pp. 468-489.

15. Bowlns, J. A., Palazotto, A, N., and Whitney, J. M., 1987, "Vibration of Symmetrically Laminated Rectangular Plates Considering Deformation and Rotary Inertia," AIAA Journal, Vol. 25, pp. 1500-1511.

16. Brogen, W. L., 1985, **Modern Control Theory,** Prentice-Hall, Englewood Cliffs, New Jersey.

17. Chandra, R., 1976, "Large Deflection Vibration of Cross-Ply Laminated Plates with Certain Edge Conditions," Journal of Sound and Vibration, Vol. 47, pp. 509-514.

18. Chandra, R. and Raju, B. B., 1975a, "Large Deflection Vibration of Angle-Ply Laminated Plates," Journal of Sound and Vibration, Vol. 40, pp. 393-408.

19. Chandra, R. and Raju, B. B., 1975b, "Large Amplitude Flextural Vibration of Cross-Ply Laminated Composite Plates," Fibre. Sci. Tech., Vol. 8, pp. 243-263.

20. Chia, C. Y. and Prabhakara, M. K., 1978, "A General Mode Approach to Nonlinear Flextural Vibrations of Laminated Rectangular Plates," Journal of Applied Mechanics, Vol. 45, pp. 623-628.

21. Chia, C. Y., 1980, **Nonlinear Analysis of Plates,** McGraw-Hill, New York.

22. Chia, C. Y., 1982, "Large Amplitude Vibrations of Laminated Rectangular Plates," Fibre Sci. Tech., Vol. 17, pp. 123-131.

23. Chia, C. Y., 1985, "Nonlinear Oscillation of Unsymmetric Angle-Ply Plate on Elastic Foundation Having Nonuniform Edge Supports," Journal of Composite Structures, Vol. 4, pp. 161-178.

24. Chon, T. S., 1971, "On the Propagation of Flextural Waves in an Orthoprotic Laminated Plate and its Response to an Impulsive Load," Journal of Composite Materials, Vol. 5, pp. 306-319.

25. Ciliberto, S. and Gollub, J. P., 1984, "Pattern Competition Leads to Chaos," Physical Review Letters, Vol. 52, pp. 922-925.

26. Ciliberto, S. and Gollub, J. P., 1985, "Chaotic Mode Competition in Parametrically Forced Surface Waves," Journal of Fluid Mechanics, Vol. 158, pp. 381-398.

27. Cooley, J. W. and Tukey, J. W., 1965, "An Algorithm for the Machine Calculation of Complex Fourier Series," Mathematical Computations, Vol. 19, pp. 297-301.

28. Croquette, V. and Pointou, C., 1981, "Cascade of Period Doubling Bifurcations and Large Stochasticity in the Motion of a Compass," Journal of Physique-Letters, Vol. 42, pp. L537-L539.

29. Dil Scinva, M., 1986, "Bending, Vibration, and Buckling of Simply Supported Thick Multilayered Orthotropic Plates: An Evaluation of a New Displacement Model," Journal of Sound and Vibration, Vol. 105, pp. 425-442.

30. Dobyns, A. L., 1981, "Analysis of Simply-Supported Orthotropic Plates Subject to Static and Dynamic Loads," AIAA Journal, Vol. 19, pp. 642-650.

31. Dokainish, M. A., and Elmedany, M. M., 1978, "On the Non-Linear Response of a Fluid Valve," Journal of Applied Mechanics, Vol. 100, pp. 675-680.

32. Doong, J. L. and Chen, T. J., 1987, "Vibration and Stability of an Initially Stressed Laminated Plate Based on a Higher-Order Deformation Theory," Composite Structures, Vol. 7, pp. 285-310.

33. Dowell, E. H., 1980, "Component Mode Analysis of Non-Linear and Non-Conservative Systems," Journal of Mechanical Design, Vol. 47, pp. 172-176.

34. Dowell, E. H. and Pezeshki, C., 1986, "On the Understanding of Chaos in Duffings Equation Including a Comparison with Experiment," Journal of Applied Mechanics," Vol. 53, pp. 5-9.

35. Eslami, H. and Kandil, O. A., 1989a, "Nonlinear Forced Vibration of Orthotropic Rectangular Plates Using the Method of Multiple Scales," AIAA Journal, Vol. 27, pp. 955-960.

36. Eslami, H. and Kandil, O. A., 1989b, "Two-Mode Nonlinear Vibration of Orthotropic Plates Using Method of Multiple Scales," AIAA Journal, Vol. 27, pp. 961-967.

37. Feng, Z. C. and Sethna, P. R., 1989, "Symmetry-Breaking Bifurcations in Resonant Surface Waves," Journal of Fluid Mechanics, Vol. 199, pp. 495-518.

38. Franklin, J. N., 1968, **Matrix Theory,** Prentice-Hall, Englewood Cliffs, New Jersey.

39. Frederickson, R., Kaplan, J. L., Yorke, E. D., and Yorke, J. A., 1983, "The Liapunov Dimension of Strange Attractors," Journal of Differential Equations, Vol. 49, pp. 185-207.

40. Gol'denviezer, A. L., 1958, "O Teorii Izgiba Plastinok Reissnera (On Reisser's Theory of the Bending of Plates)," Izvestiya AN SSSR, OTN, No. 4, pp. 102-109 (translation of the paper available at NASA Technical Translation F-27, May 1960).

41. Gollub, J. P. and Meyer, C. W., 1983, "Symmetry Breaking Instabilities on a Fluid Surface," Physica D, Vol. 6, pp. 337-346.

42. Gu, X. M. and Sethna, P. R., 1987, "Resonant Surface Waves and Chaotic Phenomena," Journal of Fluid Mechanics, Vol. 183, pp. 543-565.

43. Hencky, H., 1947, "Uber Die Berucksichtigung Der Schubverzerung in Eberen Platten," Ing. Arch. Vol. 16, pp. 72-76.

44. Hermann, G., 1955, "Influence of Large Amplitudes on Flextural Motions of Elastic Plates," Nat. Advis. Comm. Aeronaut. (U.S.A.), Tech. Note 3578.

45. Hildebrand, F. B., Reissner, E., and Thomas, G. B., 1949, "Notes on the Foundations of the Theory of Small Displacements of Orthotropic Shells," NASA Technical Note No. 1833.

46. Holmes, P. J. and Moon, F. C., 1983, "Strange Attractors and Chaos in Nonlinear Mechanics," Journal of Applied Mechanics, Vol. 50, pp. 1021-1032.

47. Hui, D., 1985a, "Effects of Geometric Imperfections on Frequency-Load Interaction of Biaxilly Compressed Antisymmetric Angle-Ply Rectangular Plates," Journal of Applied Mechanics, Vol. 52, pp. 155-162.

48. Hui, D., 1985b, "Soft-Spring Nonlinear Vibrations of Antisymmetrically Laminated Rectangular Plates," International Journal of Mechanical Science, Vol. 27, pp. 397-408.

49. Johnson, B. L. and Wandling, D. E., 1969, "Actual Popping Pressure of a Relief Valve with a Real Helical Spring Under Dynamic Load," Journal of Engineering Ind. 91, pp. 1142-1146.

50. Jones, R. M., 1973, "Buckling and Vibration of Unsymmetrically Laminated Cross-Ply Rectangular Plates," AIAA Journal, Vol. 11, pp. 1626-1632.

51. Jones, R. M., 1975, **Mechanics of Composite Materials,** McGraw-Hill, New York.

52. Kamal, K. and Durvasula, S., 1986, "Some Studies on Free Vibration of Composite Laminates," Composite Structures, Vol. 5, pp. 177-202.

53. Kapania, R. K. and Raciti, S. 1989a, "Recent Advances in Analysis of Laminated Beams and Plates, Part I: Shear Effects and Buckling," AIAA Journal, Vol. 27, pp. 923-934.

54. Kapania, R. K. and Raciti, S., 1989b, "Recent Advances in Analysis of Laminated Beams and Plates, Part II: Vibrations and Wave Propagation," AIAA Journal, Vol. 27, pp. 935-946.

55. Keolian, R. and Rudnick, I., 1984, **in Frontiers in Physical Acoustics,** edited by D. Sette, North-Holland, New York.

56. Keolian, R., Turkevich, L. A., Putterman, S. J., and Rudnick, I., 1981, "Subharmonic Sequences in the Fraday Experiment: Departures from Period Doubling," Physical Review Letters, Vol. 47, pp. 1133-1136.

57. Khdeir, A. A., 1986, "Analytical Solutions for the Statics and Dynamics of Rectangular Laminated Composite Plates Using Shearing Deformation Theories," Ph.D Dissertation, Virginia Polytechnic Institute and State University, Blacksburg, VA.

58. Khdeir, A. A., 1988, "Free Vibration of Antisymmetrically Angle-Ply Laminated Plates Including Various Boundary Conditions," Engineering Mechanics, Proceedings, 7th ASCE, EMD Conference on Engineering Mechanics, edited by R. A. Heller, and M. P. Singh, American Society of Civil Engineers, New York, pp. 284.

59. Khdeir, A. A. and Reddy, J. N., 1988, "Dynamic Response of Antisymmetric Angle-Ply Laminated Plates Subjected to Arbitrary Loading," Journal of Sound and Vibration, Vol. 126, pp. 437-445.

60. Khdeir, A. A. and Reddy, J. N., 1989, "Exact Solutions for the Transient Response of Symmetric Cross-Ply Laminates Using a Higher-Order Plate Theory," Composites Science and Technology, Vol. 34, pp. 205-224.

61. Kromm, A., 1955, "Uber die Randquerkrafte bei gestutzten Platten," ZAMM, Vol. 35, pp. 231-242.

62. Leissa, A. W., 1981, "Advances in Vibrations, Buckling, and Postbuckling Studies on Composite Plates," Composite Structures, edited by T. H. Marshall, Applied Science Publishers, London, pp. 312-334.

63. Levinson, M., 1980, "An Accurate Simple Theory of the Statics and Dynamics of Elastic Plates," Mech. Res. Commu., Vol. 7, pp. 343-350.

64. Librescu, L., 1966, "The Thermoelastic Problem of Shells and Plates Approached by Eliminating the Love-Kirchoff Hypothesis," St. Cer. Mec. Apl. Vol. 21, pp. 351-365.

65. Librescu, L., 1969, "The Elasto-Kinetic Problems in the Theory of Anistropic Shells and Plates," Part II, Plates Theory, Rev. Roum. Sci. Tech. Mec. Appl. 7,3.

66. Librescu, L., Khdeir, A. A., and Reddy, J. N., 1987, "A Comprehensive Analysis of the State of Stress of Elastic Anisotropic Flat Plates Using Refined Theories," Acta Mechanica, Vol. 70, pp. 57-81.

67. Lo, K. H., Christensen, R. M., and Wu, E. M., 1977, "A Higher-Order Theory of Plate Deformation, Part 1: Homogeneous Plates," Journal of Applied Mechanics, Vol. 44, pp. 663-668.

68. Meirovitch, L., 1980, **Computational Methods in Structural Dynamics,** Sijthoff & Noordohoff, Rockville, MD.

69. Miles, J. W., 1984, "Nonlinear Faraday Resonance," Journal of Fluid Mechanics, Vol. 146, p. 285-302.

70. Miles, J. W. and Henderson, D. H., 1990, "Parametrically Forced Surface Waves," Annual Review of Fluid Mechanics, Vol. 22, pp. 143-165.

71. Mindlin, R. D., 1951, "Influence of Rotary Inertia and Shear Deformation on Flexural Motions of Isotropic, Elastic Plates," Journal of Applied Mechanics, Vol. 18, pp. A31-A38.

72. Moon, F. C., 1980, "Experiments on Chaotic Motions of a Forced Nonlinear Oscillator: Strange Attractors," Journal of Applied Mechanics, Vol. 47, pp. 638-644.

73. Moon, F. C., 1987, **Chaotic Vibrations, an Introduction for Applied Scientists and Engineers,** Wiley-Interscience, New York.

74. Murthy, M. V. V., 1981, "An Improved Shear Deformation Theory for Laminated Anisotropic Plates," NASA TP-1903.

75. Nakashima, T., Shiramoto, K., Kondo, T., and Sasaguchi, K., 1986, "A Study on Unstable Phenomenon and Response of a Pressure Regulating Valve," Bull. JSME, Vol. 29, pp. 459-465.

76. Nayfeh, A. H., 1973, **Perturbation Methods,** Wiley-Interscience, New York.

77. Nayfeh, A. H., 1981, **Introduction to Perturbation Techniques,** Wiley-Interscience, New York.

78. Nayfeh, A. H., 1987a, "Surface Waves in Closed Basins Under Parametric and Internal Resonances," Physics of Fluids, Vol. 30, pp. 2976-2983.

79. Nayfeh, A. H., 1987b, "Parametric Excitation of Two Internally Resonant Oscillators," Journal of Sound and Vibration, Vol. 119, pp. 95-109.

80. Nayfeh, A. H., 1988, "Numerical-Perturbation Methods in Mechanics," Computers and Structures, Vol. 30, pp. 185-204.

81. Nayfeh, A. H., 1989, **in Lasers, Molecules, and Methods,** edited by J. O. Hirschfelder, R. E. Wyatt, and R. D. Coalson, Wiley-Interscience, New York, pp. 237-314.

82. Nayfeh, A. H. and Asfar, K. R., 1986, "Response of a Bar Constrained by a Non-Linear Spring to a Harmonic Excitation," Journal of Sound and Vibration, Vol. 105, pp. 1-15.

83. Nayfeh, A. H. and Balachandran, B., 1989, "Modal Interactions in Dynamical and Structural Systems," Applied Mechanics Review, Vol. 42, pp. 175-201.

84. Nayfeh, A. H. and Bouguerra, H., 1990, "Non-Linear Response of a Fluid Valve," International Journal of Non-Linear Mechanics, Vol. 25, pp. 433-449.

85. Nayfeh, A. H. and Khdeir, A. A., 1986a, "Nonlinear Rolling of Ships in Regular Beams Seas," International Shipbuilding Progress, Vol. 33, pp. 40-49.

86. Nayfeh, A. H. and Khdeir, A. A., 1986b, "Nonlinear Rolling of Biased Ships in Regular Beam Waves," International Shipbuilding Progress, Vol. 33, pp. 84-93.

87. Nayfeh, A. H. and Mook, D. T., 1979, **Nonlinear Oscillations,** Wiley-Interscience, New York.

88. Nelsson, R. B. and Lorch, D. R., 1974, "A Refined Theory for Laminated Anisotropic Plates," Journal of Applied Mechanics, Vol. 41, pp. 177-183.

89. Paslay, P. R. and Gurtin, M. E., 1980, "The Vibration Response of Linear Undamped System Resting on a Non-Linear Spring," Journal of Applied Mechanics, Vol. 27, pp. 272-274.

90. Porter, B. and Billett, R. A., 1956, "Harmonic and Subharmonic Vibration of a Continuous System Having Non-Linear Constraint," International Journal of Mechanical Science, Vol. 7, pp. 431-439.

91. Reddy, J. N., 1982, "Large Amplitude Flexural Vibrations of Layered Composite Plates with Cutouts," Journal of Sound and Vibration, Vol. 83, pp. 1-10.

92. Reddy, J. N., 1982, "On the Solutions to Forced Motions of Rectangular Composite Plates," Journal of Applied Mechanics, Vol. 49, pp. 403-408.

93. Reddy, J. N., 1983a, "A Review of the Literature on Finite-Element Modeling of Laminated Composite Plates and Shells," Shock and Vibration Digest, Vol. 15, pp. 3-8.

94. Reddy, J. N., 1983b, "Geometrically Nonlinear Transient Analysis of Laminated Composite Plates," AIAA Journal, Vol. 21, pp. 621-629.

95. Reddy, J. N., 1983c, "Dynamic (Transient) Analysis of Layered Anisotropic Composite Material Plates," International Journal of Numerical Methods in Engineering, Vol. 19, pp. 237-255.

96. Reddy, J. N., 1983d, "An Accurate Prediction of Natural Frequencies of Laminated Plates by a Higher-Order Theory," Advances in Aerospace Structures, Materials and Dynamics, AD-106, ASME Winter Annual Meeting, pp. 157-162.

97. Reddy, J. N., 1984a, "A Simple Higher-Order Theory for Laminated Composite Plates," Journal of Applied Mechanics, Vol. 51, pp. 745-752.

98. Reddy, J. N., 1984b, "A Refined Nonlinear Theory of Plates with Transverse Shear Deformation," International Journal of Solid Structures, Vol. 20, pp. 881-896.

99. Reddy, J. N., 1984c, **Energy and Variational Methods in Applied Mechanics,** Wiley-Interscience, New York.

100. Reddy, J. N., 1985, "A Review of the Literature on Finite-Element Modeling of Laminated Composite Plates," Shock and Vibration Digest, Vol. 17, pp. 3-8.

101. Reddy, J. N. and Chao, W. C., 1981, "Large Deflection and Large-Amplitude Free Vibrations of Laminated Composite-Material Plates," Computational Structures, Vol. 13, pp. 341-347.

102. Reddy, J. N. and Chao, W. C., 1982, "Nonlinear Oscillations of Laminated Anisotropic Rectangular Plates," Journal of Applied Mechanics, Vol. 49, pp. 396-402.

103. Reddy, J. N., Khdeir, A. A., and Librescu, L., 1987, "Levy Type Solution for Symmetrically Laminated Rectangular Plates Using First-Order Shear-Deformation Theory," Journal of Applied Mechanics, Vol. 54, pp. 740-742.

104. Reissner, E., 1944, "On the Theory of Bending of Elastic Plates," Journal of Mathematical Physics, Vol. 23, pp. 184-191.

105. Reissner, E., 1945, "The Effect of Transverse Shear Deformation on the Bending of Elastic Plates," Journal of Applied Mechanics, Vol. 12, pp. A69-A77.

106. Reissner, E., 1947, "On Bending of Elastic Plates," Quarterly Applied Mathematics, Vol. 5, pp. 55-68.

107. Robbin, K. A., 1977, "A New Approach to Subcritical Instability and Turbulent Transitions in a Simple Dynamo," Math. Proc. Camb. Phill. Soc., Vol. 82, pp. 309-325.

108. Rossler, O. E., 1976, "Chemical Turbulence: Chaos in a Small Reaction-Diffusion System," Z. Naturforsch, Vol. 31a, pp. 1168-1172.

109. Schmidt, R., 1977, "A Refined Nonlinear Theory of Plates with Transverse Shear Deformations," Journal of Industrial Mathematics Society, Vol. 27, Part 1, pp. 23-28.

110. Simonelli, F. and Gollub, J. P., 1989, "Surface Wave Mode Interactions: Effects of Symmetry and Degeneracy," Journal of Fluid Mechanics, Vol. 199, pp. 471-494.

111. Singleton, R. C., 1969, "An Algorithm for Computing the Mixed Radix Fast Fourier Transform," IEEE Transactions of Audio and Electroacoustics, Vol. AU-17, pp. 93-103.

112. Sivakumaran, K. S., 1987, "Natural Frequencies of Symmetrically Laminated Rectangular Plates with Free Edges," Composite Structures, Vol. 7, pp. 191-204.

113. Sivakumaran, K. S. and Chia, C. Y., 1984, "Nonlinear Vibration of Generally Laminated Anisotropic Thick Plates," Ing. Arch. Vol. 54, pp. 220-231.

114. Sivakumaran, K. S. and Chia, C. Y., 1985, "Large-Amplitude Oscillations of Unsymmetrically Laminated Anisotropic Rectangular Plates Including Shear, Rotary Inertia, and Transverse Normal Stresses," Journal of Applied Mechanics, Vol. 52, pp. 536-542.

115. Stein, M. and Jegely, D. C., 1985, "Effects of Transverse Shearing on Cylindrical Bending, Vibrations, and Buckling of Laminated Plates," AIAA Paper No. 85-0744.

116. Sun, C. T. and Chattopadhyay, S., 1975, "Dynamic Response of Anisotropic Plates Under Initial Stress Due to Impact of a Mass," Journal of Applied Mechanics, Vol. 42, pp. 693-698.

117. Sun, C. T. and Whitney, J. M., 1974, "Forced Vibrations of Laminated Composite Plates in Cylindrical Bending," Journal of the Acoustical Society of America, Vol. 55, pp. 1003-1008.

118. Sun, C. T. and Whitney, J. M., 1976, "Dynamic Response of Laminated Composite Plates Under Initial Stress," AIAA Journal, Vol. 14, pp. 268-270.

119. Timoshenko, S., 1921, "On the Correction for Shear of the Differential Equations for Transverse Vibrations of Prismatic Bars," Phil. Mag., Series 6, Vol. 41, pp. 742.

120. Ueda, Y., 1979, "Randomly Transitional Phenomena in the System Governed by Duffing's Equation," Journal of Statistical Physics, Vol. 20, pp. 181-196.

121. Umeki, M. and Kambe, T., 1989, "Nonlinear Dynamics and Chaos in Parametrically Excited Surface Waves," Journal Physical Society of Japan, Vol. 58, pp. 140-154.

122. Wantanabe, T., 1978, "Forced Vibration of Continuous System with Non-Linear Boundary Conditions," Journal of Mechanical Design, Vol. 100, pp. 487-491.

123. Whitney, J. M., 1969a, "Bending-Extensional Coupling in Laminated Plates Under Transverse Loading," Journal of Composite Materials, Vol. 3, pp. 20-28.

124. Whitney, J. M., 1969b, "The Effect of Transverse Shear Deformation on the Bending of Laminated Plates," Journal of Composite Materials, Vol. 3, pp. 534-547.

125. Whitney, J. M., 1970, "The Effect of Boundary Condition on the Response of Laminated Composites," Journal of Composite Materials, Vol. 4, pp. 192-203.

126. Whitney, J. M. and Leissa, A. W., 1969, "Analysis of Heterogeneous Anisotropic Plates," Journal of Applied Mechanics, Vol. 36, pp. 261-266.

127. Whitney, J. M. and Pagano, N. J., 1970, "Shear Deformation in Heterogeneous Anisotropic Plates," Journal of Applied Mechanics, Transactions of the ASME, pp. 1031-1036.

128. Whitney, J. M. and Sun, C. T., 1977, "Transient Response of Laminated Composite Plates Subjected to Transverse Dynamic Loading," Journal of Acoustical Society of America, Vol. 61, pp. 101-104.

129. Wolf, A., Swift, J. B., Swinney, H. L., and Vastano, J. A., 1985, "Determining Lyapunov Exponents from a Time Series," Physica-D, Vol. 16, pp. 285-317.

130. Wu, C. Y. and Vinson, J. R., 1971, "Nonlinear Oscillations of Laminated Specially Orthotropic Plates with Clamped and Simply Supported Edges," Journal of the Acoustical Society of America, Vol. 49, pp. 1561-1569.

131. Zavodney, L. D. and Nayfeh, A. H., 1988, "The Response of a Single-Degree-of-Freedom System with Quadratic and Cubic Nonlinearities to a Fundamental Parametric Resonance," Journal of Sound and Vibration, Vol. 120, pp. 63-93.

132. Zavodney, L. D., Nayfeh, A. H., and Sanchez, N. E., 1989, "The Response of a Single-Degree-of-Freedom System with Quadratic and Cubic Nonlinearities to a Principal Parametric Resonance," Journal of Sound and Vibration, Vol. 129, pp. 417-442.

133. Zavodney, L. D., Nayfeh, A. H., and Sanchez, N. E., 1990, "Bifurcations and Chaos in Parametrically Excited Single-Degree-of-Freedom Systems," Nonlinear Dynamics, Vol. 1, pp. 1-21.

Appendix A. Stiffness and Mass Matrices in Equation (3.31)

Antisymmetric cross-ply plates

The elements $k_{ij} = k_{ji}$ of the stiffness matrix [K] are given by

$$k_{11} = -\left(\alpha^2 A_{11} + \beta^2 A_{66}\right)$$

$$k_{12} = -\alpha\beta(A_{12} + a_{66})$$

$$k_{13} = \left(\frac{4}{3h^2}\right)\alpha^3 E_{11}$$

$$k_{14} = \alpha^2\left[\left(\frac{4}{3h^2}\right)E_{11} - B_{11}\right]$$

$$k_{15} = 0$$

$$k_{22} = -\left(\beta^2 A_{11} + \alpha^2 A_{66}\right)$$

$$k_{23} = -\left(\frac{4}{3h^2}\right)\beta^3 E_{11}$$

$$k_{24} = 0$$

$$k_{25} = \beta^2\left[B_{11} - \left(\frac{4}{3h^2}\right)E_{11}\right]$$

$$k_{33} = 2\left(\frac{4}{3h^2}\right)(\alpha^2 + \beta^2)D_{44} - 2\left(\frac{4}{3h^2}\right)^2\alpha^2\beta^2(H_{12} + 2H_{66})$$
$$-\left(\frac{4}{3h^2}\right)^2(\alpha^4 + \beta^4)H_{11} - \left(\frac{4}{h^2}\right)^2(\alpha^2 + \beta^2)F_{44} - (\alpha^2 + \beta^2)A_{44}$$

$$k_{34} = 2\left(\frac{4}{h^2}\right)D_{44} - \left(\frac{4}{3h^2}\right)^2\alpha\beta^2(H_{12} + 2H_{66}) + \left(\frac{4}{3h^2}\right)\alpha^3(F_{11} - H_{11})$$
$$+\left(\frac{4}{3h^2}\right)\alpha\beta^2(F_{12} + 2F_{66}) - \left(\frac{4}{h^2}\right)^2\alpha F_{44} - \alpha A_{44}$$

$$k_{35} = 2\left(\frac{4}{h^2}\right)\beta D_{44} - \left(\frac{4}{3h^2}\right)^2 \alpha^2\beta(H_{12} + 2H_{66}) + \left(\frac{4}{3h^2}\right)\beta^3(F_{11} - H_{11})$$
$$+ \left(\frac{4}{3h^2}\right)\alpha^2\beta(F_{12} + 2F_{66}) - \left(\frac{4}{h^2}\right)\beta F_{44} - \beta A_{44}$$

$$k_{44} = -\beta^2 D_{66} + 2\left(\frac{4}{h^2}\right)D_{44} - \alpha^2 D_{11} - \left(\frac{4}{3h^2}\right)^2 (\alpha^2 H_{11} + \beta^2 H_{66})$$
$$+ 2\left(\frac{4}{3h^2}\right)(\alpha^2 F_{11} + \beta^2 F_{66}) - \left(\frac{4}{h^2}\right)^2 F_{44} - A_{44}$$

$$k_{45} = -\alpha\beta\left[D_{66} + D_{12} + \left(\frac{4}{3h^2}\right)^2 (H_{12} + H_{66}) - \left(\frac{4}{3h^2}\right)(F_{12} + F_{66})\right]$$

$$k_{55} = -\alpha^2 D_{66} + 2\left(\frac{4}{h^2}\right)D_{44} - \beta^2 D_{11} - \left(\frac{4}{3h^2}\right)^2 (\alpha^2 H_{66} + \beta^2 H_{11})$$
$$+ 2\left(\frac{4}{3h^2}\right)(\alpha^2 F_{66} + \beta^2 F_{11}) - \left(\frac{4}{h^2}\right)F_{44} - A_{44}$$

The elements $m_{ij} = m_{ji}$ of the mass matrix [M] are given by

$$m_{11} = m_{22} = -I_1$$

$$m_{33} = -\left(\frac{4}{3h^2}\right)I_7(\alpha^2 + \beta^2) - I_1$$

$$m_{34} = \left(\frac{4}{3h^2}\right)\bar{I}_5\alpha$$

$$m_{35} = \left(\frac{4}{3h^2}\right)\bar{I}_5\beta$$

$$m_{44} = m_{55} = -\bar{I}_3$$

and the remaining elements are zero.

Antisymmetric cross-ply plate strips

The elements $k_{ij} = k_{ji}$ of the stiffness matrix [K] are given by

$$k_{11} = -\alpha^2 A_{22}$$

$$k_{12} = \left(\frac{4}{3h^2}\right)\alpha^3 E_{11}$$

$$k_{13} = \alpha^2\left[\left(\frac{4}{3h^2}\right)E_{11} - B_{11}\right]$$

$$k_{22} = -\alpha^2\left[A_{44} - 2\left(\frac{4}{h^2}\right)D_{44} + \left(\frac{4}{h^2}\right)^2 F_{44}\right] - \alpha^4\left(\frac{r}{3h^2}\right)^2 H_{11}$$

$$k_{23} = -\alpha\left[A_{44} - 2\left(\frac{4}{h^2}\right)D_{44} + \left(\frac{4}{h^2}\right)^2 F_{44}\right] - \left(\frac{4}{3h^2}\right)\alpha^3(H_{11} - F_{11})$$

$$k_{33} = -\left[A_{44} - 2\left(\frac{4}{h^2}\right)D_{44} + \left(\frac{4}{h^2}\right)^2 F_{44}\right] - \alpha^2\left[\left(D_{11} + \frac{4}{3h^2}\right)\alpha^2 H_{11} + 2\left(\frac{4}{3h^2}\right)F_{11}\right]$$

The elements $m_{ij} = m_{ji}$ of the mass matrix [M] are given by

$$m_{11} = -I_1$$

$$m_{22} = -I_1 - \left(\frac{4}{3h^2}\right)^2 \alpha^2 I_7$$

$$m_{23} = \left(\frac{4}{3h^2}\right)\alpha \bar{I}_5$$

$$m_{33} = -\bar{I}_3$$

and the remaining elements are zero.

Appendix B. Constants Appearing in Equation (3.42)

$C_1 = k_{11}/m_{11}$

$C_2 = k_{12}/m_{11}$

$C_3 = k_{13}/m_{11}$

$C_4 = 0$

$C_5 = (m_{33}k_{22} - m_{23}k_{23})/d$

$C_6 = (m_{33}k_{23} - m_{23}k_{33})/d$

$C_7 = 0$

$C_8 = (-m_{23}k_{22} + m_{22}k_{23})/d$

$C_9 = (-m_{23}k_{23} + m_{22}k_{33})/d$

$b_1 = 0$

$b_2 = m_{33}/d$

$b_3 = -m_{23}/d$

where $d = 1/(m_{22}m_{23} - m_{23}^2)$, the m_{ij}, and the k_{ij} are given in Appendix A.

Appendix C. Constants Appearing in Equations (5.32) and (5.33)

$$e_1 = A_{11}/I_1$$

$$e_2 = A_{66}/I_1$$

$$e_3 = (A_{12} + A_{66})/I_1$$

$$e_4 = c_1 E_{11}/I_1$$

$$e_5 = (B_{11} - c_1 E_{11})/I_1$$

$$e_6 = c_1^2 I_7/I_1$$

$$e_7 = c_1 \bar{I}_5/I_1$$

$$e_8 = c_1^2 H_{11}/I_1$$

$$e_9 = 2c_1^2(H_{12} + 2H_{66})/I_1$$

$$e_{10} = c_1(F_{11} - c_1 H_{11})/I_1$$

$$e_{11} = c_1(F_{12} + 2F_{66} - c_1 H_{12} - 2c_1 H_{66})/I_1$$

$$e_{12} = (A_{44} - 2c_2 D_{44} + c_2^2 F_{44})/I_1$$

$$e_{13} = A_{12}/I_1$$

$$e_{14} = 3A_{11}/(2I_1)$$

$$e_{15} = (\frac{1}{2} A_{11} + A_{66})/I_1$$

$$e_{16} = 2(A_{12} + 2A_{66})/I_1$$

$$e_{17} = 1/I_1$$

$$e_{18} = c_1 \bar{I}_5/\bar{I}_3$$

$$e_{19} = c_1(F_{11} - c_1 H_{11})/\bar{I}_3$$

$$e_{20} = c_1(F_{12} + 2F_{66} - c_1 H_{12} - 2c_1 H_{66})/\bar{I}_3$$

$$e_{21} = (A_{44} - 2c_2 D_{44} + c_2^2 F_{44})/\bar{I}_3$$

$$e_{22} = (B_{11} - c_1 E_{11})/\bar{I}_3$$

$$e_{23} = (D_{12} + D_{66} + c_1^2 H_{12} + c_1^2 H_{66} - 2c_1 F_{12} - 2c_1 F_{66})/\bar{I}_3$$

$$e_{24} = (D_{66} + c_1^2 H_{66} - 2c_1 F_{66})/\bar{I}_3$$

$$e_{25} = (D_{11} - c_1^2 H_{11} - 2c_1 F_{11})/\bar{I}_3$$

VITA

The author, Jamal F. Nayfeh, was born in Kuwait, March 2, 1960. He obtained a Bachelor Degree in Civil Engineering from Kuwait University in 1983. He earned a Masters Degree in Mechanical Engineering from Yarmouk University, Irbid, Jordan in 1985. In 1985, he joined Virginia Polytechnic Institute and State University and in December 1990 he will receive a Doctor of Philosophy in Engineering Mechanics. He will join the faculty of the Department of Mechanical Engineering and Aerospace Sciences at the University of Central Florida in Orlando.